AD NUMBER

ADB017944

NEW LIMITATION CHANGE

TO

Approved for public release, distribution unlimited

FROM

Distribution authorized to U.S. Gov't. agencies only; Test and Evaluation; Dec 1976. Other requests shall be referred to the Air Force Flight Dynamics Laboratory, Attn: FBR, Wright-Patterson AFB, OH 45433

AUTHORITY

AFFDL ltr, 13 Jul 1979

AFFDL-TR-76-161

A FINITE ELEMENT MACH BOX PROCEDURE FOR FLUTTER PREDICTION OF PANELS IN THREE-DIMENSIONAL SUPERSONIC UNSTEADY POTENTIAL FLOW

DECEMBER 1976

TECHNICAL REPORT AFFDL-TR-76-161
FINAL REPORT FOR PERIOD JUNE 1976 - DECEMBER 1976

AIR FORCE FLIGHT DYNAMICS LABORATORY
AIR FORCE WRIGHT AERONAUTICAL LABORATORIES
AIR FORCE SYSTEMS COMMAND
WRIGHT-PATTERSON AIR FORCE BASE, OHIO 45433

NOTICE

When Government drawings, specifications, or other data are used for any purpose other than in connection with a definitely related Government procurement operation, the United States Government thereby incurs no responsibility nor any obligation whatsoever; and the fact that the Government may have formulated, furnished, or in any way supplied the said drawings, specifications, or other data, is not to be regarded by implication or otherwise in any manner licensing the holder or any other person or corporation, or conveying any rights or permission to manufacture, use, or sell any patented invention that may in any way be related thereto.

This technical report has been reviewed and is approved for publication.

James J. Olsen

JAMES J. OLSEN
Project Engineer

FOR THE COMMANDER

Howard L. Farmer

HOWARD L. FARMER, Colonel, USAF
Chief, Structural Mechanics Division

Copies of this report should not be returned unless return is required by security considerations, contractual obligations, or notice on a specific document.

THIS REPORT HAS BEEN DELIMITED
AND CLEARED FOR PUBLIC RELEASE
UNDER DOD DIRECTIVE 5200.20 AND
NO RESTRICTIONS ARE IMPOSED UPON
ITS USE AND DISCLOSURE.

DISTRIBUTION STATEMENT A

APPROVED FOR PUBLIC RELEASE;
DISTRIBUTION UNLIMITED.

UNCLASSIFIED

SECURITY CLASSIFICATION OF THIS PAGE (When Data Entered)

REPORT DOCUMENTATION PAGE

READ INSTRUCTIONS BEFORE COMPLETING FORM

1. REPORT NUMBER: AFFDL-TR-76-161
2. GOVT ACCESSION NO.
3. RECIPIENT'S CATALOG NUMBER
4. TITLE (and Subtitle): A FINITE ELEMENT MACH BOX PROCEDURE FOR FLUTTER PREDICTIONS OF PANELS IN THREE-DIMENSIONAL SUPERSONIC UNSTEADY POTENTIAL FLOW
5. TYPE OF REPORT & PERIOD COVERED: Final Report, June 1976-December 1976
6. PERFORMING ORG. REPORT NUMBER
7. AUTHOR(s): T. Y. YANG
8. CONTRACT OR GRANT NUMBER(s)
9. PERFORMING ORGANIZATION NAME AND ADDRESS: AFSC (AFWAL) AF Flight Dynamics Laboratory (FBR) Structural Mechanics Division, WPAFB, Ohio 45433
10. PROGRAM ELEMENT, PROJECT, TASK AREA & WORK UNIT NUMBERS: 230705
11. CONTROLLING OFFICE NAME AND ADDRESS: Air Force Flight Dynamics Laboratory Structural Mechanics Division Wright-Patterson AFB, Ohio 45433
12. REPORT DATE: December 1976
13. NUMBER OF PAGES: 92
14. MONITORING AGENCY NAME & ADDRESS (if different from Controlling Office)
15. SECURITY CLASS. (of this report): UNCLASSIFIED
15a. DECLASSIFICATION DOWNGRADING SCHEDULE

16. DISTRIBUTION STATEMENT (of this Report)

Distribution limited to U.S. Government agencies only; test and evaluation; statement applied in December 1976. Other requests for this document must be referred to AF Flight Dynamics Laboratory, (FBR), Wright-Patterson AFB, Ohio 45433.

17. DISTRIBUTION STATEMENT (of the abstract entered in Block 20, if different from Report)

N/A

18. SUPPLEMENTARY NOTES

N/A

19. KEY WORDS (Continue on reverse side if necessary and identify by block number)

Aeroelasticity	Finite Elements	Mach Box
Panel Flutter	Supersonic Flow	

20. ABSTRACT (Continue on reverse side if necessary and identify by block number)

A finite element formulation and solution procedure are developed for flutter predictions of rectangular panels with one surface exposed to three-dimensional supersonic unsteady potential flow. The effect of in-plane force is included. Each element is divided into several Mach boxes. The aerodynamic influence coefficients between each pair of sending and receiving boxes are computed by the method of Gaussian quadrature. The aerodynamic matrix is based on the numerically computed velocity potentials for all boxes.

DD FORM 1 JAN 73 1473 EDITION OF 1 NOV 65 IS OBSOLETE

UNCLASSIFIED

SECURITY CLASSIFICATION OF THIS PAGE (When Data Entered)

012 320

This development is particularly useful in the low supersonic range for panels with chord-span ratio less than about one, while the piston theory does not give satisfactory solution. Examples are demonstrated by using the 16 d.o.f. rectangular plate elements. Results for flutter boundaries for the unstressed panels agree well with an alternative Galerkin's modal solution. The examples demonstrate that flutter boundaries are dominated by higher modes for panels with higher chord-span ratio. They also demonstrate that the dominating flutter boundaries abruptly change modes as the Mach number is varied. The beneficial effect of in-plane tension is demonstrated.

FOREWORD

This report was prepared by Dr. T. Y. Yang, Visiting Scientist in the Optimization Group, Analysis and Optimization Branch, Structural Mechanics Division, Air Force Flight Dynamics Laboratory, Air Force Wright Aeronautical Laboratories, Air Force Systems Command, Wright-Patterson Air Force Base, Ohio. This work was performed under Project Nr. 2307, "Research in Flight Vehicle Dynamics," Task Nr. 230705, "Basic Research in Structures and Dynamics."

The manuscript was released by the author in December 1976 for publication as a technical report. The report covers work conducted from June 1976 through December 1976.

TABLE OF CONTENTS

ILLUSTRATIONS

LIST OF ILLUSTRATIONS (Continued)

LIST OF ILLUSTRATIONS (Continued)

LIST OF ILLUSTRATIONS (Continued)

SYMBOLS

a, b	=	length and width of the rectangular plate finite element as defined in Fig. 1.
[A]	=	aerodynamic matrix of the panel system
B_x, B_{xs}	=	number of boxes in the stream and cross-stream directions, respectively
D	=	$Eh^3/12(1 - \gamma^2)$, bending rigidity with γ being Poisson's ratio
F	=	$N_x/\ell^2\omega_1{}^2\sigma h$, Initial in-plane tension parameter
$f_j(x,y)$	=	shape function associated with degree of freedom "j"
g	=	structural damping coefficient
h	=	panel thickness
i, j	=	subscripts indicate d.o.f. number
[K]	=	stiffness matrix of the panel system
k_ℓ, k_ε	=	$\omega\ell/V$, $\omega\varepsilon/V$, respectively, reduced frequency
ℓ	=	length of panel in stream direction
[M]	=	mass matrix of the panel system
M	=	Mach number
m, n	=	receiving box index numbers in the stream and cross-stream directions, respectivley
[N]	=	incremental stiffness matrix of the panel system
N_x, N_y, N_{xy}	=	panel in-plane line forces
r, s	=	$(m - \lambda)$, $(n - \nu)$, respectively
u, v	=	transformed variables of integration based on $\varepsilon/2$ as reference length, $u\beta/2 = x_m - \varepsilon$, $v/2 = y_n - \eta$
V	=	speed of undisturbed airstream

w	=	width of panel in cross-stream direction
w_j	=	downwash velocity at panel surface for d.o.f. "j"
x, y	=	panel coordinates as defined in Fig. 1
$\bar{x}$, $\bar{y}$	=	x/ℓ, y/w, respectively
x_m, y_n	=	values of x/ε and y/ε at center of box m,n
α_ϕ	=	aerodynamic influence coefficient relating the velocity potential at a box to unit downwash on another box (Eq. 12)
β	=	$(M^2 - 1)^{\frac{1}{2}}$
ε	=	w/B_{xs}, box width
ξ, η	=	values of x/ε and y/ε at any point in the sending box
μ	=	panel-air mass density ratio, $\sigma h/\rho\ell$
λ, ν	=	sending box index number in the stream and cross-stream directions, respectively
ρ	=	density of undisturbed airstream
σ	=	density of panel
τ	=	length-width ratio of box as defined in Fig. 1
$\phi_j(m,n)$	=	velocity potential at center of box m,n for d.o.f. "j"
$\bar{\phi}(m,n)$	=	velocity potential at center of box m,n due to unit downwash over box λ,ν
ω	=	frequency of flutter motion
ω_1	=	first natural frequency of the panel
Ω	=	$(\omega_1/\omega)^2(1 + ig)$
$\bar{\Omega}$	=	$M^2 k_\varepsilon/\beta^2$

SECTION I

INTRODUCTION

Ever since the earliest days of manned flight, panel flutter has been known as one of the most important problems in the design of aircraft, missiles, launched vehicles, and spacecraft. Extensive progress in wind tunnel tests and theoretical studies has been achieved. The basic theories and an account of the developments on panel flutter can be found in, among other books, a recent text by Dowell (Reference 1). A list of keyed bibliography and collection of some significant survey papers and original papers were prepared by Garrick (Reference 2).

The theoretical solution for a panel flutter problem usually requires an accurate aerodynamic and structural theory to formulate a set of complex eigenvalue equations of motion interacted between the panel and the flow. One of the most common theoretical methods is the modal method where the aerodynamic pressure and the inertial and elastic forces of the panel are obtained by assuming the displacements as composed of a number of natural modes and generalized coordinates. The natural frequencies and corresponding normal mode shapes are obtained either theoretically or experimentally, or both. Since the finite element method is powerful and practical in the free vibration analysis of panels with arbitrary geometrical and boundary conditions, it is commonly used in obtaining natural frequencies and mode shapes in the modal method.

As an alternative approach, the finite element workers have formulated the matrix of aerodynamic pressure by using the

displacement functions as composed of the nodal degrees of freedom and shape functions rather than the generalized coordinates and natural mode shapes. Such approach can directly solve for the flutter frequencies and corresponding normal mode shapes without having to seek the natural frequencies and modes and choose the number of modes before the eigensolution, and also without having to compute the flutter mode shapes after the eigensolution. Such approach permits expression of the equations of motion in an elegant and straightforward form. Such approach also permits generality in panel configurations and boundary conditions, and allows for flexibility to accurately include physical effect such as in-plane forces.

The finite element method was first extended to the panel flutter problems by Olson (Reference 3). He formulated the aerodynamic matrix explicitly for an infinite plate element. Olson (Reference 4) later formulated the aerodynamic matrices for two rectangular (12 and 16 d.o.f.) and an 18 d.o.f. triangular plate elements. Simultaneously, but independently, Appa and Somashekar (Reference 5) formulated the aerodynamic matrix for a 12 d.o.f. rectangular plate element. Appa, Somashekar and Shah (Reference 6) later extended their work by accounting for skew panels and yawed flow by means of coordinate transformation. Sander, Bon, and Geradin (Reference 7) employed the CQ conforming quadrilateral plate finite element for flutter analysis of rectangular panels with yawed flow and in-plane stresses.

In all the above finite element works (References 3 - 7), Lighthill's linearized piston theory was employed. The Mach numbers considered were above approximately 1.6. Recently, Yang (Reference 8) developed a finite element procedure using the exact linearized two-dimensional theory (strip theory) for unsteady supersonic flow to formulate an infinite plate finite element by means of numerical integration. The flutter speed considered thus could be in the lower supersonic range. Such formulation cannot, however, be adequately applied to the more general case of rectangular panels with finite aspect ratios.

In this report, the three-dimensional supersonic unsteady potential flow theory is employed to formulate the plate finite elements so that the flutter problems of the finite panels in low supersonic range can be treated.

The aerodynamic matrix is derived by using the principle of virtual work. The aerodynamic forces or velocity potentials that produce the work are obtained for each d.o.f. by the Mach box method. Each finite element is divided into several boxes. The aerodynamic influence coefficients for each pair of sending and receiving boxes are evaluated, for each d.o.f., by the method of Gaussian quadrature. The velocity potential at each receiving box is obtained, for each d.o.f., by summation of the product of corresponding downwash and influence coefficients for all sending boxes. It should be noted that a similar box method was used by Cunningham (Reference 9) in conjunction with a Galerkin's modal method for panel flutter analysis. Such 3-D aerodynamic theory was also employed by Dowell and Voss (Reference 10) in a theoretical and experimental correlation study of panel flutter.

The 16 d.o.f. conforming rectangular plate element (Reference 11) was used for example demonstrations. Flutter boundaries were found for clamped rectangular panels with various aspect ratios. The thickness ratios required to prevent flutter of an aluminum panel at sea level were plotted for Mach numbers ranging from 1.05 to 3. Results found are in favorable agreement with Cunninhgam's solution (Reference 9).

The initial in-plane tensile stresses were then included in finding the flutter boundaries for a clamped aluminum panel. The thickness ratios required to prevent flutter of the panel at 25,000 feet altitude were obtained for Mach numbers ranging from 1.05 to 2.0 for various values of tension. It was found that the dominating flutter mode changed abruptly as Mach number was varied.

SECTION II

FORMULATION OF EQUATIONS OF MOTION

The free vibration equations of motion for a finite element panel subjected to the effect of stiffness, in-plane force, inertia, and aerodynamic pressure may be written as

$$[K]\{q\} + [N]\{q\} + [M]\{\ddot{q}\} + [A]\{q\} = \{0\} \tag{1}$$

where [K], [N], [M], and [A] are, respectively, the stiffness, incremental stiffness, mass, and aerodynamic matrices assembled for the whole finite element system. The vector {q} contains the nodal degrees of freedom for the whole panel system. In this section, only the system aerodynamic matrix is formulated.

1. PRINCIPLE OF VIRTUAL WORK

For a system of plate finite elements, the deflection and aerodynamic pressure may be written by separating the time and space variables as,

$$\begin{aligned} \bar{z}(x,y,t) &= z(x,y)e^{i\omega t} \\ \bar{p}(x,y,t) &= p(x,y)e^{i\omega t} \end{aligned} \tag{2}$$

where the coordinates are defined in Fig. 1.

The strain energy for the panel system is equal to the work produced by the aerodynamic pressure

$$U = \frac{1}{2}\iint z(x,y)p(x,y)\ dxdy \tag{3}$$

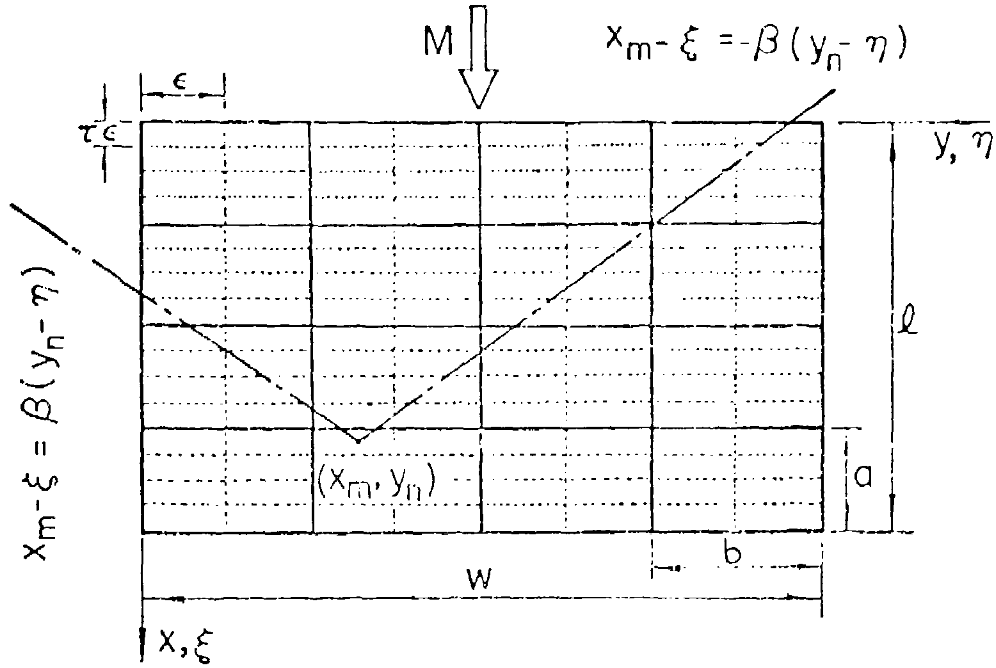

Figure 1. Panel divided into finite elements (solid lines) and boxes (dash lines) with coordinates, dimensions, and Mach cone

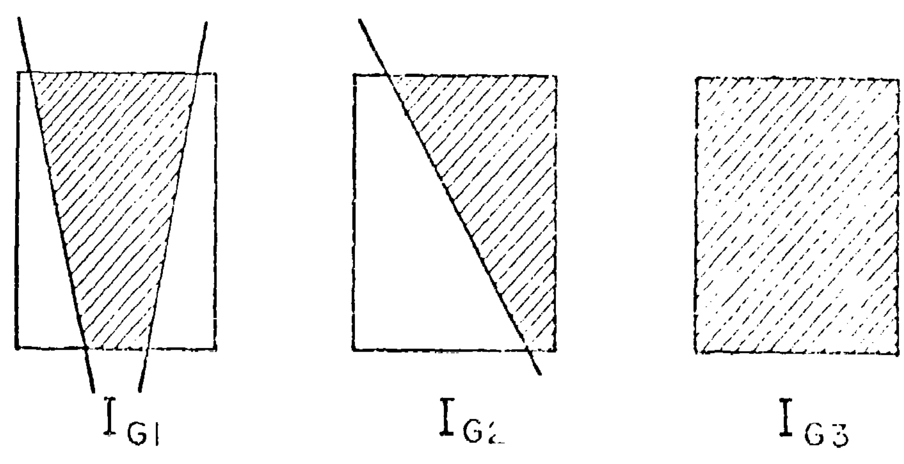

Figure 2. Three forms of integrals for computing the aerodynamic influence coefficients

The deflection function for the total finite element system may be assumed as

$$z(x,y) = \sum_{j=1}^{N} f_j(x,y)q_j = \{f\}^T\{q\} \tag{4}$$

where $f_j(x,y)$ represents the assembled shape function corresponding to the nodal d.o.f. "q_j" and N is the number of degrees of freedom for the entire panel system. Usually, q_j represents deflection, slopes, twist, and curvatures of the plate at the nodal point j.

Similarly, the aerodynamic pressure may be assumed as

$$p(x,y) = \sum_{j=1}^{N} P_j(x,y)q_j = \{P\}^T\{q\} \tag{5}$$

where $P_j(x,y)$ is defined in Eq. (8) as the pressure function associated with the shape function $f_j(x,y)$ and d.o.f. "q_j."

Substituting Eqs. (4) and (5) into (3), the strain energy expression becomes

$$U = \frac{1}{2} \{q\}^T[A]\{q\} \tag{6}$$

with

$$[A] = \iint \{f\}\{P\}^T \, dxdy \tag{7}$$

Using the principle of virtual work, it can be interpreted that Eq. (7) yields the aerodynamic matrix.

2. AERODYNAMIC MATRIX AND AERODYNAMIC PRESSURE

The aerodynamic perturbation pressure is obtained from the linearized three-dimensional supersonic unsteady potential flow theory. When associated

with the d.o.f. "q_j" and the shape function $f_j(x,y)$, the perturbation pressure may be expressed in terms of the velocity potential through the relation (see, for example, Ref. 12),

$$P_j(\bar{x},\bar{y}) = -\frac{\rho V}{\ell}\left(\frac{\partial \phi_j}{\partial \bar{x}} + i\,\frac{\omega \ell}{V}\,\phi_j\right) \tag{8}$$

where ϕ_j is the velocity potential associated with d.o.f. "q_j".

The coefficient for the i<u>th</u> row and j<u>th</u> column of the aerodynamic matrix [A] is obtained by substituting Eq. (8) into Eq. (7).

$$A_{ij} = -\frac{\rho V}{\ell}\iint f_i(\bar{x},\bar{y})\left(\frac{\partial \phi_j}{\partial \bar{x}} + i\,\frac{\omega \ell}{V}\,\phi_j\right)d(\ell\bar{x})\,d(w\bar{y}) \tag{9}$$

Performing integration by parts and assuming restrained trailing edge, Eq. (9) becomes

$$A_{ij} = \frac{\rho V}{\ell}\iint \phi_j\left(\frac{\partial f_i}{\partial \bar{x}} - i\,\frac{\omega \ell}{V}\,f_i\right)d(\ell\bar{x})\,d(w\bar{y}) \tag{10}$$

where the quantity within the parentheses is the complex conjugate of the downwash ratio for unit d.o.f. "q_i" and unit panel length. The coefficient A_{ij} is evaluated numerically through the following simple summation

$$A_{ij} = \frac{\rho V}{\ell}\sum \phi_j\left(\frac{\partial f_i}{\partial \bar{x}} - i\,\frac{\omega \ell}{V}\,f_i\right)\cdot(\text{Box Area}) \tag{11}$$

where the summation is to be made for every box and the quantities related to ϕ_j and f_i are evaluated numerically at the center of each box. The method for numerically evaluating the velocity potential at the center of each box is given as follows.

3. VELOCITY POTENTIAL AND AERODYNAMIC INFLUENCE COEFFICIENT

The method of Mach box as employed by Cunningham in Reference 9 is used here to derive the aerodynamic influence coefficients between each pair of boxes and the resulting velocity potentials at each box.

In this method, each finite element is divided into several equal-size boxes as shown in Fig. 1. The numbers of boxes in the stream and cross-stream directions are defined as B_X and B_{XS}, respectively. The width and length of each box are defined as ϵ and $\tau\epsilon$, respectively, where $\epsilon = w/B_{XS}$ and $\tau = \ell B_{XS}/wB_X$. The boxes are numbered in sequence from the origin with m (or λ) and n (or ν) as the box number in the stream and the cross-stream directions, respectively. The numbers (m,n) and (λ,ν) refer to the receiving and sending boxes, respectively.

The boxes are assumed as sufficiently small so that the downwash over any sending box is considered as uniformly distributed at any instant, and the resulting perturbation pressure at the center of each receiving box represents the average of the pressure distributed over the box.

The velocity potential at the center of a receiving box (m,n) due to a uniformly distributed but otherwise unspecified downwash $w(\lambda,\nu)$ over the sending box (λ,ν) can be expressed, for harmonic motion, as

$$\bar{\phi}(m,n) = \epsilon\, w(\lambda,\nu)\alpha_{\phi}(r,s) \tag{12}$$

where the relative locations in stream and cross-stream directions, respectively, between the two boxes are defined as $r = m - \lambda$ and $s = n - \nu$. The aerodynamic influence coefficient from Reference 9 is,

$$\alpha_\phi(r,s) = \frac{1}{2\pi}\int_{u_1}^{u_2} e^{-i(\beta\bar{\Omega}/2)u}\left\{\cos^{-1}\frac{v_1}{u} - \cos^{-1}\frac{v_2}{u} + \int_{v_1}^{v_2}\frac{\cos[\frac{\beta\bar{\Omega}}{2M}(u^2-v^2)^{\frac{1}{2}}] - 1}{(u^2 - v^2)^{\frac{1}{2}}}\,dv\right\}du \tag{13}$$

where all the parameters are defined in the List of Symbols.

In Eq. (13), the surface integration limits u_1, u_2, v_1, and v_2 result in only three different forms I_{G1}, I_{G2}, and I_{G3} as shown in Fig. 2.

The first form is for any portion of a sending box(λ, ν) cut by both sides of the Mach cone so that $v_2 = -v_1 = u$ and $s = 0$.

$$I_{G1} = \frac{1}{2}\int_{u_1}^{u_2} e^{-i(\beta\bar{\Omega}/2)u}\, J_0(\frac{\beta\bar{\Omega}}{2M}\,u)du \tag{14}$$

where J_0 is the Bessel function of the first kind of order zero.

The second form is for portions of a box cut by one side of the Mach cone so that the limits $v_2 = u$ and $v_1 = 2s - 1 \geq 1$.

$$I_{G2} = \frac{1}{2\pi}\int_{u_1}^{u_2} e^{-i(\beta\bar{\Omega}/2)u}\left\{\cos^{-1}\frac{v_1}{u} + \int_{v_1}^{u}\frac{\cos[\frac{\beta\bar{\Omega}}{2M}(u^2 - v^2)^{\frac{1}{2}}] - 1}{(u^2 - v^2)^{\frac{1}{2}}}\,dv\right\}du \tag{15}$$

The third form is for boxes that are completely within the Mach cone and also for portions of boxes ahead of the point where the Mach line cuts the side of the box.

$$I_{G3} = \frac{1}{2\pi}\int_{u_1}^{u_2} e^{-i(\beta\bar{\Omega}/2)u}\left\{\cos^{-1}\frac{v_1}{u} - \cos^{-1}\frac{v_2}{u} + \int_{v_1}^{v_2}\frac{\cos[\frac{\beta\bar{\Omega}}{2M}(u^2-v^2)^{\frac{1}{2}}] - 1}{(u^2 - v^2)^{\frac{1}{2}}}\,dv\right\}du \tag{16}$$

The complete $\alpha_\phi(r,s)$ for any one sending box (λ,ν) consists of I_{G1}, I_{G2}, or I_{G3}, or a combination of I_{G1} and I_{G2}, or of I_{G2} and I_{G3}. The types of integrals and limits of integration for computing $\alpha_\phi(r,s)$ for all possible relative locations of box$(\lambda, \nu)$and the Mach cone from(m, n) are given in Reference 9.

The evaluation of the above three integrals is carried out through the method of Gaussian quadrature. In the subsequent numerical examples, three Gaussian points are used in both x and y directions for computing I_{G3}. Five Gaussian points in both x and y directions are used for computing I_{G1} and I_{G2}.

Once all possible values of the aerodynamic influence coefficient $\alpha_{\phi}(r,s)$ are obtained for a certain shape function $f_j(\bar{x},\bar{y})$, the total velocity potential at the center of a receiving box (m,n) for the downwash associated with the same shape function is a weighted sum of the $\bar{\phi}_j(m,n)$ defined in Eq. (12)

$$\phi_j(m,n) = V\varepsilon \sum_{\lambda} \sum_{\nu} \frac{w_j(\lambda,\nu)}{V} \alpha_{\phi}(r,s) \tag{17}$$

The summation is extended over all the sending boxes. The downwash ratios $w_j(\lambda,\nu)/V$ for a unit d.o.f. "q_j" are the total time derivatives of the shape function $f_j(\bar{x},\bar{y})e^{i\omega t}$

$$\frac{w_j}{V} = \frac{1}{\ell}\left(\frac{\partial f_j}{\partial \bar{x}} + i\,\frac{\omega \ell}{V} f_j\right) \tag{18}$$

Once the velocity potentials are obtained for each box for each shape function, they can readily be substituted into Eq. (11) for computing the aerodynamic matrix for the entire panel system.

SECTION III

FORMULATION FOR FLUTTER DETERMINANT IN TERMS OF FINITE ELEMENT SHAPE FUNCTIONS

In the present finite element flutter formulation, the parameters are so grouped and nondimensionalized that the solution is general enough to include every parameter. Assuming harmonic motion with natural frequency ω, the equations of motion (1) are rewritten in an element form as

$$\left\{\Omega\left[c_1[k] + Fc_2[n]\right] - \left[c_3[m] - c_4[A]\right]\right\}\{q\} = \{0\} \tag{19}$$

where $\Omega = \omega_1{}^2/\omega^2(1 + ig)$ is the flutter eigenvalue parameter, and

$$\begin{aligned} c_1 &= \frac{\mu(\ell/a)^5 D}{\omega_1{}^2 \sigma h \ell^4} \quad ; \quad c_2 = \mu(\ell/a)^3 \quad ; \\ c_3 &= \mu(\ell/a) \quad ; \quad c_4 = \left(\frac{\ell}{a}\right)^3\left(\frac{\varepsilon}{\ell}\right)\left(\frac{1}{k_\ell}\right)^2\left(\frac{\tau\varepsilon^2}{ab}\right) \end{aligned} \tag{20}$$

The element matrix terms are obtained as

$$\begin{aligned} k_{ij} = \int_0^1 \int_0^1 \Big[&\frac{\partial^2 f_i}{\partial \bar{x}^2}\frac{\partial^2 f_j}{\partial \bar{x}^2} + \left(\frac{a}{b}\right)^4 \frac{\partial^2 f_i}{\partial \bar{y}^2}\frac{\partial^2 f_j}{\partial \bar{y}^2} + \nu\left(\frac{a}{b}\right)^2 \frac{\partial^2 f_i}{\partial \bar{x}^2}\frac{\partial^2 f_j}{\partial \bar{y}^2} \\ &+ \nu\left(\frac{a}{b}\right)^2 \frac{\partial^2 f_j}{\partial \bar{x}^2}\frac{\partial^2 f_i}{\partial \bar{y}^2} + 2(1 - \nu)\left(\frac{a}{b}\right)^2 \frac{\partial^2 f_i}{\partial \bar{x}\partial \bar{y}}\frac{\partial^2 f_j}{\partial \bar{x}\partial \bar{y}}\Big] d\bar{x}d\bar{y} \end{aligned} \tag{21}$$

$$n_{ij} = \int_0^1 \int_0^1 \left[\frac{\partial f_i}{\partial \bar{x}}\frac{\partial f_j}{\partial \bar{x}} + \frac{N_y}{N_x}\frac{\partial f_i}{\partial \bar{y}}\frac{\partial f_j}{\partial \bar{y}} + \frac{N_{xy}}{N_x}\frac{\partial f_i}{\partial \bar{x}}\frac{\partial f_j}{\partial \bar{y}} + \frac{N_{xy}}{N_x}\frac{\partial f_j}{\partial \bar{x}}\frac{\partial f_i}{\partial \bar{y}}\right] d\bar{x}d\bar{y} \tag{22}$$

$$m_{ij} = \int_0^1 \int_0^1 f_i f_j \, d\bar{x}d\bar{y} \tag{23}$$

$$A_{ij} = \sum \frac{\phi_j}{V\varepsilon}\left(\frac{\partial f_i}{\partial \bar{x}} - i\,\frac{\omega a}{V} f_i\right) \tag{24}$$

The shape functions $f_i(\bar{x},\bar{y})$ are usually cubic or higher order functions of nondimensional coordinate variables $\bar{x}$ and $\bar{y}$. Their differentiations with respect to $\bar{x}$ and $\bar{y}$ are performed analytically. The subscript "i" indicates the degree of freedom number with which the shape function is associated. Eqs. (19-24) are suitable for any plate finite element so long as it is a displacement model with assumed shape functions. According to the state-of-the-art of the finite element development, the stiffness matrix [k], mass matrix [m], and incremental stiffness matrix [n] have been formulated analytically and explicitly for almost every plate and shell finite element. Only the aerodynamic matrix [A] remains to be formulated and it is to be obtained by numerical integration here.

Eq. (19) constitutes an eigenvalue problem. The flutter solution is obtained by first assuming a value of reduced frequency k_ℓ, then varying the air-panel mass ratio $1/\mu$ incrementally and solving for the corresponding eigenvalues Ω or $(\omega_1/\omega)^2(1 + ig)$. When the structural damping coefficient g changes its value from negative to positive, the panel goes from the stable region to unstable region, and vice versa. The values of k_ℓ and $1/\mu$ that correspond to zero g value define the flutter boundary and the corresponding mode shape defines the flutter mode. The complex eigenvalue problem is solved by using a subroutine in EISPACK provided by Argonne National Laboratory.

Before performing analysis for each class of problems, a convergence study by varying the meshes of Mach boxes and finite elements must be made in order to find the suitable meshes needed for obtaining converged results. Such meshes depend on the panel geometry, boundary conditions, flow speed, and flutter modes. However, due to the enormous computations needed for obtaining massive data in this study, not the finest meshes are used. Most of the present results are compared with those obtained by the modal method (Reference 9) and good results are obtained.

SECTION IV

RESULTS

The 16 d.o.f. conforming rectangular plate finite elements were employed to demonstrate the present formulation and procedure. The examples chosen were rectangular panels, stressed as well as unstressed, with clamped edges. For the unstressed panels, a sophisticated analytical solution by Cunningham (Reference 9) using the box method (400 boxes) and Galerkin's modal approach (6 to 16 modes) was available for comparison.

In all examples studied here, the flutter mode shapes were assumed as symmetrical about the center chord-line of the panel. Thus, only half of each panel was modeled by finite elements. In all cases, two elements in the cross stream direction were used for half of the panel. The number of elements in the stream direction varied from 4 to 10 dependent on the dominating flutter mode shapes. Each element was divided into 4 by 2 boxes in the stream and cross stream directions, respectively.

It is important to note that symmetry does not exist for the mesh of boxes unless the Mach cone apex is located at the center chord-line of the panel. The boxes on the other (disregarded) half of the panel can, however, still be accounted for since their deflection shapes are known by symmetry.

Case 1 Clamped Panels with Various Chord-span Ratios at $M = 1.3$

The rectangular panels with all edges clamped and chord-span ratios (ℓ/w) equal to 0, 1/4, 1/2, 1, 2, and 4 were studied for $M = 1.3$.

The resulting flutter boundaries are presented as plots of each dominating mode with the air-panel mass ratio $1/\mu$ as the vertical coordinate and the stiffness parameter $\omega_1 \ell/V$ as the horizontal coordinate. The values of reduced frequency k_ℓ or $\omega\ell/V$ are marked along each curve. The results for the infinite panel with $\ell/w = 0$ are in exact agreement with those obtained by Cunningham, therefore, they are not presented here.

Fig. 3 shows that for the wide panel with $\ell/w = 1/4$, the first mode flutter boundary crosses the second mode flutter boundary. The critical flutter boundaries are thus dominated by the first mode in the high mass ratio range and by the second mode in the low mass ratio range. A slight amount of structural damping was also included ($g = 0.01$). The results agree well with those obtained by Cunningham (Reference 9).

The first flutter mode shape (real part) corresponding to point A ($k_\ell = 0.635$) in Fig. 3 is shown in Fig. 4. It is seen that, due to the effect of the flow, the mode is not symmetrical about the cross stream centerline. The maximum deflection occurs at a point behind the center of the panel. The second flutter mode shape (real part) for the center chord-line of the panel corresponding to point B ($k_\ell = 1.59$) in Fig. 3 is shown in Fig. 5. The effect of the flow that pushes down the front part of the panel is seen.

Fig. 6 shows that, as the panel width is reduced ($\ell/w = 1/2$), the first mode boundary shifts to the left and the second mode boundary becomes the critical flutter boundary. Again, the results agree well with Cunningham's solution.

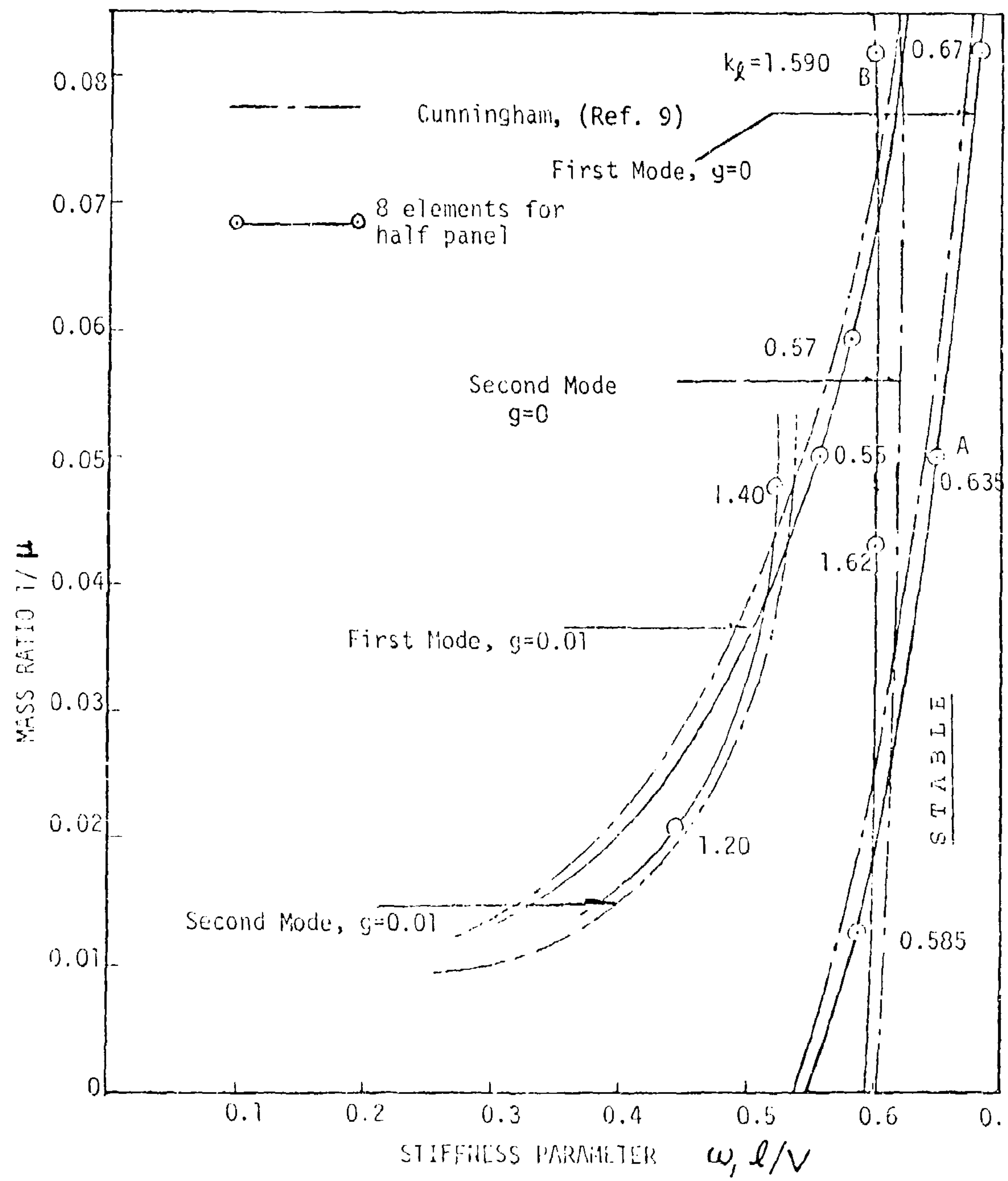

Figure 3 Flutter boundaries for clamped panel with $\ell/w = 1/4$ and $M = 1.3$

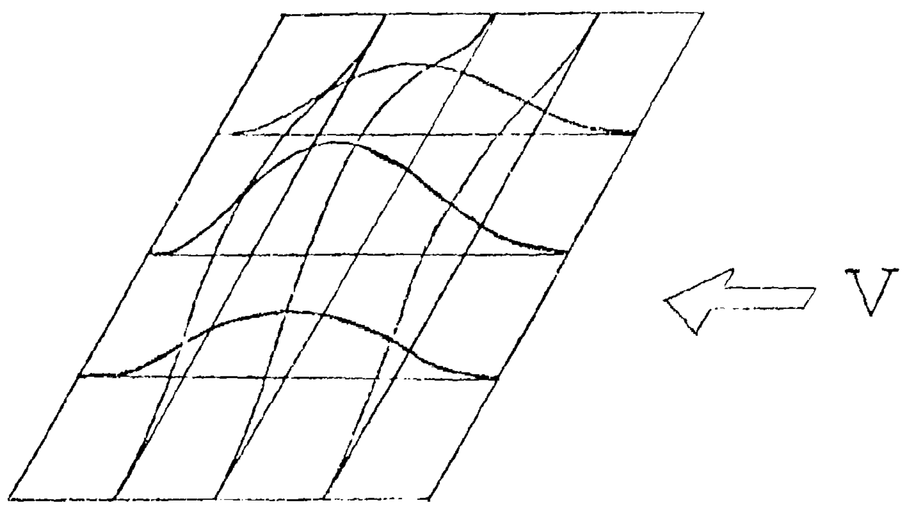

Figure 4. The first mode shape (real part) for panel corresponding to point A in Fig. 3

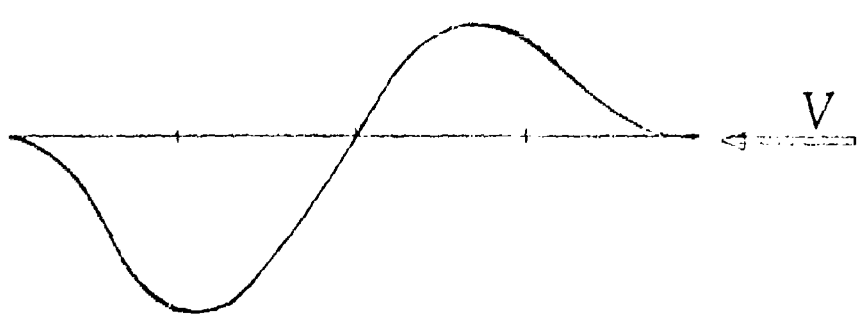

Figure 5 The second mode shape (real part) for the center line of panel corresponding to point B in Fig. 3

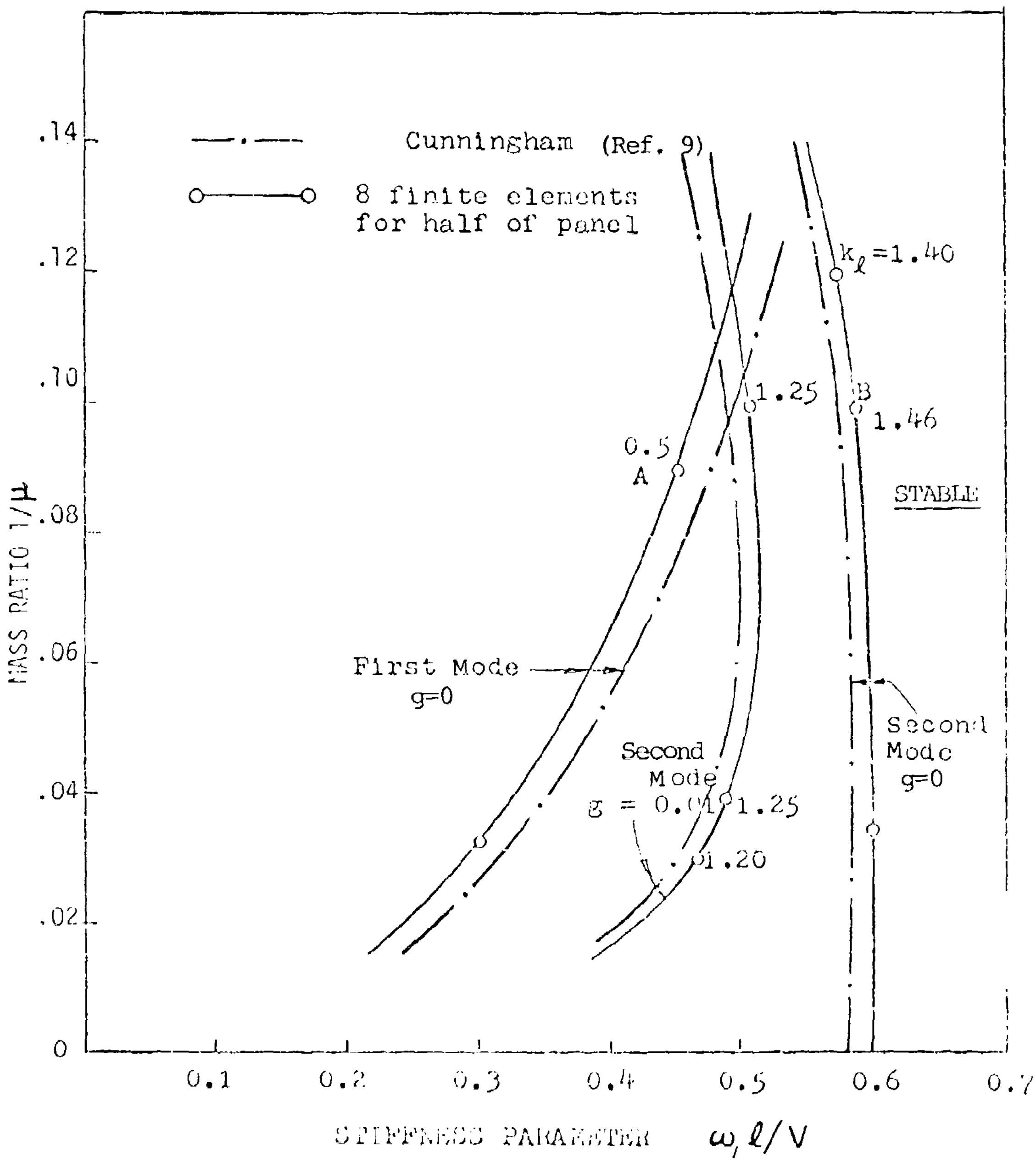

Figure 6 Flutter boundaries for clamped panel with $\ell/w = 1/2$ and $M = 1.3$

The first and second flutter mode shapes (real part) corresponding to points A and B in Fig. 6 are plotted in Figs. 7 and 8, respectively. They are quite similar to those shown in Figs. 4 and 5.

Fig. 9 shows that, as the panel becomes square, the third and fourth mode boundaries emerge and the third mode boundary becomes the critical flutter boundary. The results are in good agreement with Cunningham's solution. The results for the first mode boundary obtained by Houbolt using the piston theory are also shown in the figure.

The third and fourth flutter mode shapes (real part) corresponding to points A and B in Fig. 9 are shown in Figs. 10 and 11, respectively. The effect of the flow that tends to blow flat the front part of the panel is seen.

Fig. 12 shows that, for a long panel with $\ell/w = 2$, the fifth mode flutter boundary becomes dominant in the low mass ratio range and the first mode boundary dominates the high mass ratio range. It also shows that Houbolt's solution for first mode and this solution are very close. There are, however, some discrepancies between this solution and Cunningham's solution for the first mode boundary. This may be due to the fact that the stiffness coupling effect between assumed beam natural modes was uniformly neglected by Cunningham

Such coupling effect can become significant as the chord-span ratio increases. It should be noted that, due to the limited number of elements and boxes used, the present results are not the most accurate that this approach can produce.

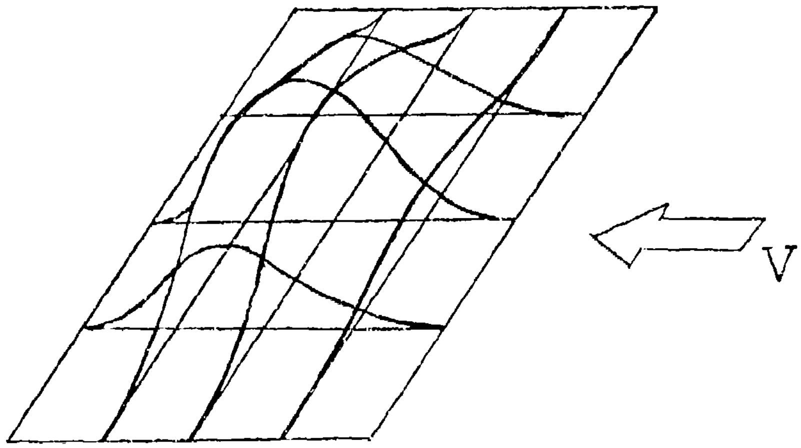

Figure 7 The first mode shape (real part) for panel corresponding to point A in Fig. 6

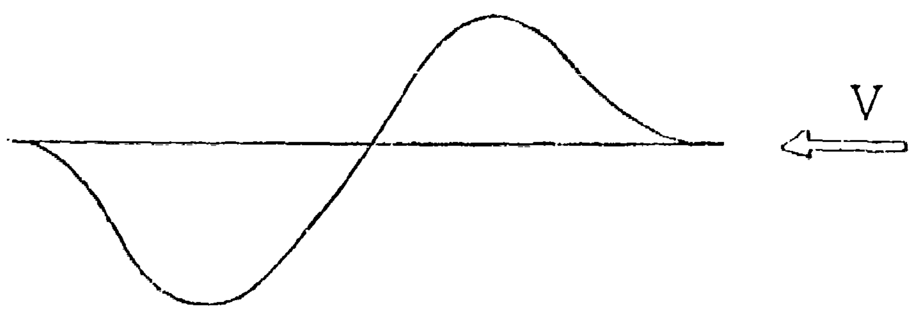

Figure 8 The second mode shape (real part) for the center line of panel corresponding to point B in Fig. 6

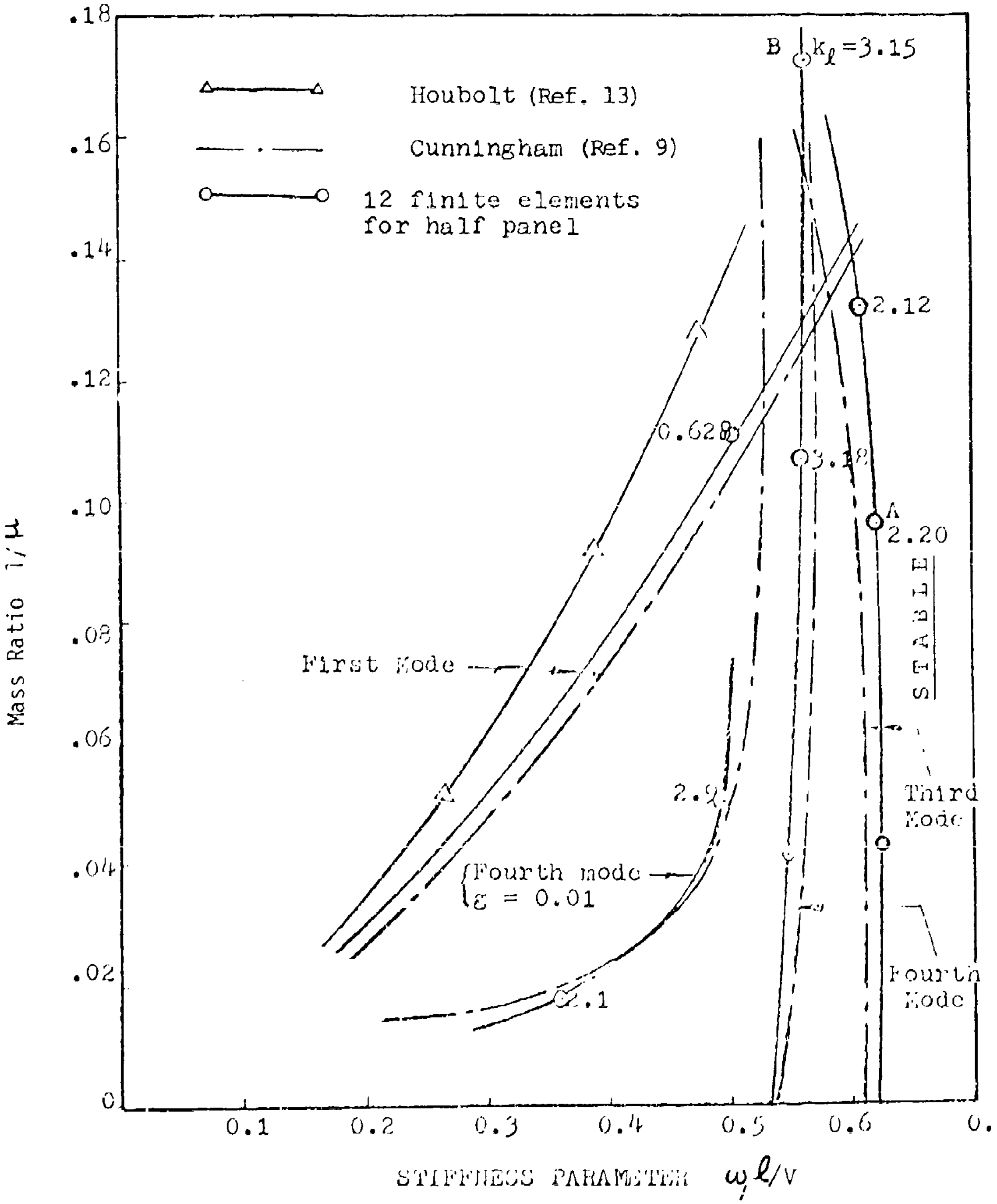

Figure 9 Flutter boundaries for clamped panel with $\ell/w = 1$ and $M = 1.3$

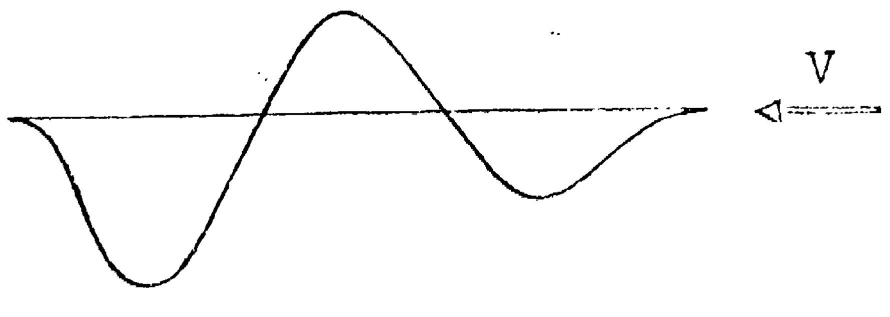

Figure 10 The third mode shape (real part) for the center line of panel corresponding to point A in Fig. 9

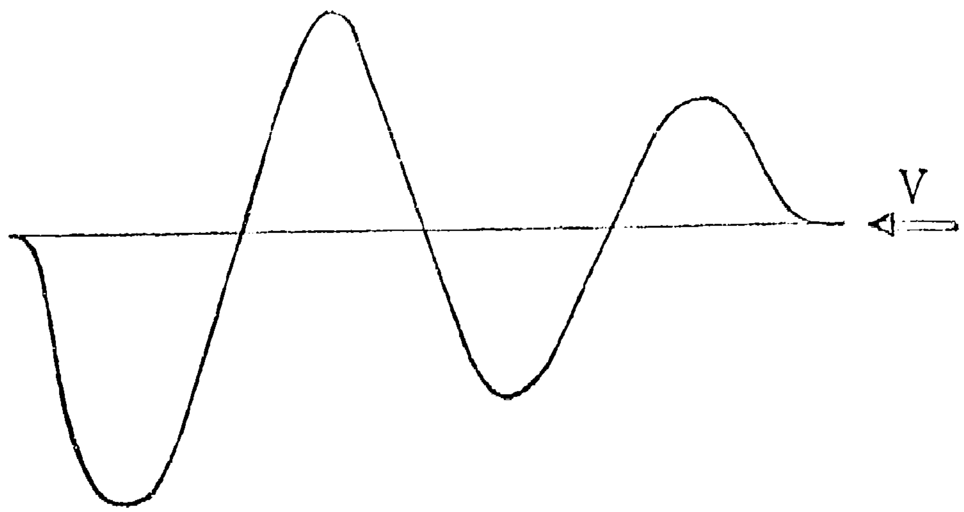

Figure 11 The fourth mode shape (real part) for the center line of panel corresponding to point B in Fig. 9

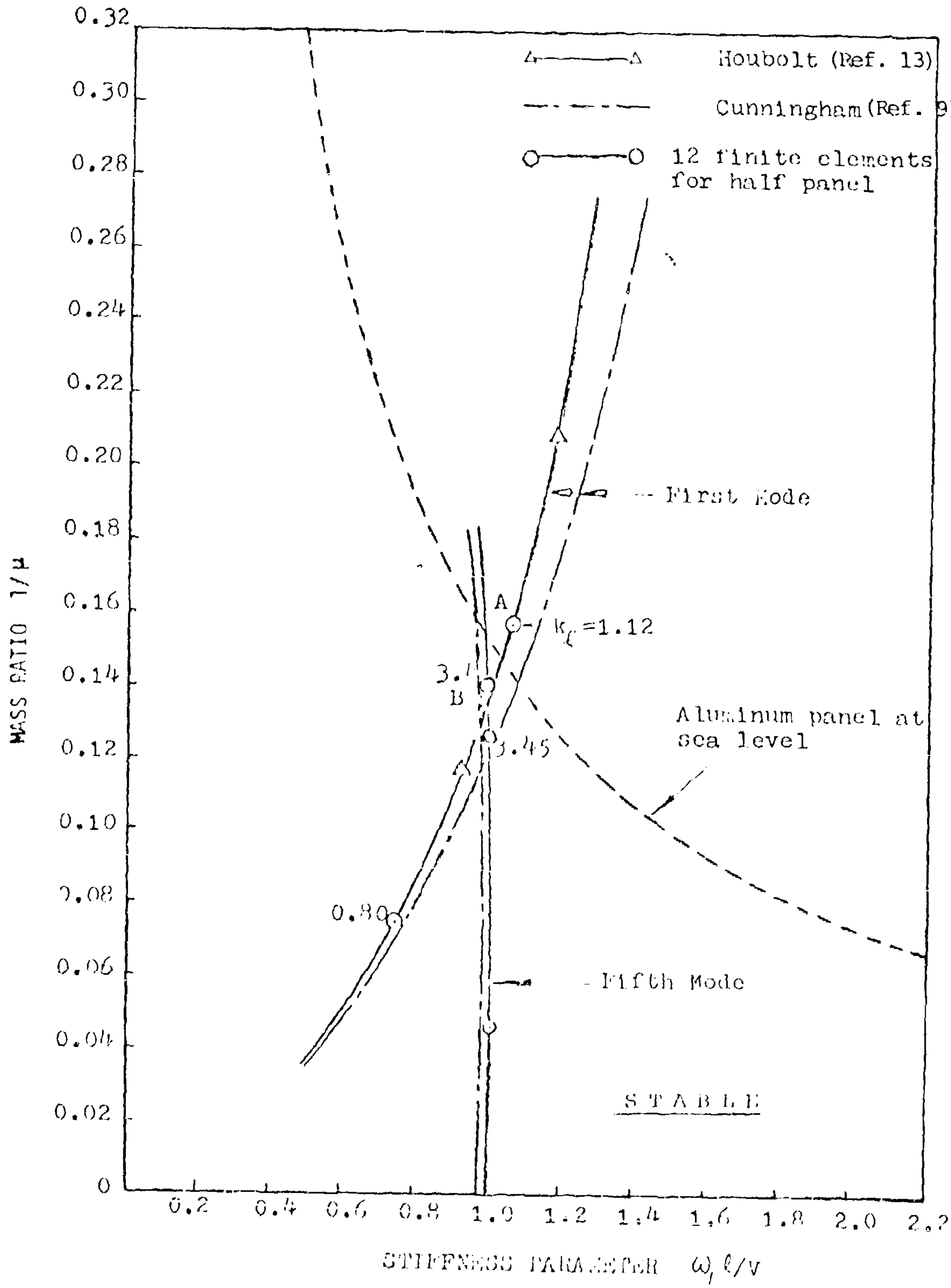

Figure 12 Flutter boundaries for clamped panel with $\ell/w = 2$ and $M = 1.3$

The first and third flutter mode shapes (real part) corresponding to points A and B in Fig. 12 are shown in Figs. 13 and 14, respectively. The difference between a symmetrical *in vacuo* first mode and the first flutter mode with front part blown flat is clearly shown in Fig. 13.

Fig. 15 shows that, for a very long panel with $\ell/w = 4$, the tenth mode flutter boundary dominates the lower mass ratio range while the first mode boundary dominates the upper mass ratio range. The discrepancy between the present solution and Cunningham's solution may be attributed to the same reasons as explained for Fig. 6. Houbolt's solution for first mode boundary is also shown.

The second and tenth flutter mode shapes (real part) corresponding to points A and B in Fig. 15 are plotted in Figs. 16 and 17, respectively.

Case 2 Clamped Panel with $\ell/w = 2$ at Various Mach Numbers

A clamped panel with $\ell/w = 2$ and with one surface exposed to air stream with various Mach numbers was studied. One of the main purposes was to establish a curve for the thickness ratios required to prevent flutter of panel at various air speeds and at sea level.

The first mode flutter boundaries for panel with $\ell/w = 2$ and M = 1.05, 1.1; 1.4, 1.5; 2.0, and 3.0 are shown in Figs. 18, 19, and 20, respectively. Corresponding to each curve, a dashed parabola is shown. Each parabola is plotted for the equation $xy = C$ or $(\rho\ell/\sigma h)(\omega_1 \ell/V) = C$. The constant C is dependent upon

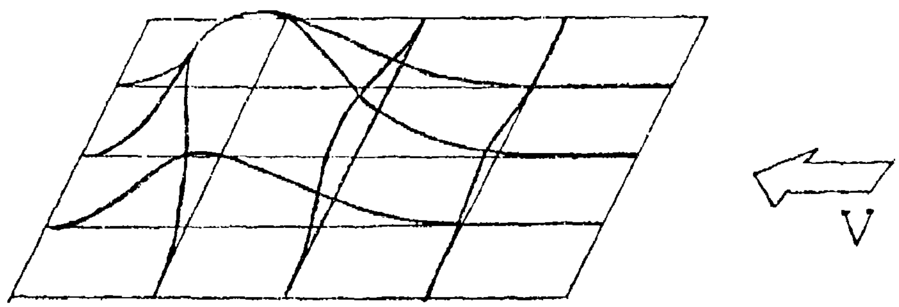

Figure 13 The first mode shape (real part) for panel corresponding to point A in Fig. 12.

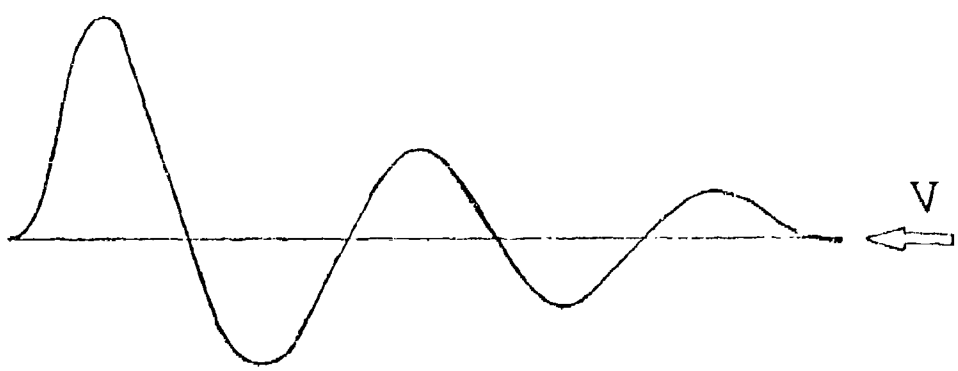

Figure 14 The fifth mode shape (real part) for the center line of panel corresponding to point B in Fig. 12.

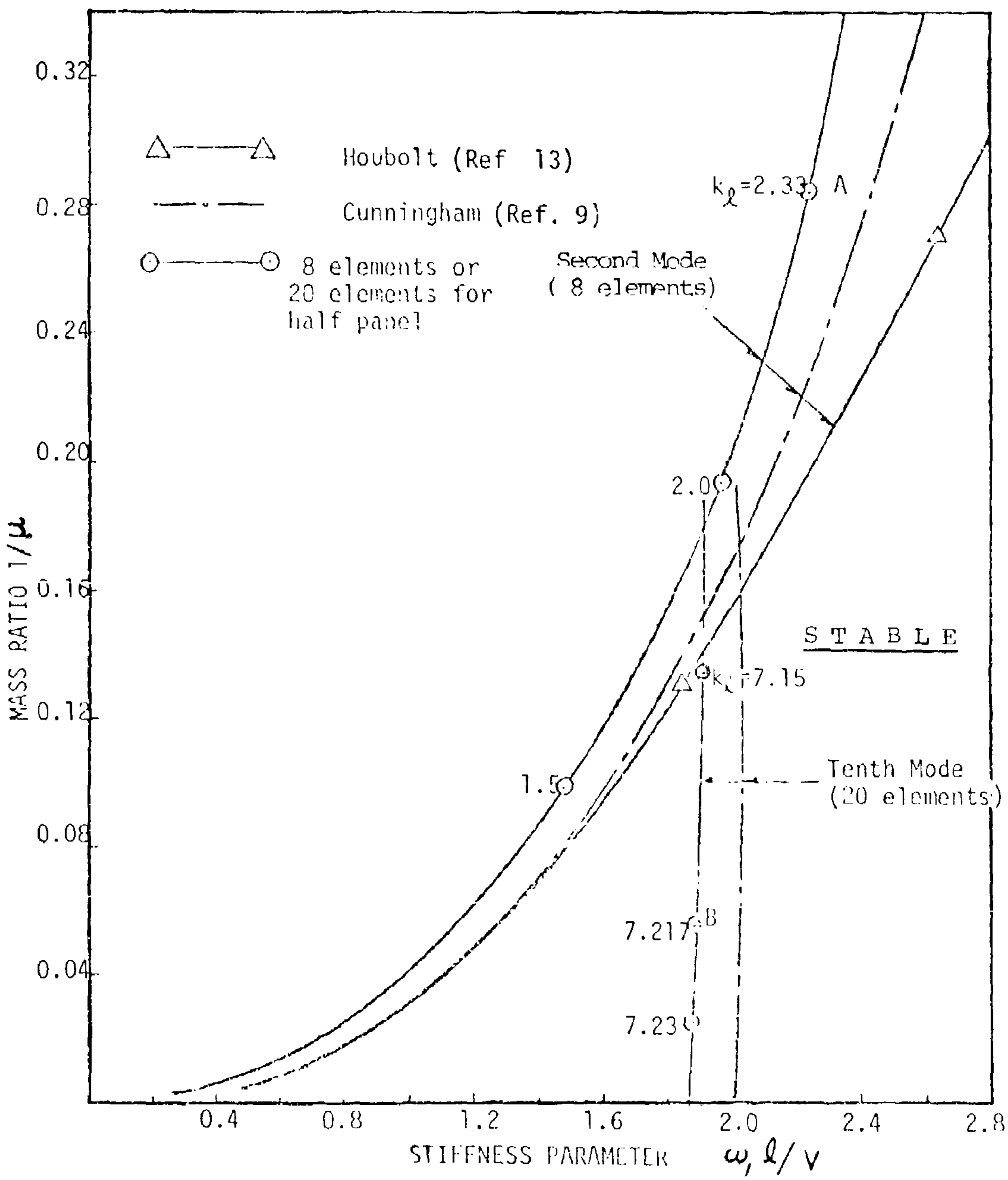

Figure 15 Flutter boundaries for clamped panel with $\ell/w = 4$ and $M = 1.3$

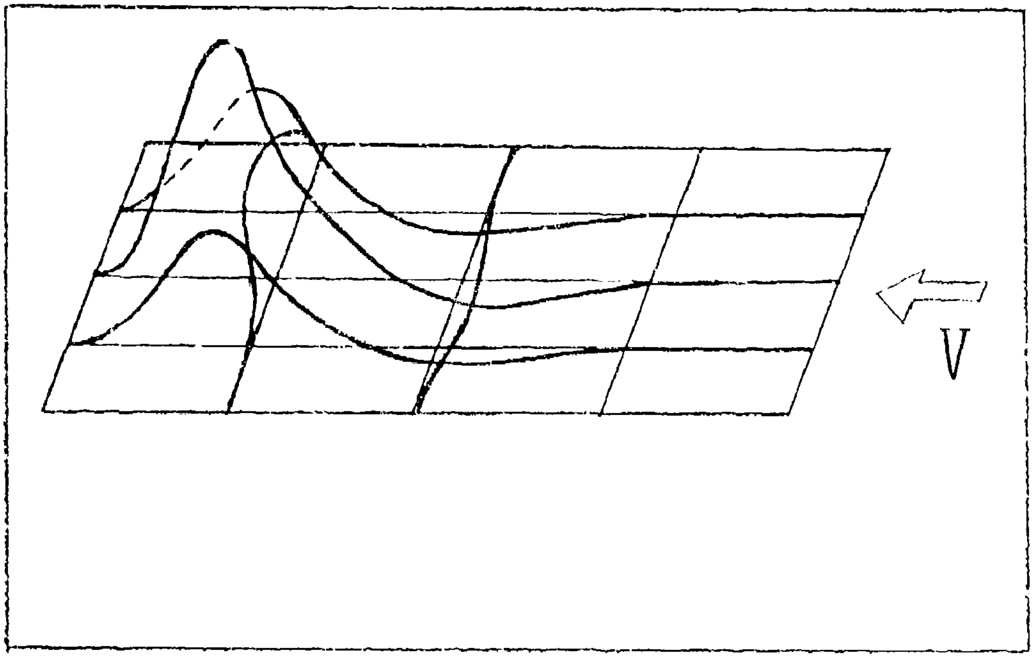

Figure 16 The second mode shape (real part) for panel corresponding to point A in Fig. 15.

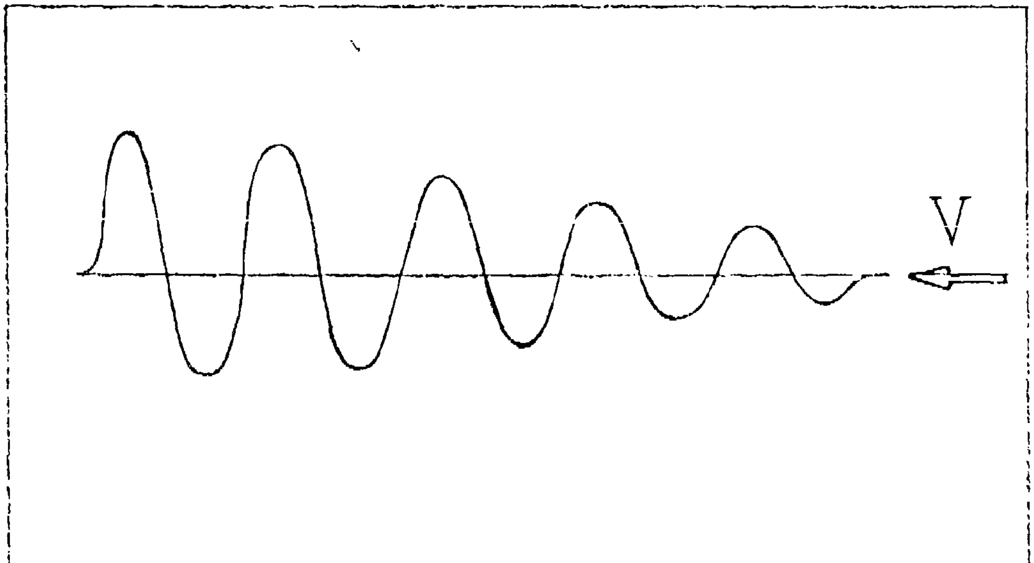

Figure 17 The tenth mode shape (real part) for the center line of panel corresponding to point B in Fig. 15.

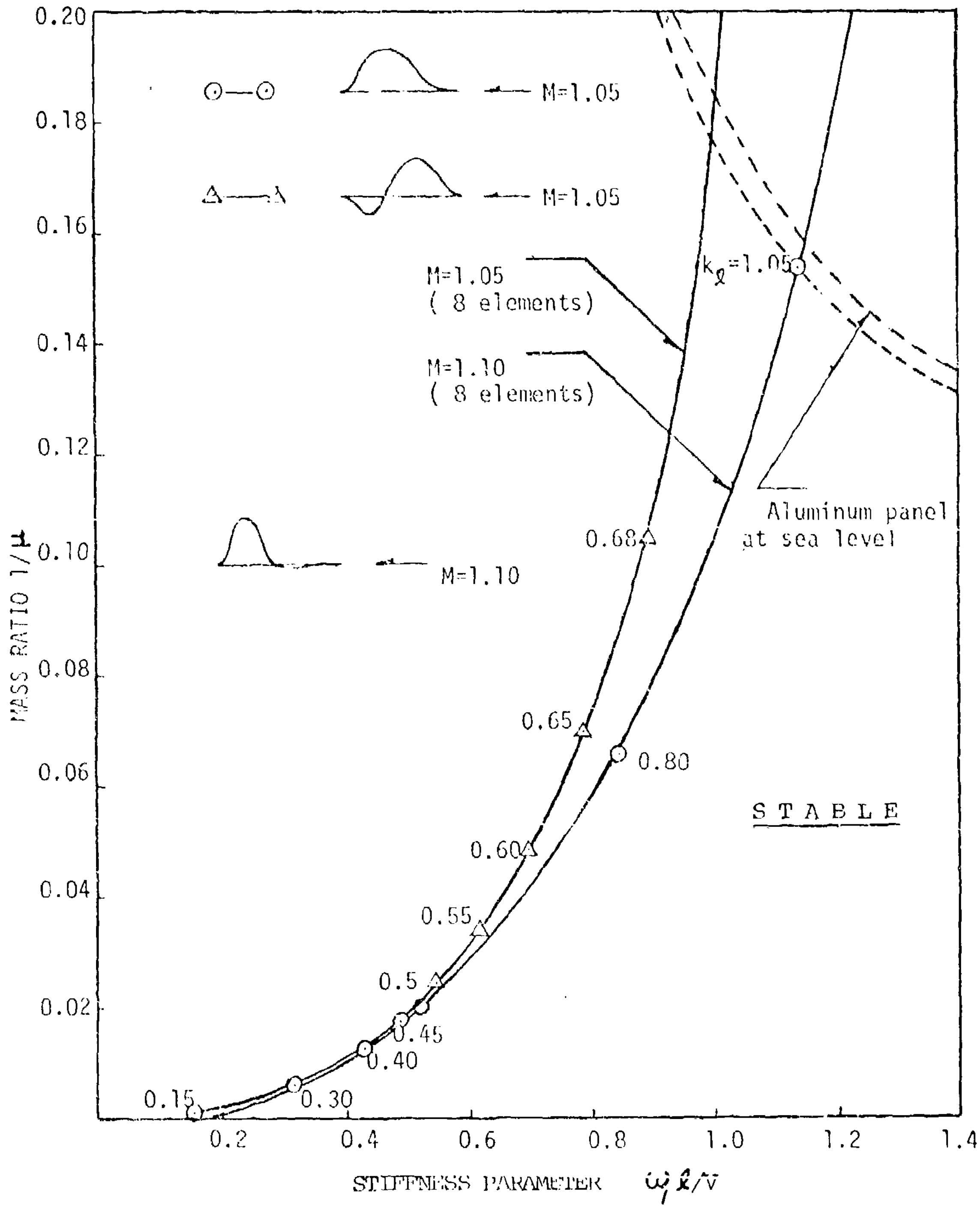

Figure 18 Flutter boundaries for clamped panel with $\ell/w = 2$ and $M = 1.05$, 1.10.

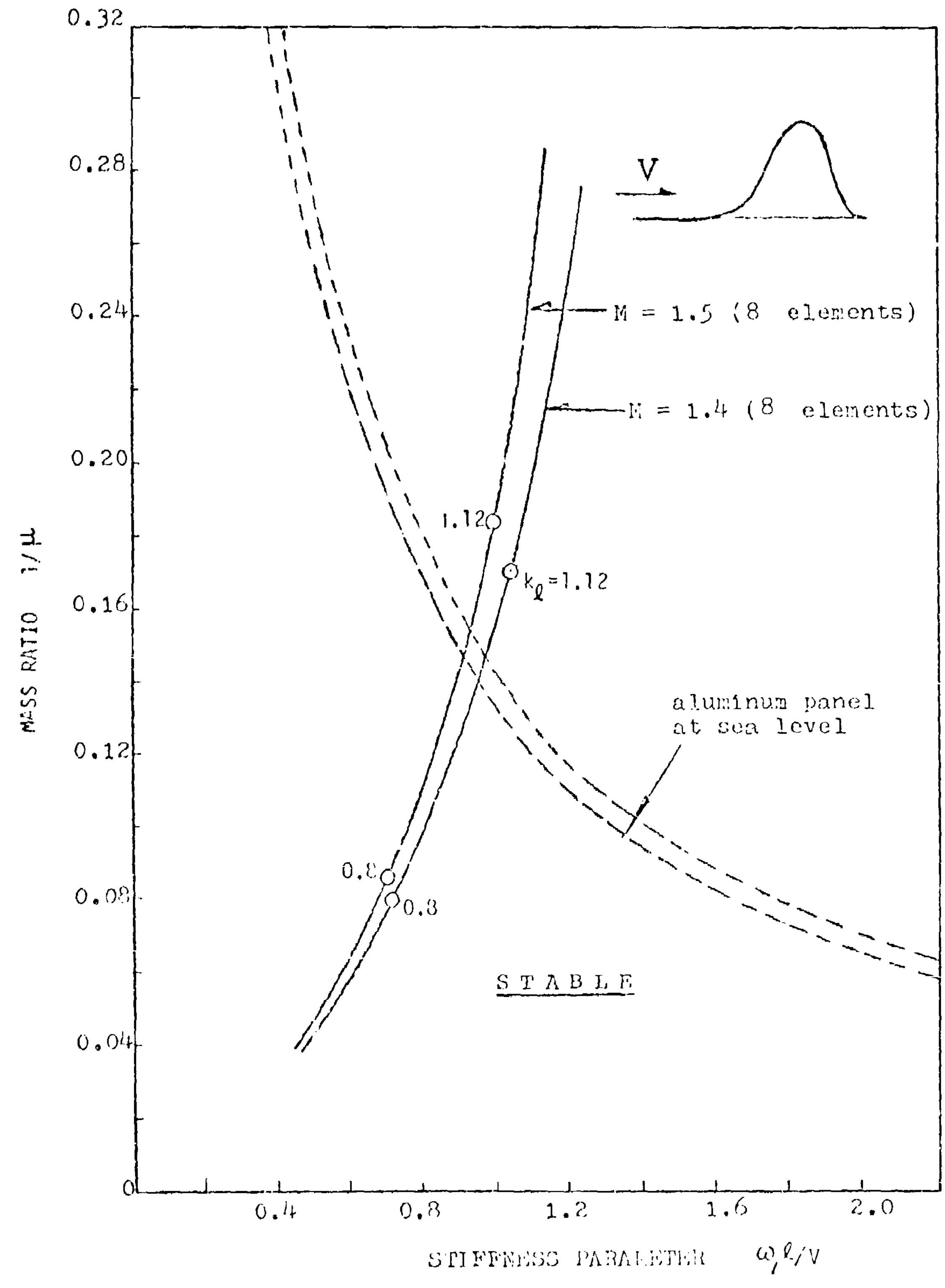

Figure 19 Flutter boundaries for clamped panel with $\ell/w = 2$ and M = 1.40, 1.50.

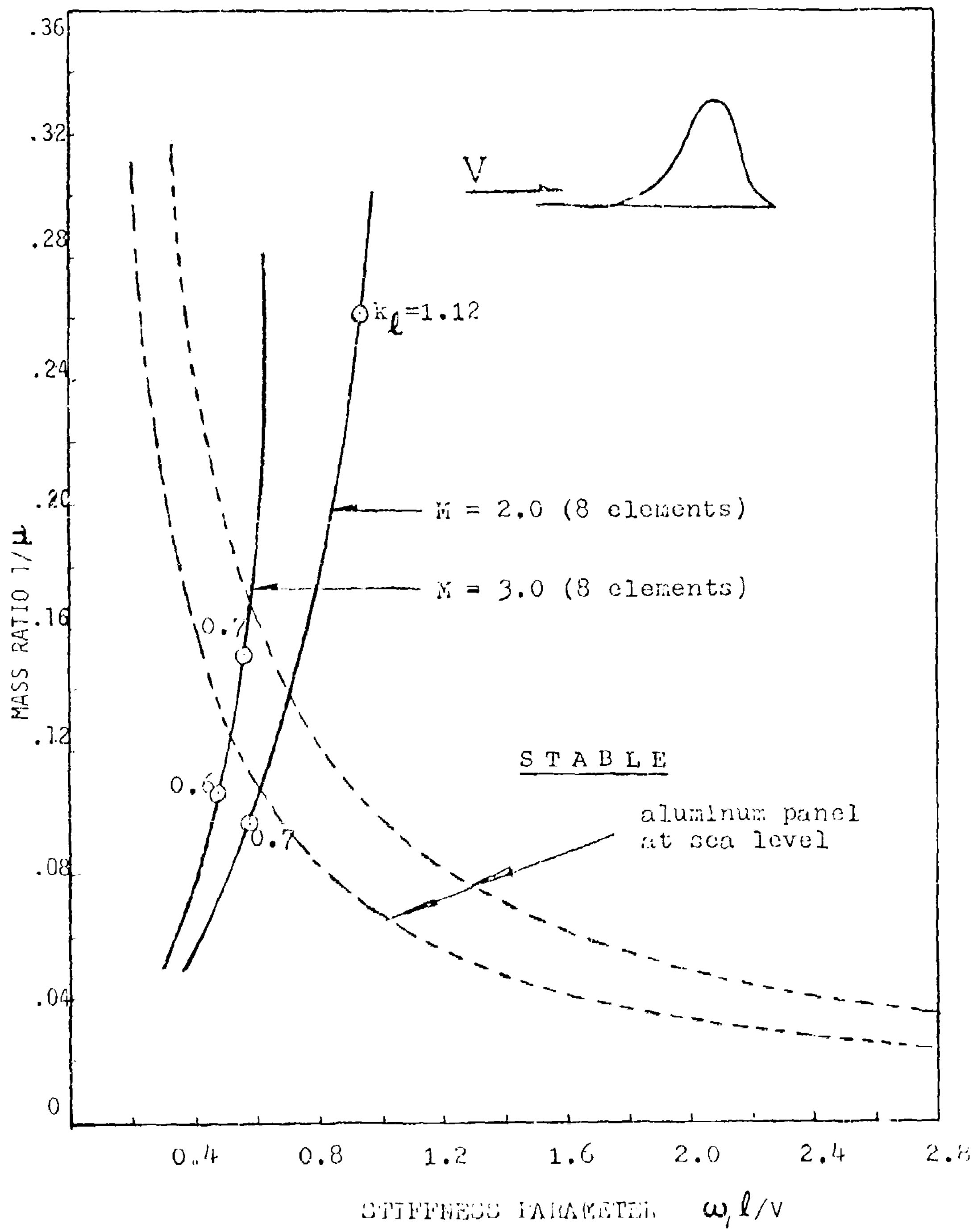

Figure 20 Flutter boundaries for clamped panel with $\ell/w = 2$ and $M = 2.0$ and 3.0.

the densities of the aluminum and the air at sea level, the dimensions of the panel, the air speed, and the bending rigidity of the panel. The intersecting point between a pair of dashed and solid curves gives the thickness ratio h/ℓ required to prevent flutter of the aluminum panel at sea level. For all Mach numbers considered here, the first mode flutter boundaries are critical for the dashed curves for the sea level altitude.

The results are shown in Fig. 21. The present results are slightly on the unconservative side as compared to the results of Cunningham.

Case 3 Pinned-Edge Panels with Various Chord-Span Ratios at M = 1.3

The panels with simply-supported edges and various chord length-span width ratios were studied. The flow speed considered was M = 1.3. The dominating flutter boundaries for panels with ℓ/w = 0.25, 0.5, 1.0, and 2.0 are shown in Figs. 22, 24, 26 and 28, respectively. They are all in good agreement with those found by Cunningham (Reference 9).

Fig. 22 shows that the first mode flutter boundary is the critical boundary for panels with ℓ/w = 0.25. The mode shape (real part) is shown in Fig. 23.

Fig. 24 shows that the second mode flutter boundary is the critical boundary for panels with ℓ/w = 0.5. The first and second flutter mode shapes (real part) are shown in Fig. 25.

Fig. 26 shows that the third mode flutter boundary is the critical boundary for panel with ℓ/w = 1.0. The first mode boundary found by Hedgepeth (Reference 14) using the piston theory is also shown in the figure. The corresponding first and third flutter mode shapes (real part) are shown in Fig. 27.

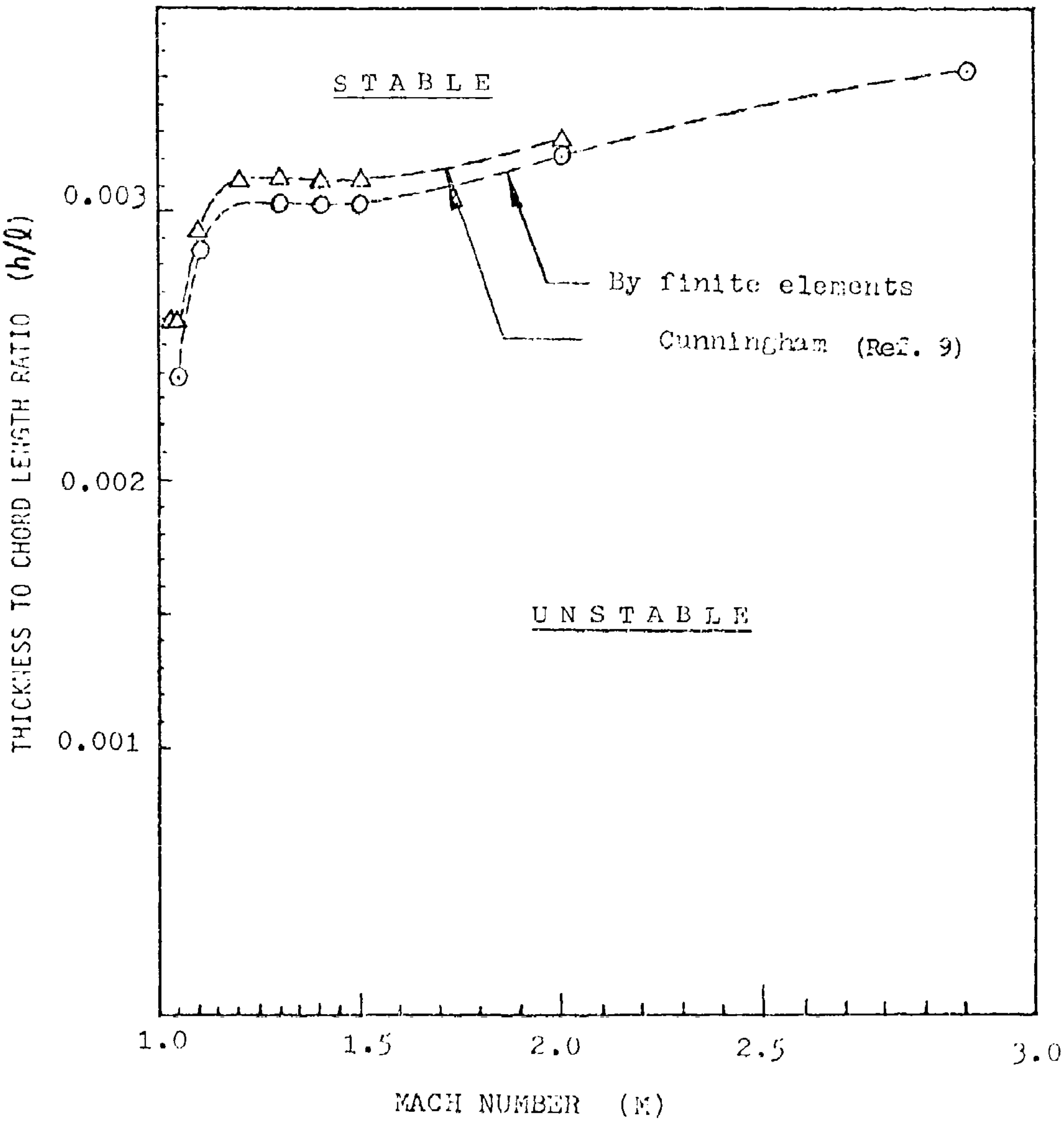

Figure 21 Thickness required to prevent flutter for clamped aluminum panel with $\ell/w = 2$ at sea level.

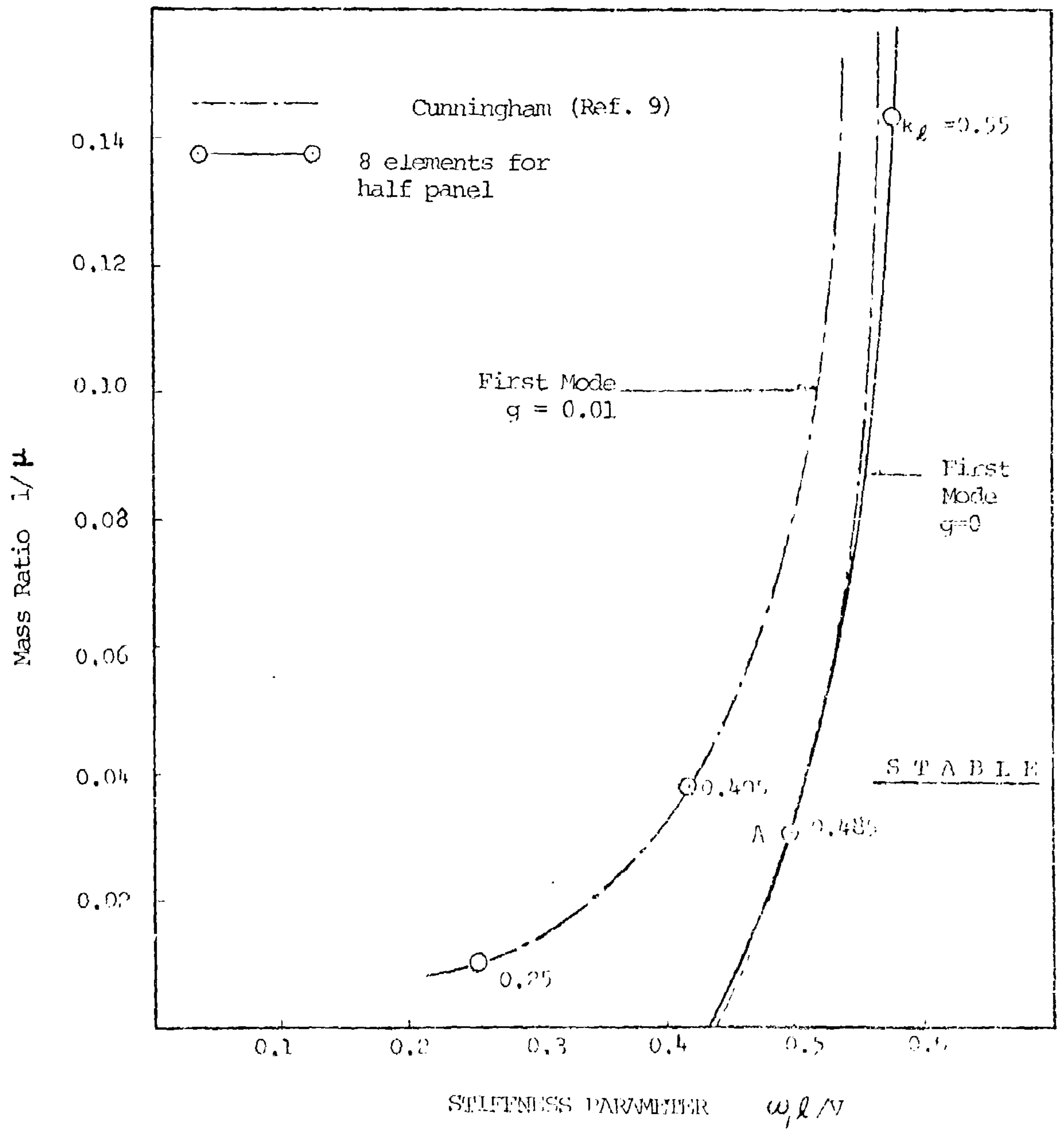

Figure 22 Flutter boundaries for pinned edge panel with $\ell/w = 1/4$ and $M = 1.3$.

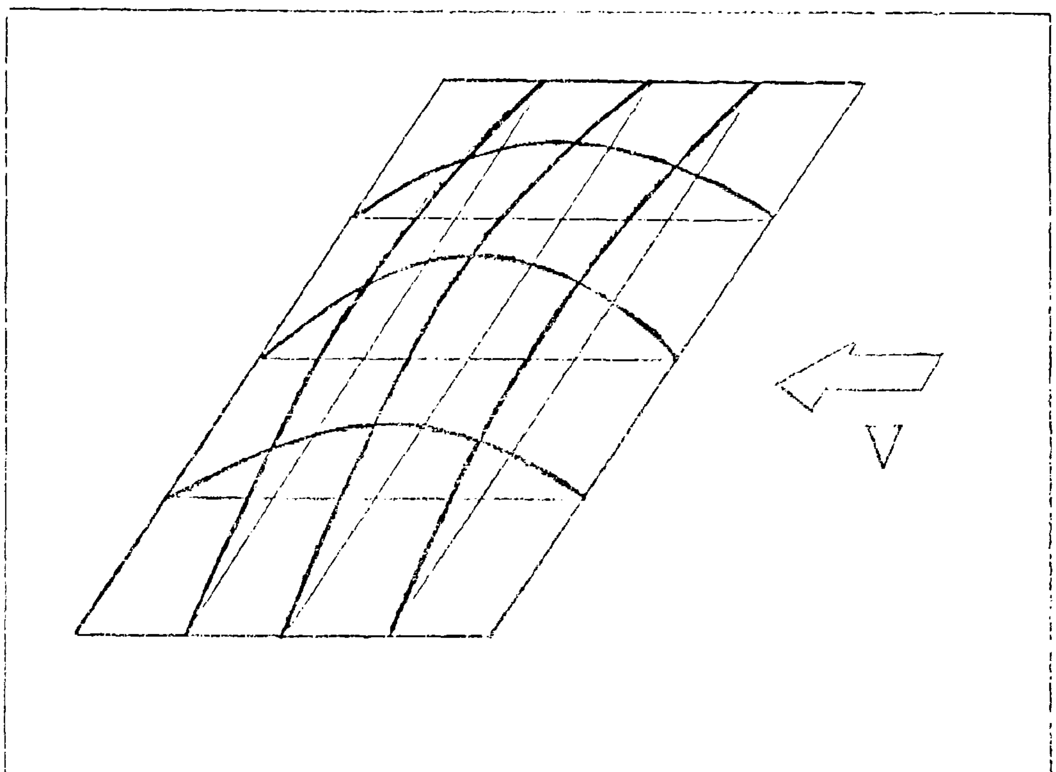

Figure 23 The First Mode Shape (Real Part) for Panel Corresponding
to Point A in Fig. 22.

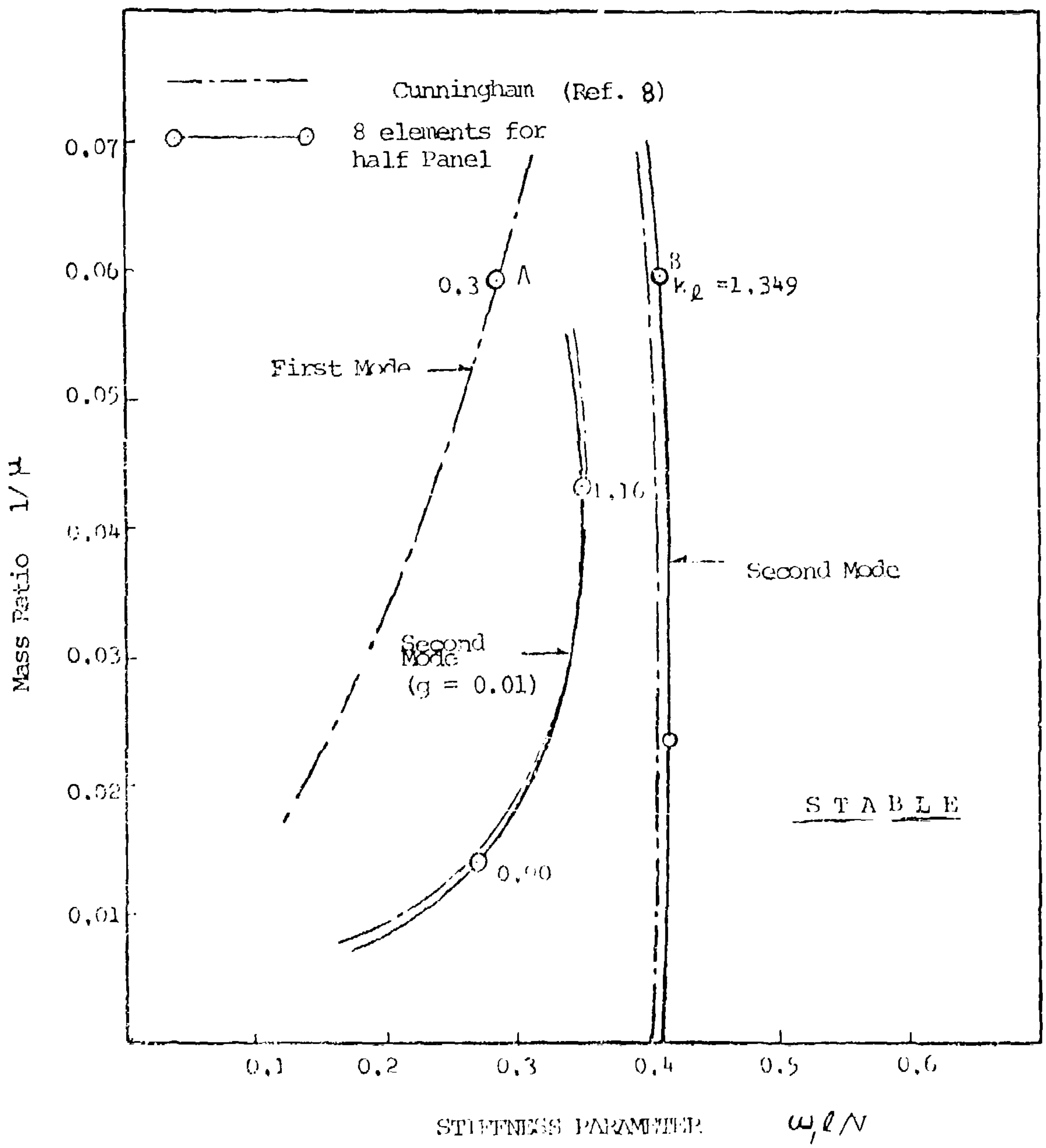

Figure 24 Flutter boundaries for pinned-edge panel with $\ell/w = 1/2$ and M = 1.3.

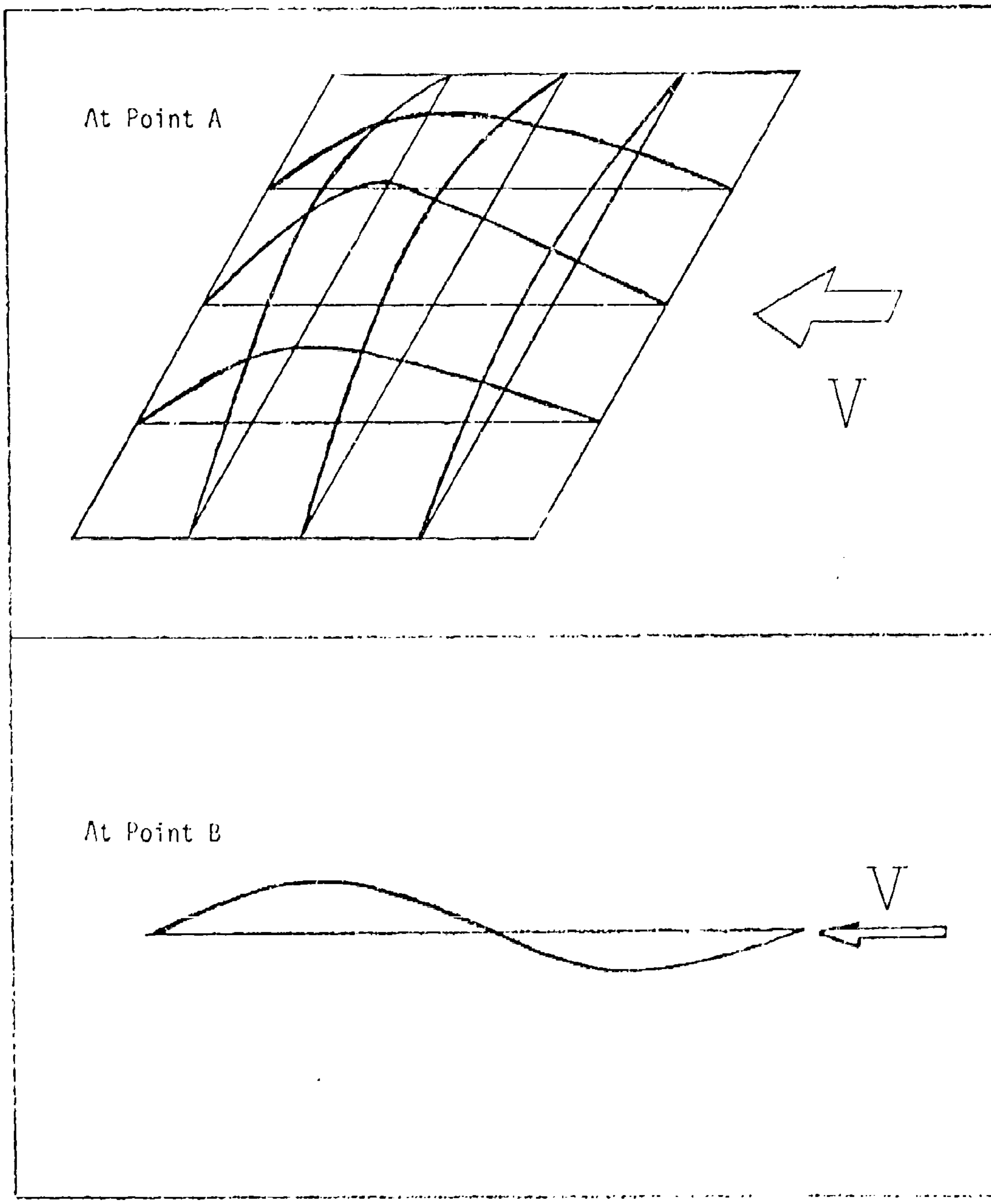

Figure 25 The First Mode Shape (Real Part) for Panel Corresponding to Point A in Fig. 24 and the Second Mode Shape (Real Part) for the Center Line of Panel Corresponding to Point B in Fig. 24.

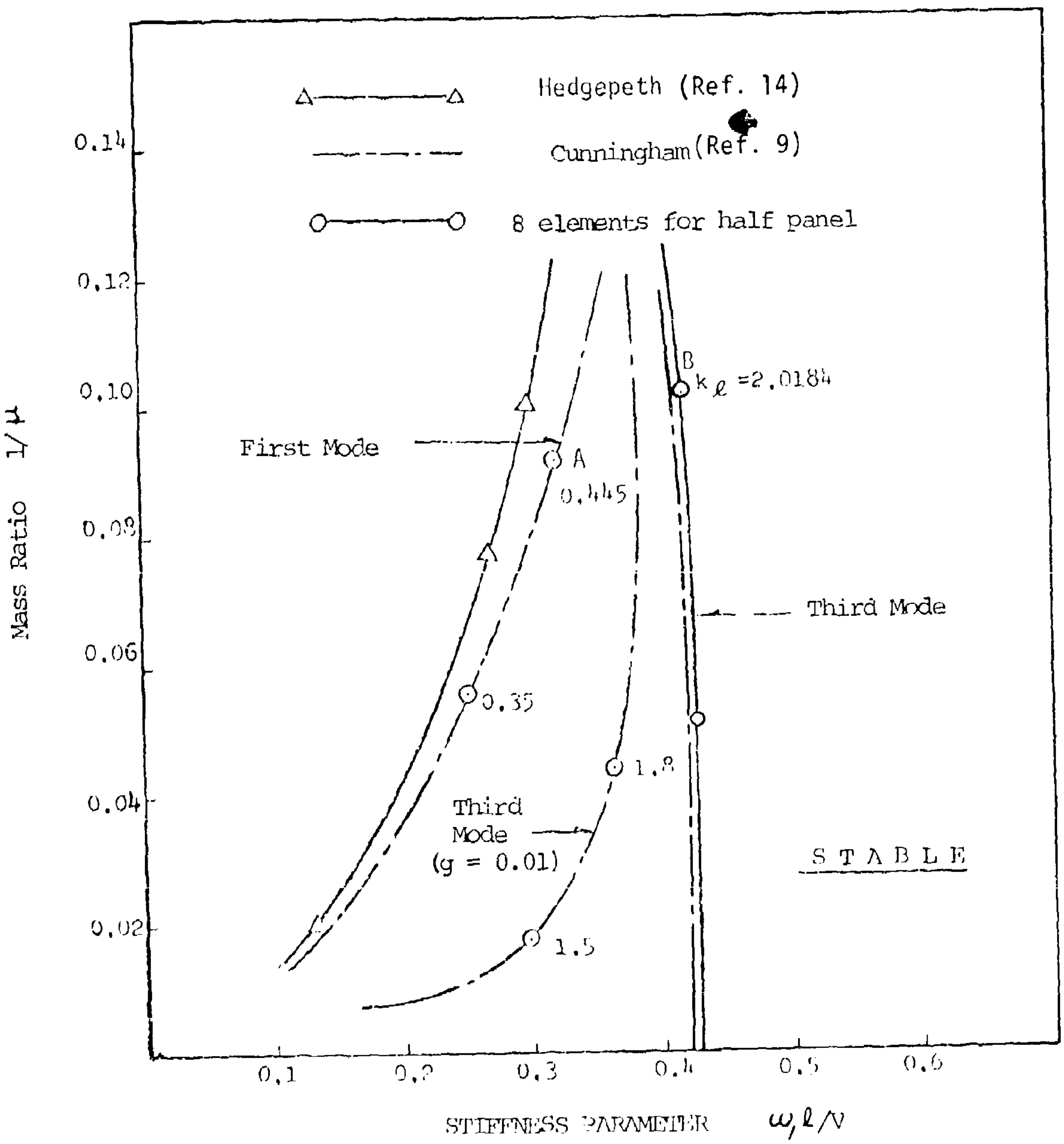

Figure 26 Flutter boundaries for pinned-edge panel with $\ell/w = 1$ and $M = 1.3$.

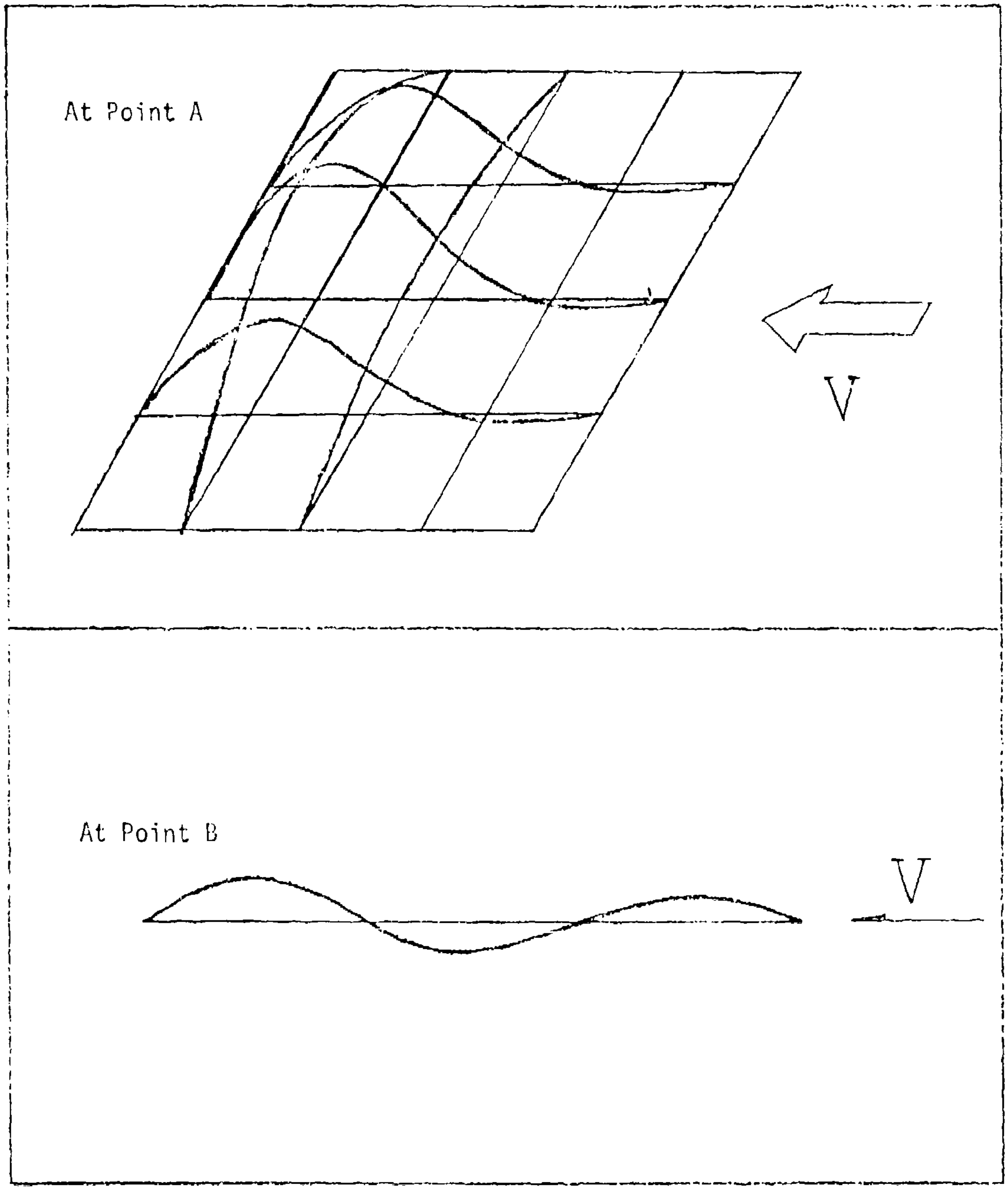

Figure 27 The First Mode Shape (Real Part) for Panel Corresponding to Point A in Fig. 26 and the Third Mode Shape (Real Part) for the Center Line of Panel Corresponding to Point B in Fig. 26.

Fig. 28 shows that the fifth mode flutter boundary is the critical boundary for panels with $\ell/w = 2.0$. The results by Hedgepeth and Cunningham are seen to be in good agreement with the present results. The corresponding first and fifth flutter mode shapes (real part) are shown in Fig. 29.

Case 4 Clamped Square Panels with Various Tension Parameters and Mach Numbers

One of the advantages of the finite element method is that the effect of in-plane forces can be included in a direct and accurate fashion. To demonstrate this, a square clamped panel was chosen and four different tension parameters F = 0.01, 0.1, 0.5, and 1 were considered. The flutter boundaries were obtained for various Mach numbers.

Fig. 30 shows the dominating first mode flutter boundaries and the hyperbola for the square, aluminum panel at 25,000 feet above sea level and at M = 1.1. Four values of tension parameters were included.

The mode shapes (real part) corresponding to points A (F = 0.01) and point B (F = 0.1) of the flutter boundaries in Fig. 30 are plotted in Figs. 31 and 32. The mode shapes for the case F = 0.5 and 1.0 are similar to those shown in Figs. 31 and 32. They are thus not shown here.

Fig. 33 shows the first and the third mode flutter boundaries for M = 1.2 and various tension parameters. For aluminum panels at 25,000 feet above sea level (dashed parabola), the third mode boundaries are the critical flutter boundaries. The first flutter mode shapes (real part) corresponding to points A and B in Fig. 33 are presented in Figs. 34 and 35, respectively.

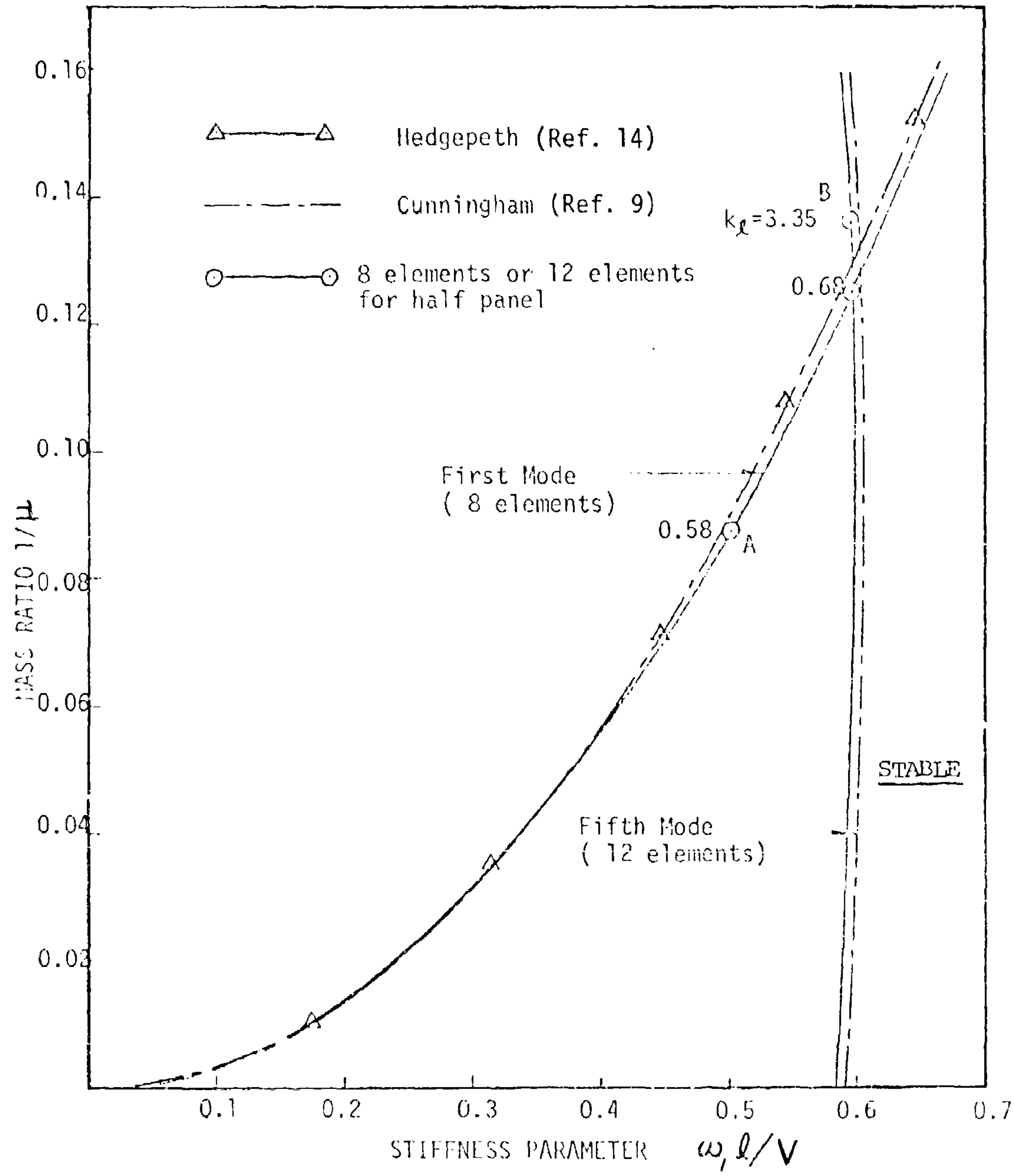

Figure 28 Flutter boundaries for pinned-edge panel with $\ell/w = 2$ and $M = 1.3$.

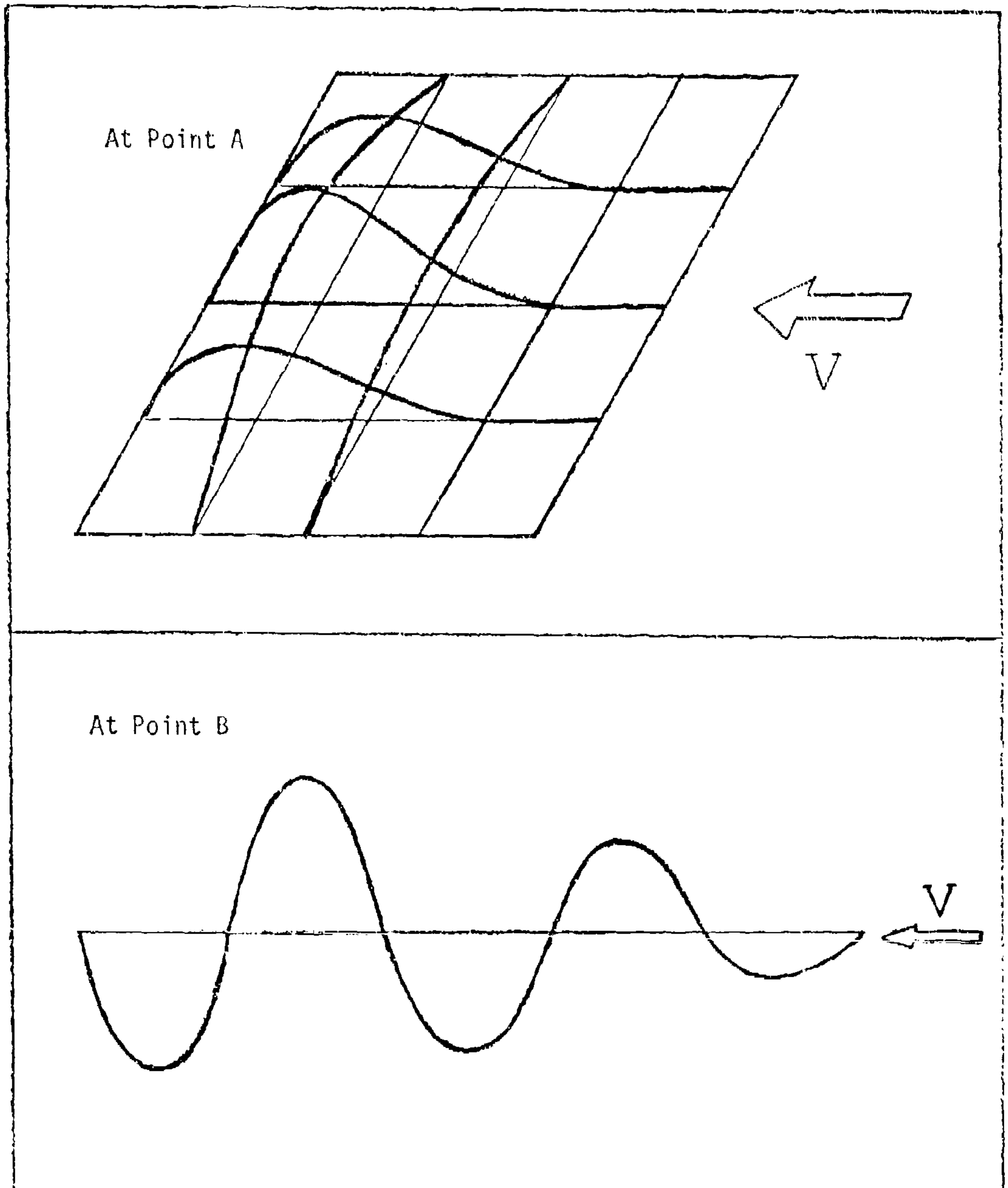

Figure 29 The First Mode Shape (Real Part) for Panel Corresponding to Point A in Fig. 28 and the Fifth Mode Shape (Real Part) for the Center Line of Panel Corresponding to Point B in Fig. 28.

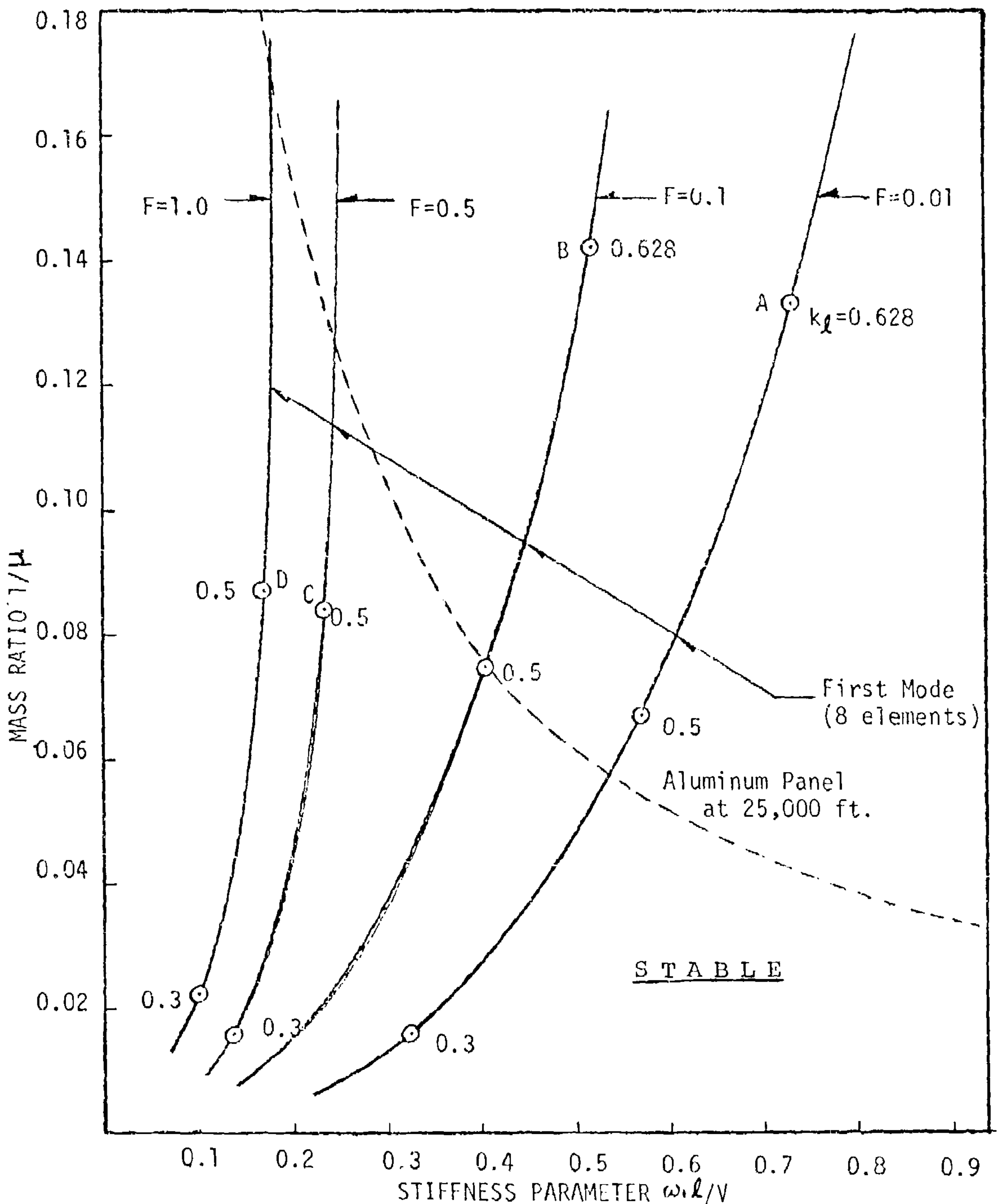

Figure 30. Flutter boundaries for clamped panels of ℓ/w =1.0 with M= 1.1 and various tension parameters F.

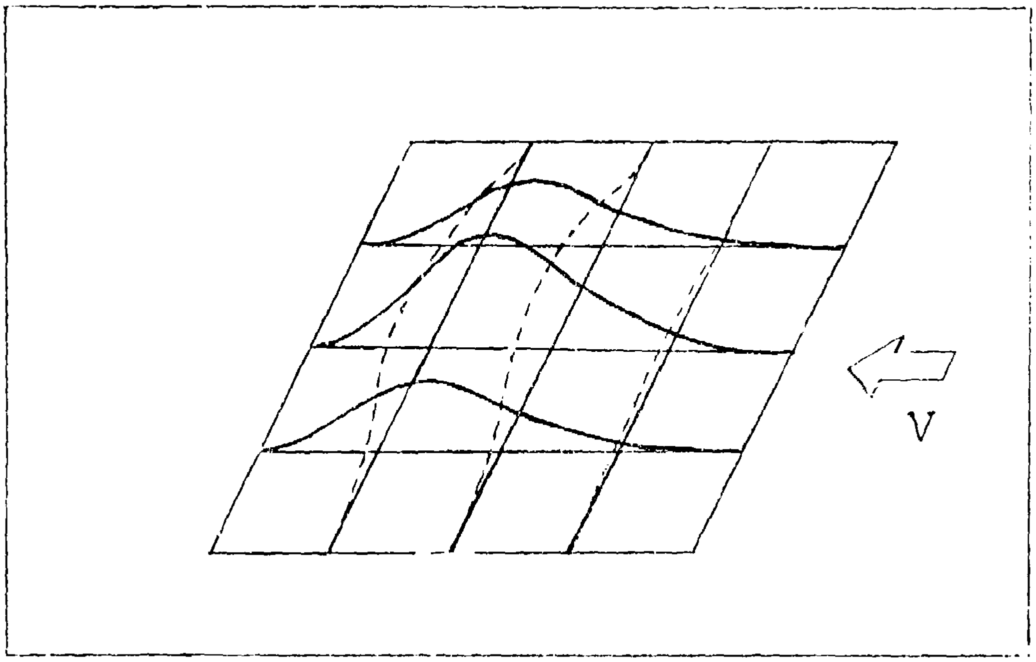

Figure 31 The First Mode Shape (Real Part) for Panel Corresponding to Point A in Fig. 30.

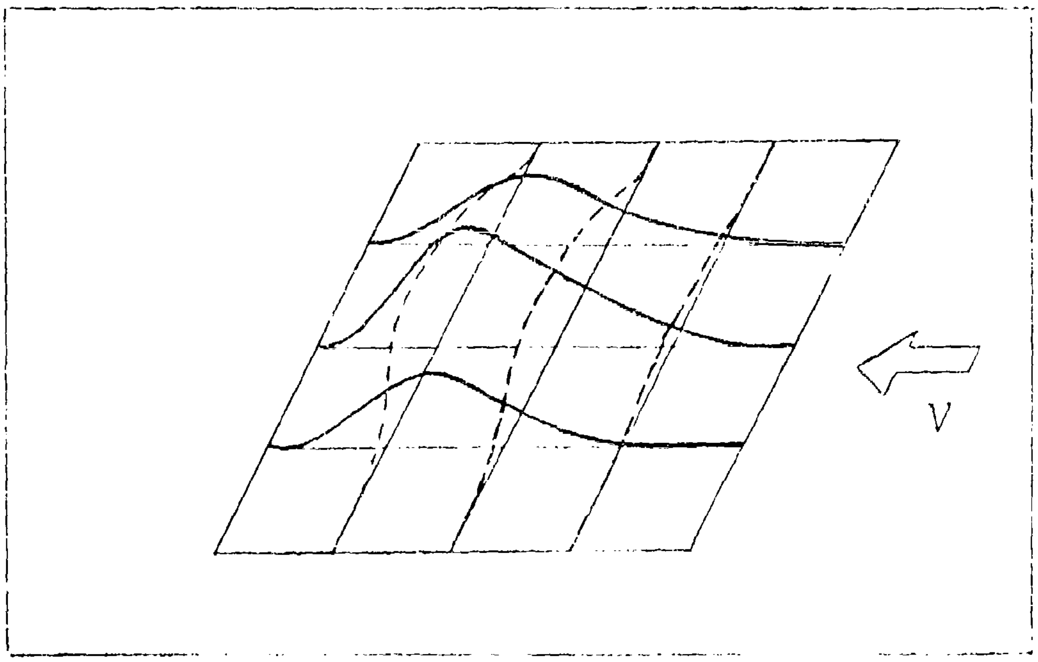

Figure 32 The First Mode Shape(Real Part) for Panel Corresponding to Point B in Fig. 30.

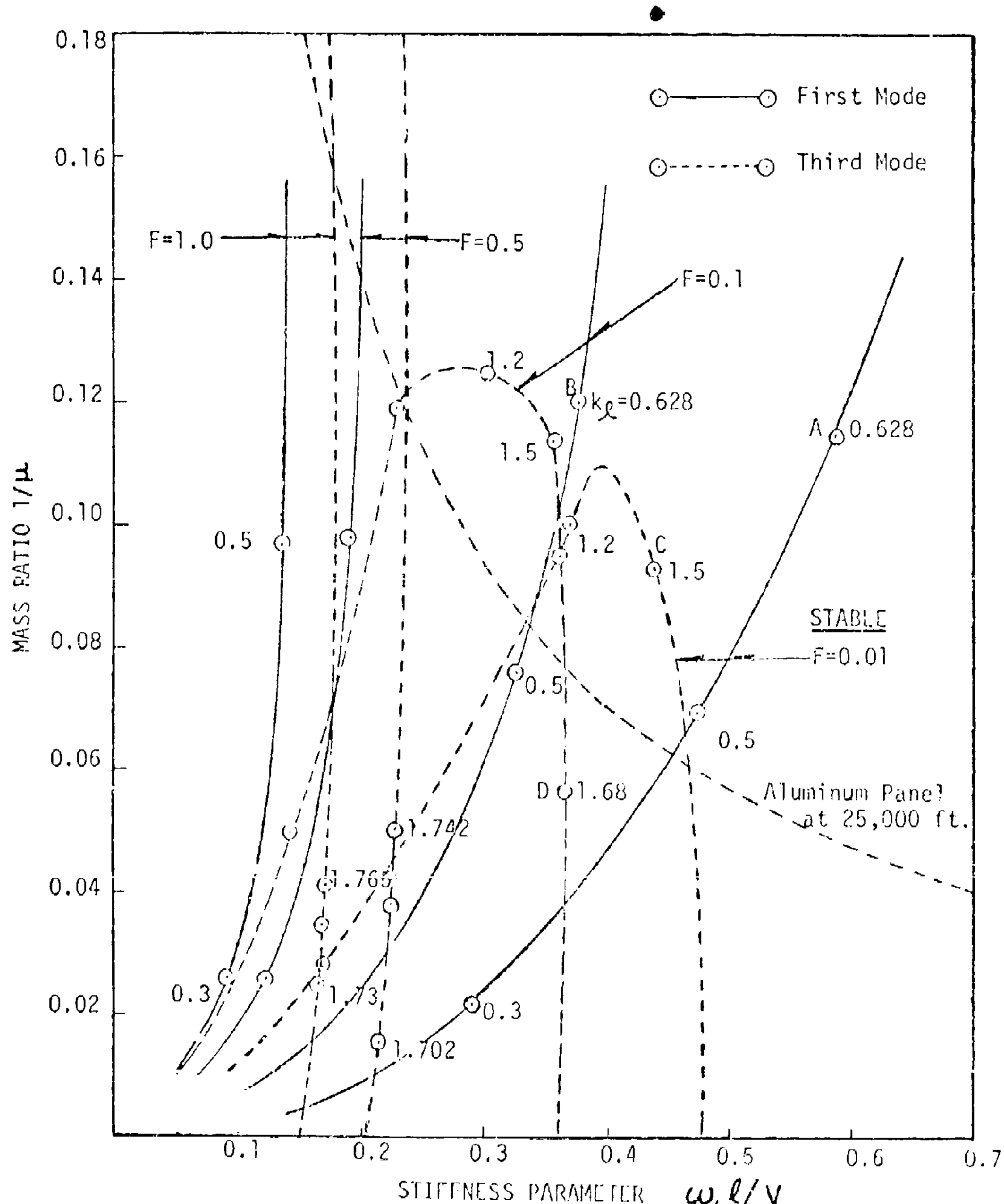

Figure 33 Flutter boundaries for clamped panels of ℓ/w=1.0 with M=1.2 and various tension parameters F

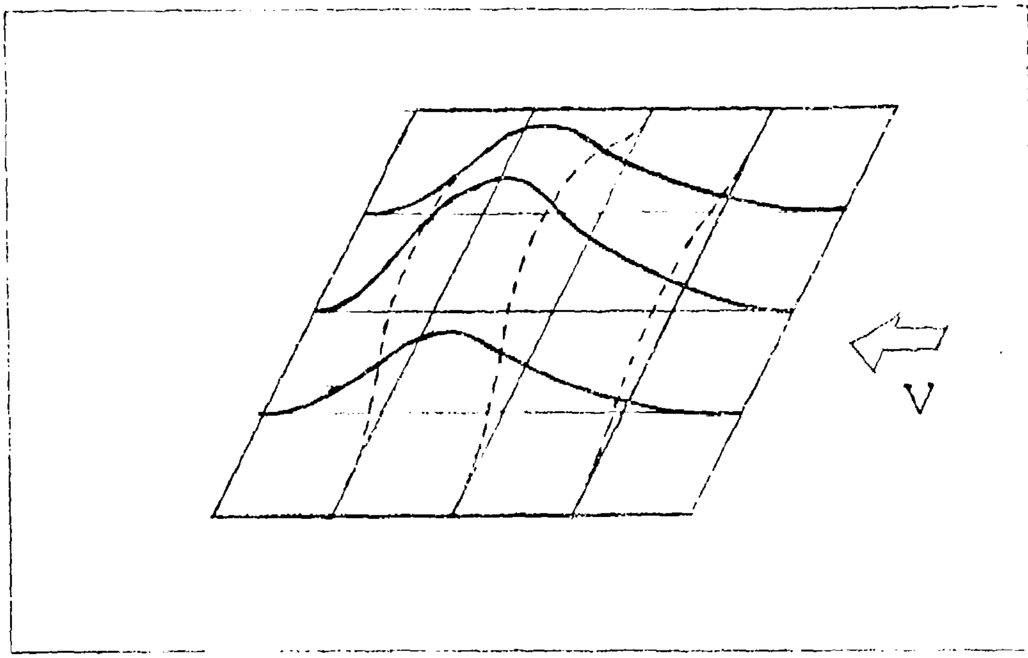

Figure 34 The First Mode Shape(Real Part) for Panel Corresponding to Point A in Fig. 33.

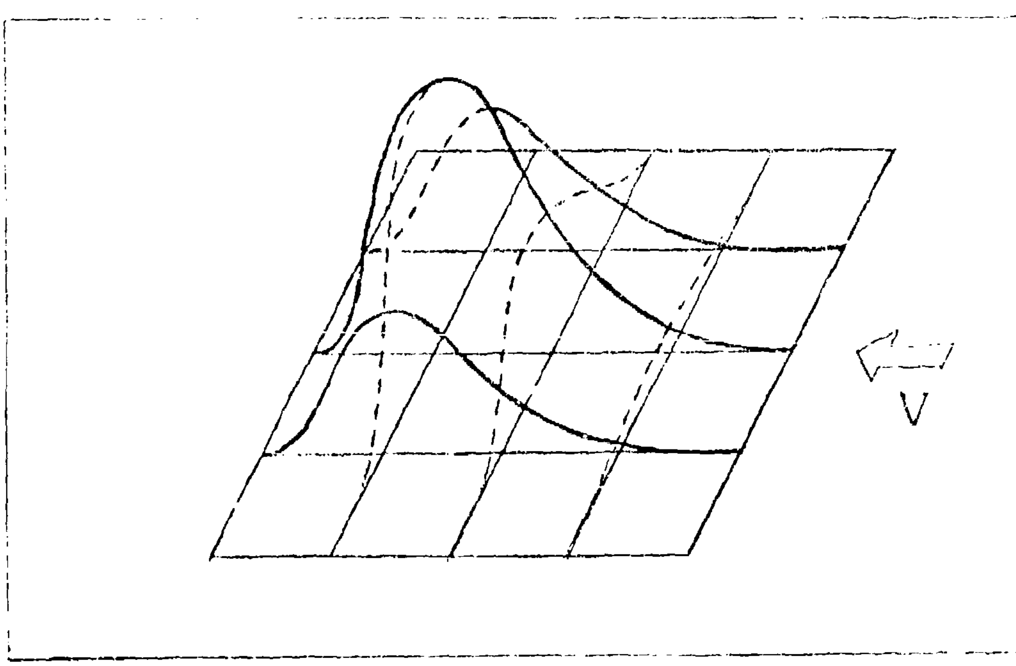

Figure 35 The First Mode Shape (Real Part) for Panel Corresponding to Point B in Fig. 33.

The third flutter mode shapes (real part) for the center chord lines corresponding to points C, D, E, and F are shown in Fig. 36.

Fig. 37 shows the first mode flutter boundaries for M = 1.3 and the third mode flutter boundaries for M = 1.3, 1.32, 1.35 for various values of tension. The flutter boundaries are dominated by the third mode. Since the flutter mode shapes are similar to those shown in the previous figures, they are not presented here.

Fig. 38 shows the flutter boundaries for M = 1.4, 1.45, 1.48 and various tension parameters. The third mode flutter boundaries shift to the right as the Mach number increases. It is interesting to see that the top portions of the third mode flutter boundaries begin to bend down to the left as the Mach number increases.

Fig. 39 shows that for M = 1.5 and various values of tension, the third mode flutter boundaries continue to bend down rapidly with a slight increase in Mach number.

Figs. 40 and 41 show that for M = 1.52 and 1.54 and various values of tension, the third mode flutter boundaries bend down substantially to be small loops. They only dominate the lower range of the mass ratio.

Fig 42 shows that for M = 1.6, all the third mode flutter boundaries disappear and the first mode flutter boundaries once again become the critical boundaries. Such a phenomenon is also the case for M = 2.0 as shown in Fig. 43.

Also shown in Figs. 37-43 are the dashed parabolas for an aluminum panel at 25,000 feet above sea level.

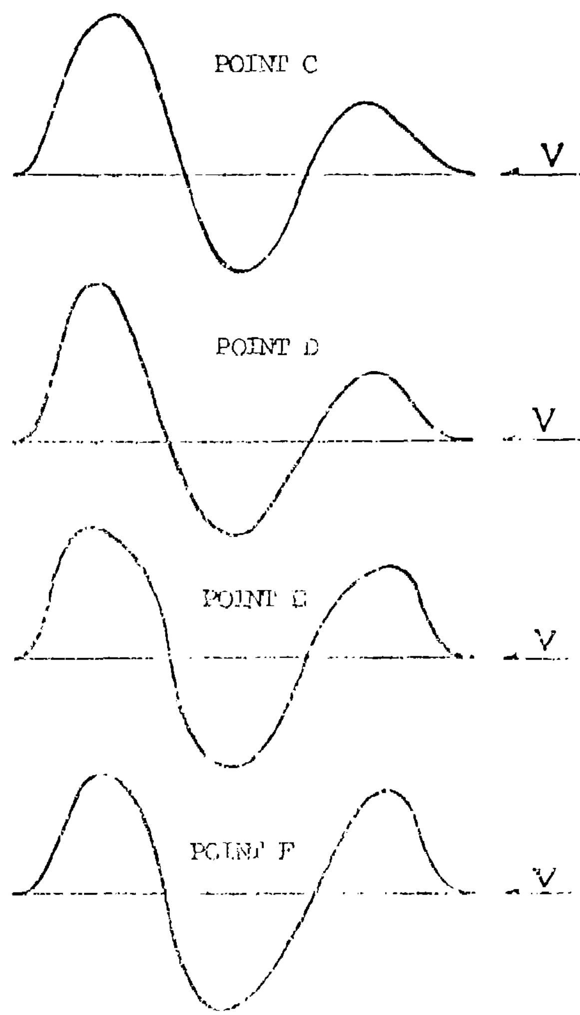

Figure 36 The Third Mode Shape (Real Part) for the Center Line of Panel with various tension parameter Corresponding to Point C, D, E, and F respectively in Fig. 35.

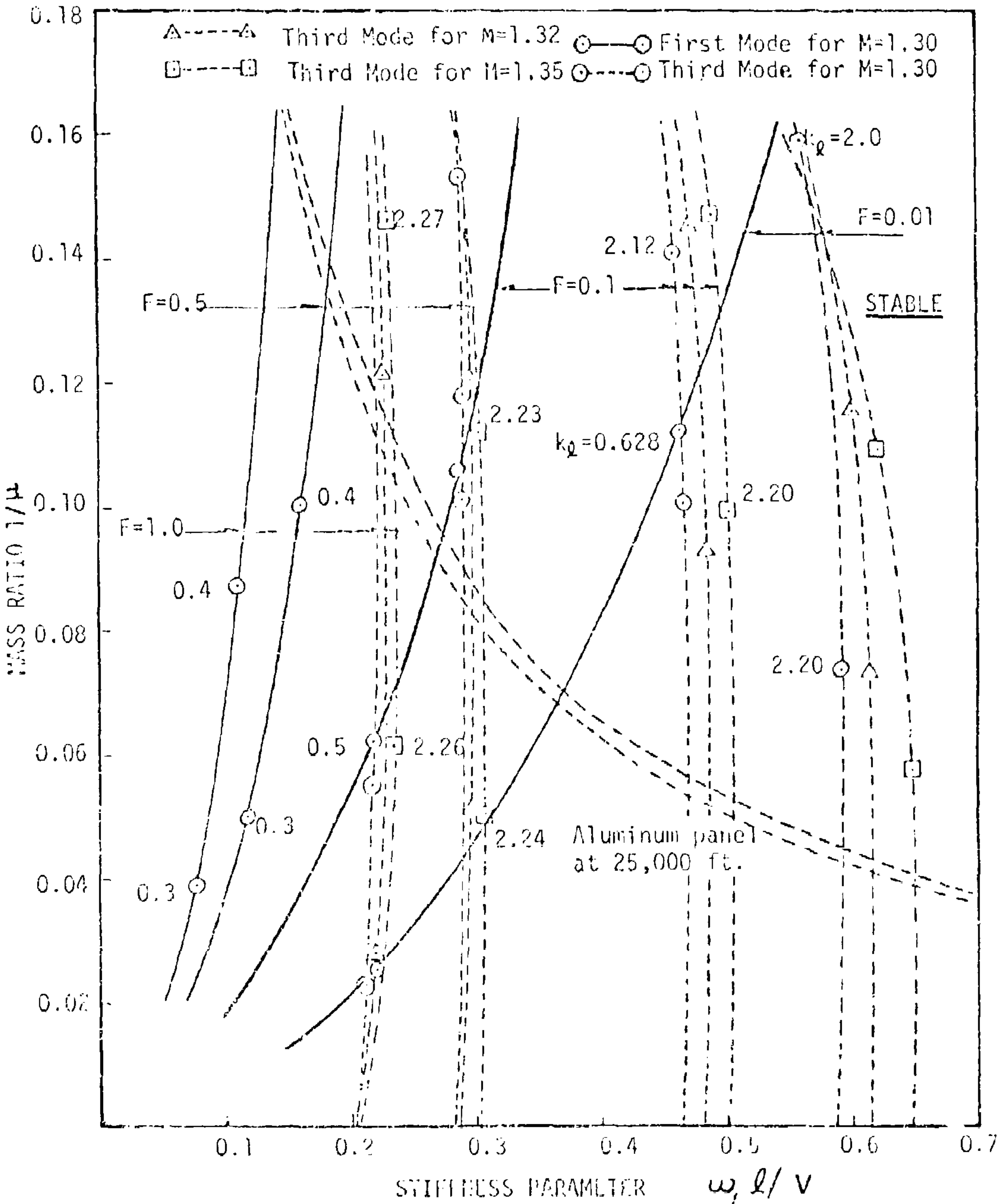

Figure 37 Flutter boundaries for clamped panels of $\ell/w=1.0$ with M 1.3, M=1.32, M=1.35 and various values of tension parameters F.

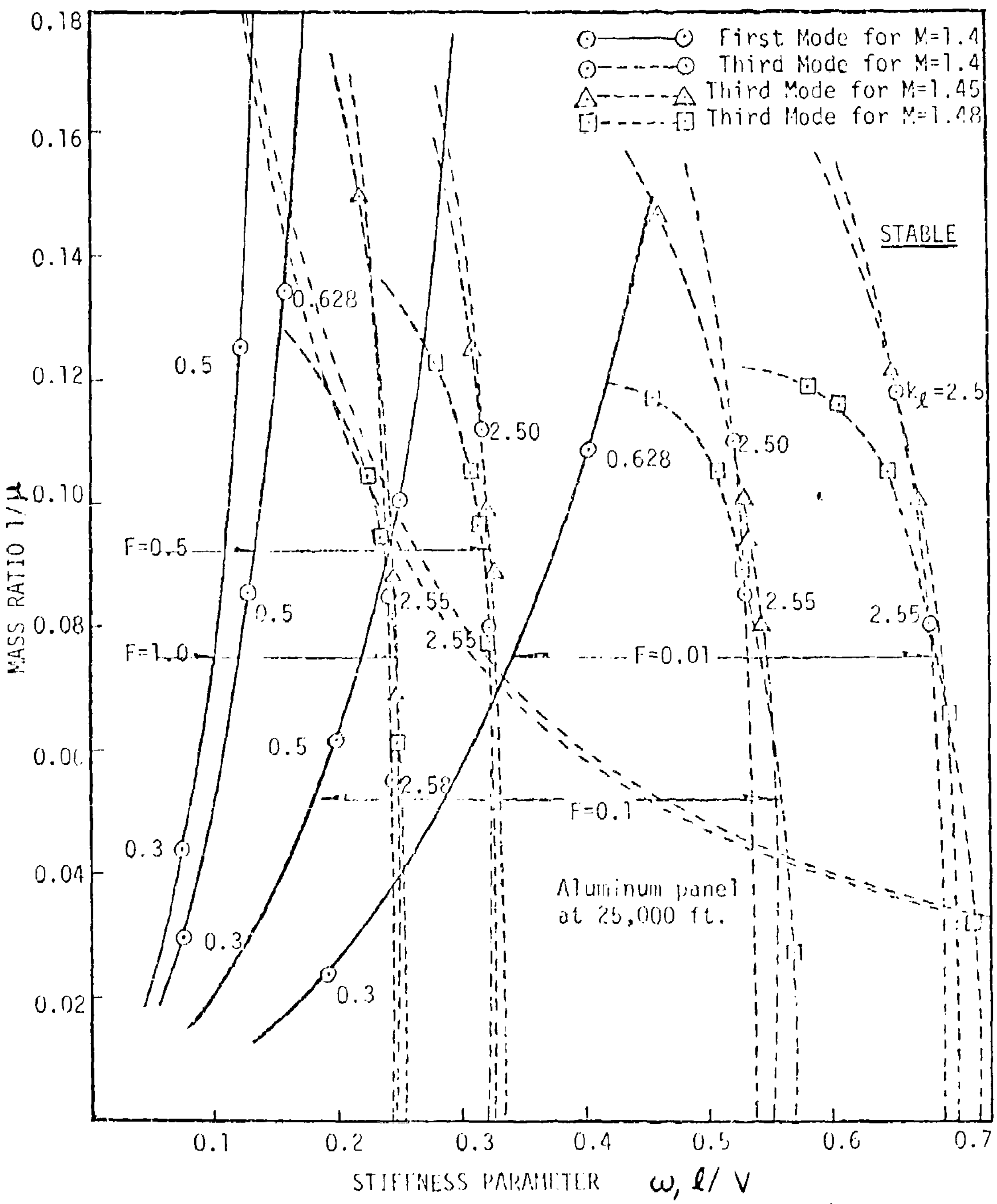

Figure 38 Flutter boundaries for clamped panels with $\ell/w=1.0$ with M=1.4, M=1.45, M=1.48 and various values of tension parameters F.

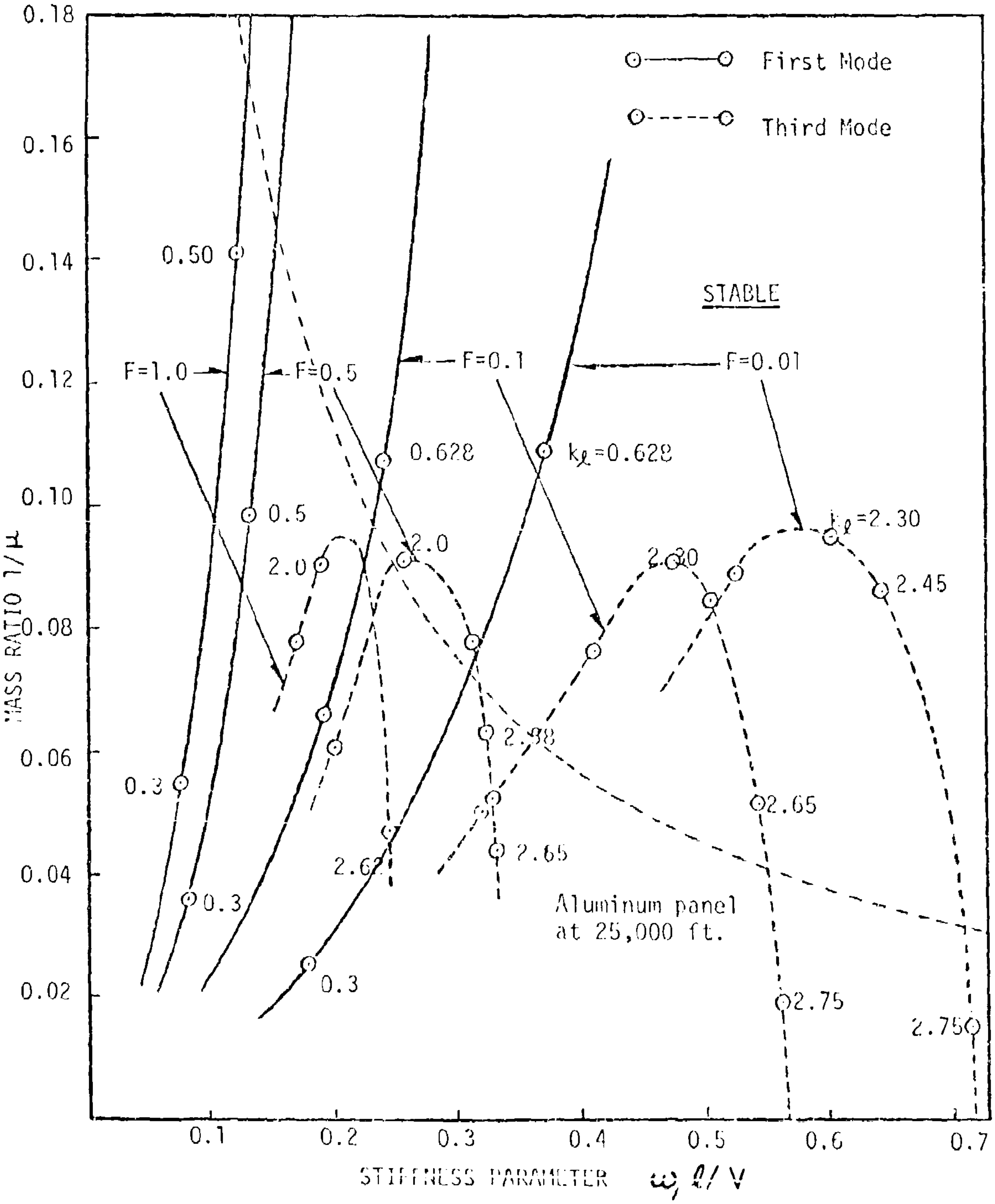

Figure 39 Flutter boundaries for clamped panels of ℓ/w 1.0 with M=1.5 and various values of tension parameters F.

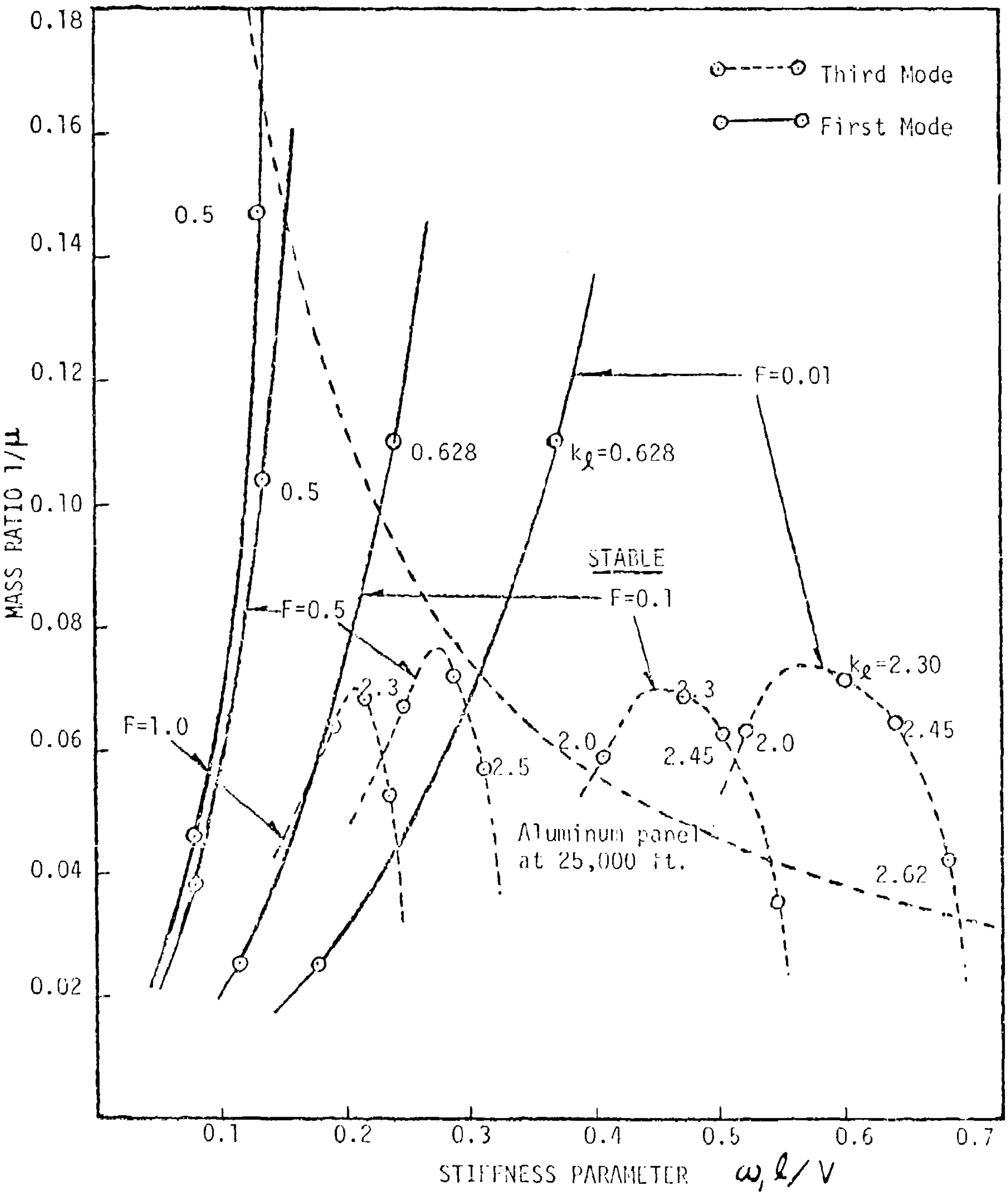

Figure 40. Flutter boundaries for clamped panels of ℓ/w=1.0 with M=1.52 and various values of tension parameters F.

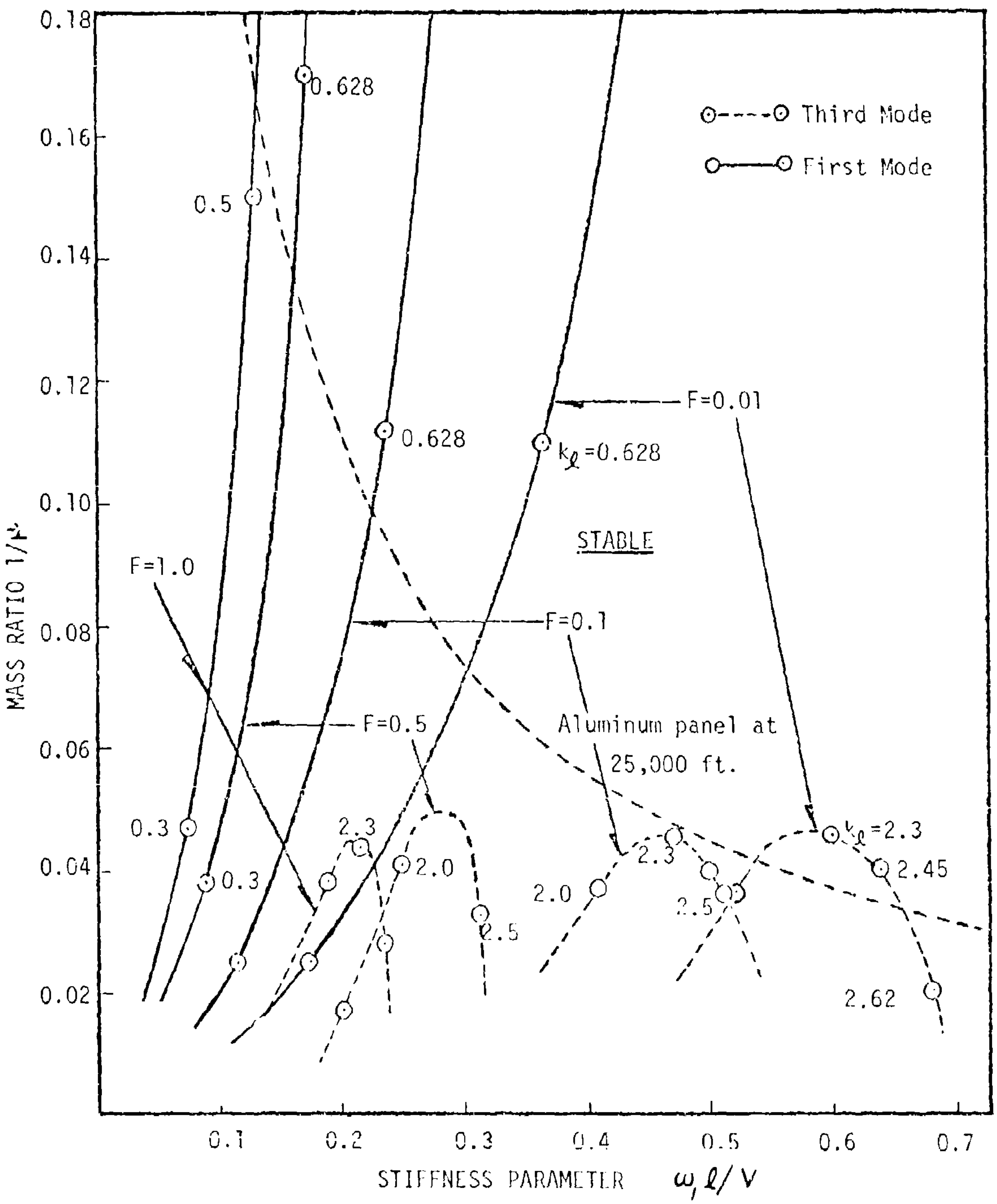

Figure 41 Flutter boundaries for clamped panels of ℓ/w=1.0 with M=1.54 and various values of tension parameters F.

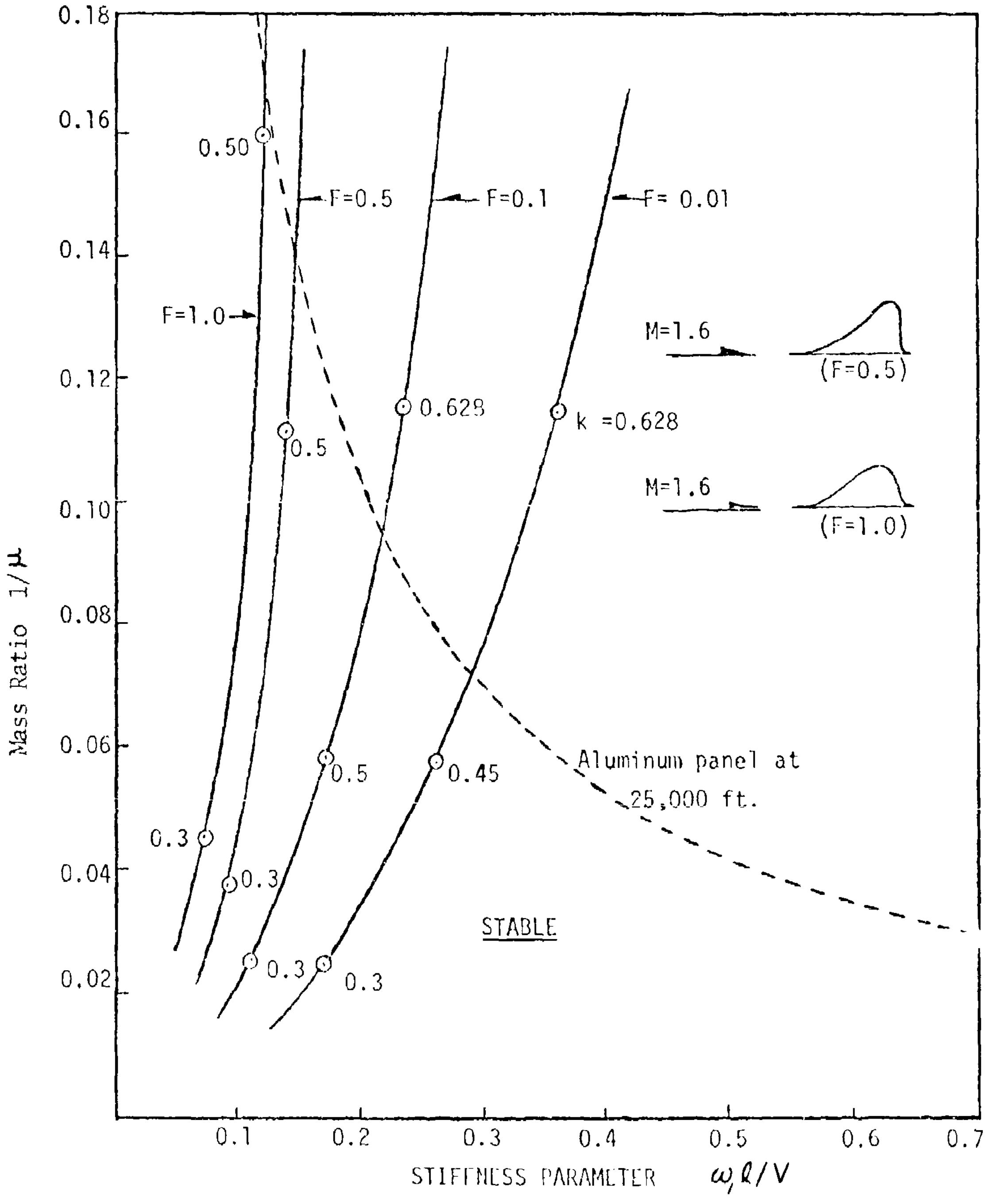

Figure 42 Flutter boundaries for clamped panels of ℓ/w=1.0 with M=1.6 and various values of tension parameters F.

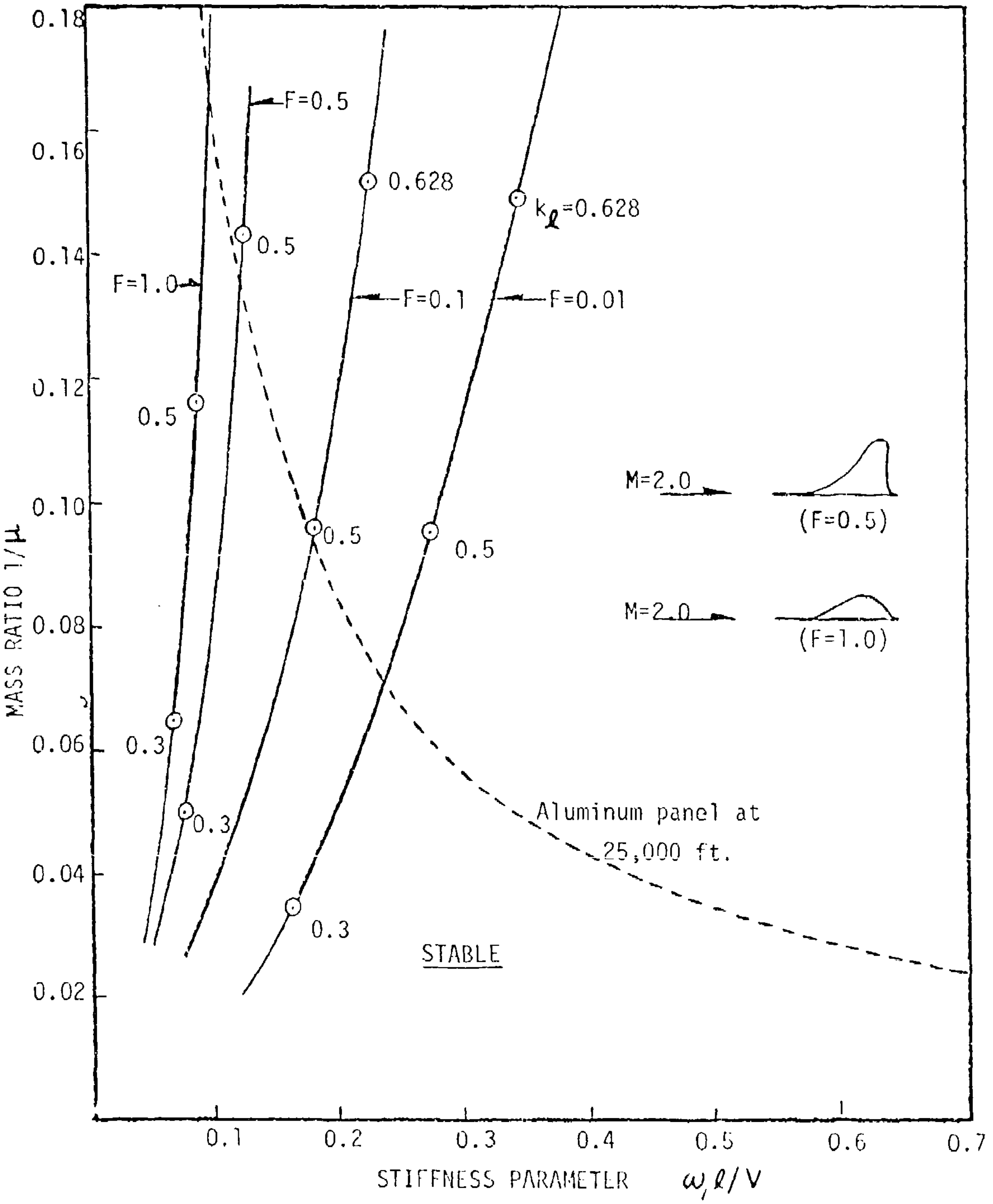

Figure 43 Flutter boundaries for clamped panel of $\ell/w=1.0$ with $M=2.0$ and various values of tension parameters F.

By collecting all the intersecting points between the dashed parabolas and the critical flutter boundaries in Figs. 30, 33, and 37-43, the results for thickness ratios required to prevent flutter of the panel are shown in Fig. 44 for various values of Mach numbers and tension.

In Fig. 44, the critical flutter boundaries were dominated by the third mode in the Mach region between approximately 1.2 and 1.5. For other lower and higher Mach regions, the first mode flutter boundaries dominate. The sharp drops in the curves are due to the abrupt changes in critical flutter modes.

The beneficial effect of introducing in-plane tensions to reduce the required panel thickness to avoid flutter is clearly demonstrated. Fig. 44 should be of value to panel flutter analysts and designers.

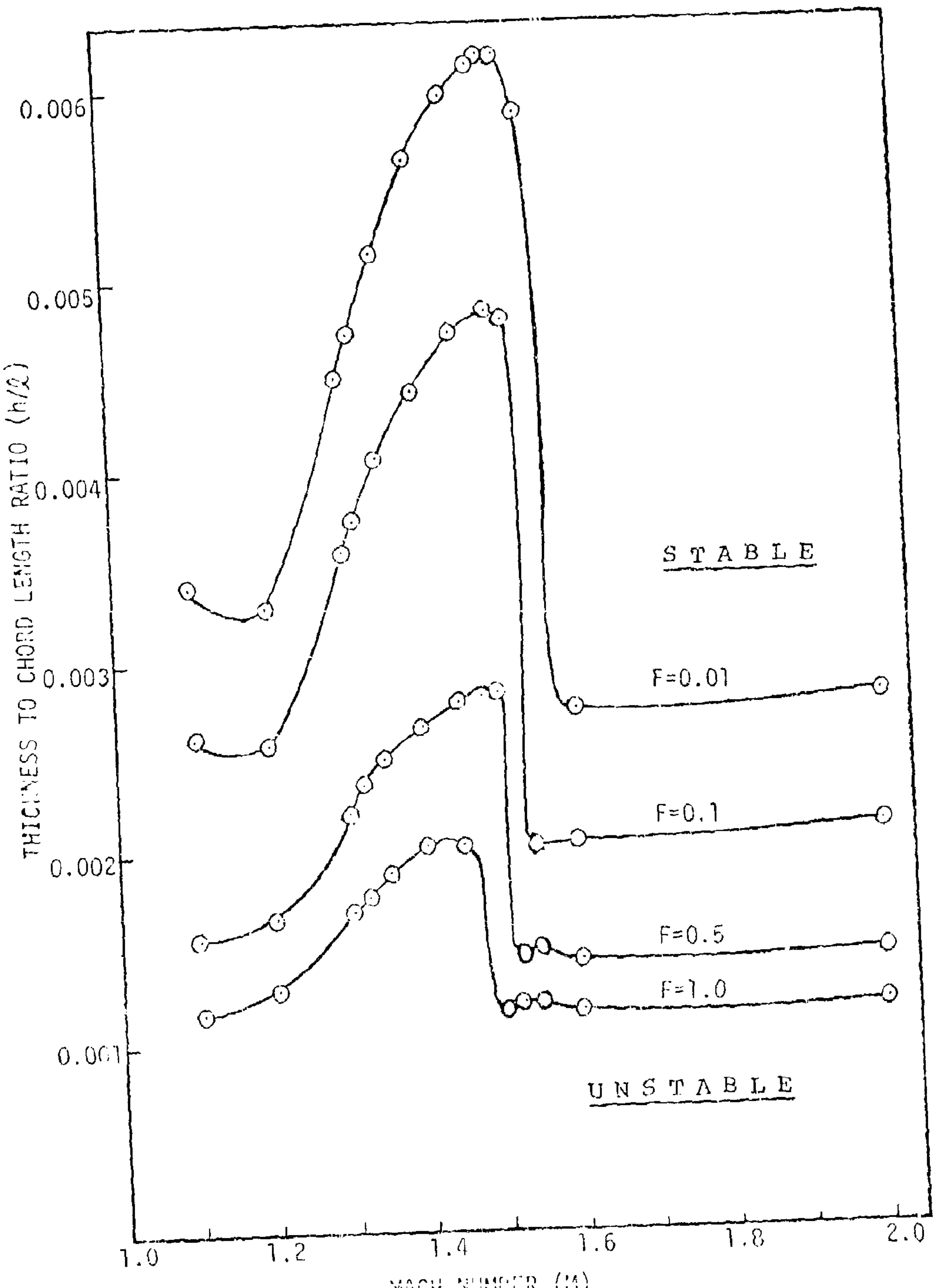

Figure 44 Thickness ratio required to prevent flutter for various values of tension parameter F for a square clamped aluminum panel at 25,000 ft. above sea level

SECTION V

CONCLUDING REMARKS

A basic finite element procedure for panel flutter analysis has been developed and performed with examples. The following concluding remarks may be made.

(1) The three-dimensional supersonic unsteady potential flow theory was employed. This theory allows the treatment of panels with finite aspect ratio. It is particularly advantageous at low supersonic range ($1 < M < \sqrt{2}$) for panels with chord-span ratio less than one, when the piston theory does not give satisfactory results.

(2) The finite element method offers a set of elegant and straightforward eigenvalue equations. It can be used directly to solve for flutter frequencies and mode shapes without requiring the natural vibration frequencies and mode shapes before the eigensolution, and also without requiring the computation of mode shapes after the eigensolution.

(3) If the modal method is used in panel flutter analysis, one could use the natural frequencies and modes found by the finite element method. Such procedure is, however, basically different from the present finite element method.

(4) The formulations here (Eqs. 19-24) are general. They are readily applicable to any plate finite element displacement model whose shape functions are known.

(5) The present results agree well with Galerkin's modal solution by Cunningham.

(6) The critical flutter boundaries for a square clamped panel change modes abruptly as the Mach number is varied.

(7) Fig. 44 clearly demonstrates the beneficial effect of in-plane tensions.

(8) The present development may provide a basic finite element procedure for panel flutter analysis. The present results may provide useful data to the flutter analysts and designers.

(9) A logical next step appears to be the development of a method using triangular plate finite elements combined with triangular Mach boxes. Such development will be of great value to the flutter predictions of wing panels with arbitrary configurations. It is suggested that the triangular element developed by Bell (Reference 15) be used.

REFERENCES

1. Dowell, E.H., Aeroelasticity of Plates and Shells, Noordhoff International Publishing, Leyden, The Netherlands, 1975.

2. Garrick, I.E., Aerodynamic Flutter, AIAA Selected Reprint Series, Vol. V, March 1969.

3. Olson, M.D., "Finite Elements Applied to Panel Flutter," AIAA Journal, Vol. 5, December 1967, pp. 2267-2270.

4. Olson, M.D., "Some Flutter Solutions Using Finite Elements," AIAA Journal, Vol. 8, April 1970, pp. 747-752.

5. Appa, K. and Somashekar, B.R., "Application of Matrix Displacement Methods in the Study of Panel Flutter," AIAA Journal, Vol. 7, January 1969, pp. 50-53.

6. Appa, K., Somashekar, B.R., and Shah, C.G., "Discrete Element Approach to Flutter of Skew Panels with Inplane Forces under Yawed Supersonic Flow," AIAA Journal, Vol. 8, November 1970, pp. 2017-2022.

7. Sander, G., Bon, C., and Geradin, M., "Finite Element Analysis of Supersonic Panel Flutter," International Journal for Numerical Methods in Engineering, Vol. 7, 1973, pp. 379-394.

8. Yang, T.Y., "Flutter of Flat Finite Element Panels in a Supersonic Potential Flow," AIAA Journal, Vol. 13, November 1975, pp. 1502-1507.

9. Cunningham, H.J., "Flutter Analysis of Flat Rectangular Panels Based on Three-Dimensional Supersonic Unsteady Potential Flow," NASA-TR R-256, 1967.

10. Dowell, E.H. and Voss, H.M., "Theoretical and Experimental Panel Flutter Studies in the Mach Number Range 1.0 to 5.0," AIAA Journal, Vol. 3, December 1965, pp. 2292-2304.

11. Bogner, F.K., Fox, R.L., and Schmit, L.A., "The Generation of Interelement - Compatible Stiffness and Mass Matrices by the Use of Interpolation Formulas," Proceedings of the Conference on Matrix Methods in Structural Mechanics, Air Force Flight Dynamics Laboratory, TR-66-80, 1966, pp. 397-443.

12. Watkins, E.E., "Three Dimensional Supersonic Theory," AGARD Manual on Aeroelasticity, November 1960, Part II, Chapter 5.

13. Houbolt, J.C., "A Study of Several Aerothermoelastic Problems of Aircraft Structures in High Speed Flight," Doctor of T.S. Thesis, The Swiss Federal Institute of Technology, Leeman, Zürich, 1958.

14. Hedgepeth, J.M., "Flutter of Rectangular Simply-Supported Panels at High Supersonic Speeds," Journal of Aeronautical Sciences, Vol. 24, No. 8, August 1957, pp. 563-573, 586.

15. Bell, K., "A Refined Triangular Plate Bending Finite Element," International Journal for Numerical Methods in Engineering, Vol. 1, 1969, pp. 101-122.

APPENDIX

THE COMPUTER PROGRAM

The description and listing of the computer program are provided in this appendix. The flow chart is given on pages 69 and 70. The procedure for input is given on pages 62, 67, and 68. The use of the program is demonstrated by considering an example of a square clamped panel with $k_\ell = 0.5$, $M = 1.2$, and $F = 0.1$. Both input and output data are provided.

The stiffness, mass, and incremental stiffness matrices are based on the known explicit coefficients. These coefficients are read in as input data given on pages 63-66. The program uses the subroutine EISPACK for solving the general complex eigenvalue equations.

INPUT DATA

1. **Control Card** (2F5.2, 7I3, 4F7.4)

Columns 1-5	Panel chordwise length (XL)
6-10	Panel spanwise width (YL)
11-13	Number of elements in chordwise direction (NX)
14-16	Half number of elements in spanwise direction (NY)
17-19	Number of boxes in streamwise (or chordwise) direction for one element (IBX)
20-22	Number of boxes in cross-streamwise (or spanwise) direction for one element (IBY)
23-25	Total number of degrees of freedom for the panel (NXD)
26-28	Number of nodes in streamwise direction (NDX)
29-31	Number of nodes in cross-streamwise direction (NDY)
32-38	Structural damping coefficient (SG)
39-45	Mach number (MACH)
46-52	Starting value for the mass ratio range (MUO)
53-59	Increment for the values of mass ratios (XINCR)

2. **Element matrix** cards (8I4, 2I2, 2I4, 2I6)

Read in the data given on pages 63-66.

TABLE I DATA INFØRMATIØN FØR QQ(I,J), QM(I,J) and QN(I,J)

QQ(I,J)-ELEMENT STIFFNESS MATRIX
QM(I,J)-ELEMENT MASS MATRIX
QN(I,J)-ELEMENT INCREMENTAL STIFFNESS MATRIX

MATRIX LOCATION	CARD NUMBER	QQ(I,J) DATA JS(1) 1-4	JS(2) 5-8	JS(3) 9-12	JS(4) 13-16	JS(5) 17-20	JS(6) 21-24	JS(7) 25-28	JS(8) 29-32	INDEX IZ 33-34	IY 35-36	QM(I,J) DATA JM(1) 37-40	JM(2) 41-44	QN(I,J) DATA JB(1) 45-50	JB(2) 51-56
(1, 1)	1	156	35	156	35	72	25	-0	1	-0	-0	169	1	78	175
(2, 1)	2	78	35	22	35	6	25	6	5	1	-0	143	6	13	350
(2, 2)	3	52	35	4	35	8	25	-0	1	2	-0	13	3	26	525
(3, 1)	4	22	35	78	35	6	25	6	5	-0	1	143	6	33	525
(3, 2)	5	11	35	11	35	1	50	6	5	1	1	121	36	11	2100
(3, 3)	6	4	35	52	35	8	25	-0	1	-0	2	13	3	2	175
(4, 1)	7	11	35	11	35	1	50	1	5	1	1	121	36	11	2100
(4, 2)	8	22	105	2	35	2	75	2	15	2	1	11	18	11	1575
(4, 3)	9	2	35	22	105	2	75	2	15	1	2	11	18	1	1050
(4, 4)	10	4	105	4	105	8	225	-0	1	2	2	1	9	2	1575
(5, 1)	11	54	35	-156	35	-72	25	-0	1	-0	-0	117	2	27	175
(5, 2)	12	27	35	-22	35	-6	25	-6	5	1	-0	33	4	9	700
(5, 3)	13	13	35	-78	35	-6	25	-0	1	-0	1	169	12	39	1050
(5, 4)	14	13	70	-11	35	-1	50	-1	10	1	1	143	72	13	4200
(5, 5)	15	156	35	156	35	72	25	-0	1	-0	-0	169	1	78	175
(6, 1)	16	27	35	-22	35	-6	25	-6	5	1	-0	33	4	9	700
(6, 2)	17	18	35	-4	35	-8	25	-0	1	2	-0	3	2	9	525
(6, 3)	18	13	70	-11	35	-1	50	-1	10	1	1	143	72	13	4200
(6, 4)	19	13	105	-2	35	-2	75	-0	1	2	1	13	36	13	3150
(6, 5)	20	78	35	22	35	6	25	6	5	1	-0	143	6	13	350
(6, 6)	21	52	35	4	35	8	25	-0	1	2	-0	13	3	26	525
(7, 1)	22	-13	35	78	35	6	25	-0	1	-0	1	-169	12	-13	350
(7, 2)	23	-13	70	11	35	1	50	1	10	1	1	-143	72	-13	4200
(7, 3)	24	-3	35	26	35	-2	25	-0	1	-0	2	-13	4	-3	350
(7, 4)	25	-3	70	11	105	-1	150	-1	30	1	2	-11	24	-1	1400
(7, 5)	26	-22	35	-78	35	-6	25	-6	5	-0	1	-143	6	-11	175
(7, 6)	27	-11	35	-11	35	-1	50	-6	5	1	1	-121	36	-11	2100
(7, 7)	28	4	35	52	35	8	25	-0	1	-0	2	13	3	2	175
(8, 1)	29	-13	70	11	35	1	50	1	10	1	1	-143	72	-13	4200
(8, 2)	30	-13	105	2	35	2	75	-0	1	2	1	-13	36	-13	3150
(8, 3)	31	-3	70	11	105	-1	150	-1	30	1	2	-11	24	-1	1400
(8, 4)	32	-1	35	2	105	-2	225	-0	1	2	2	-1	12	-1	1050
(8, 5)	33	-11	35	-11	35	-1	50	-1	5	1	1	-121	36	-11	2100
(8, 6)	34	-22	105	-2	35	-2	75	-2	15	2	1	-11	18	-11	1575
(8, 7)	35	2	35	22	105	2	75	2	15	1	2	11	18	1	1050

TABLE I DATA INFØRMATIØN FØR QQ(I,J), QM(I,J) and QN(I,J), continued ...

(8, 8)	36	4	105	4	105	8	225	-0	1	2	2	1	9	2	1575
(9, 1)	37	-54	35	-54	35	72	25	-0	1	-0	-0	81	4	-27	175
(9, 2)	38	-27	35	-13	35	6	25	-0	1	1	-0	39	8	-9	700
(9, 3)	39	-13	35	-27	35	6	25	-0	1	-0	1	39	8	-13	350
(9, 4)	40	-13	70	-13	70	1	50	-0	1	1	1	169	144	-13	4200
(9, 5)	41	-156	35	54	35	-72	25	-0	1	-0	-0	117	2	-78	175
(9, 6)	42	-78	35	13	35	-6	25	-0	1	1	-0	169	12	-13	350
(9, 7)	43	22	35	-27	35	6	25	6	5	-0	1	-33	4	11	175
(9, 8)	44	11	35	-13	70	1	50	1	10	1	1	-143	72	11	2100
(9, 9)	45	156	35	156	35	72	25	-0	1	-0	-0	169	1	78	175
(10, 1)	46	27	35	13	35	-6	25	-0	1	1	-0	-39	8	9	700
(10, 2)	47	9	35	3	35	2	25	-0	1	2	-0	-9	8	-9	2100
(10, 3)	48	13	70	13	70	-1	50	-0	1	1	1	-169	144	13	4200
(10, 4)	49	13	210	3	70	1	150	-0	1	2	1	-13	48	-13	12600
(10, 5)	50	78	35	-13	35	6	25	-0	1	1	-0	-169	12	13	350
(10, 6)	51	26	35	-3	35	-2	25	-0	1	2	-0	-13	4	-13	1050
(10, 7)	52	-11	35	13	70	-1	50	-1	10	1	1	143	72	-11	2100
(10, 8)	53	-11	105	3	70	1	150	1	30	2	1	11	24	11	6300
(10, 9)	54	-72	35	-22	35	-6	25	-6	5	1	-0	-143	6	-13	350
(10,10)	55	52	35	4	35	8	25	-0	1	2	-0	13	3	26	525
(11, 1)	56	13	35	27	35	-6	25	-0	1	-0	1	-39	8	13	350
(11, 2)	57	13	70	13	70	-1	50	-0	1	1	1	-169	144	13	4200
(11, 3)	58	3	35	9	35	2	25	-0	1	-0	2	-9	8	3	350
(11, 4)	59	3	70	13	210	1	150	-0	1	1	2	-13	48	1	1400
(11, 5)	60	22	35	-27	35	6	25	6	5	-0	1	-33	4	33	525
(11, 6)	61	11	35	-13	70	1	50	1	10	1	1	-143	72	11	2100
(11, 7)	62	-4	35	18	35	-8	25	-0	1	-0	2	3	2	-2	175
(11, 8)	63	-2	35	13	105	-2	75	-0	1	1	2	13	36	-1	1050
(11, 9)	64	-22	35	-78	35	-6	25	-6	5	-0	1	-143	6	-33	525
(11,10)	65	11	35	11	35	1	50	6	5	1	1	121	36	11	2100
(11,11)	66	4	35	52	35	8	25	-0	1	-0	2	13	3	2	175
(12, 1)	67	-13	70	-13	70	1	50	-0	1	1	1	169	144	-13	4200
(12, 2)	68	-13	210	-3	70	-1	150	-0	1	2	1	13	48	13	12600
(12, 3)	69	-3	70	-13	210	-1	150	-0	1	1	2	13	48	-1	1400
(12, 4)	70	-1	70	-1	70	1	450	-0	1	2	2	1	16	1	4200
(12, 5)	71	-11	35	13	70	-1	50	-1	10	1	1	143	72	-11	2100
(12, 6)	72	-11	105	3	70	1	150	1	30	2	1	11	24	11	630
(12, 7)	73	2	35	-13	105	2	75	-0	1	1	2	-13	36	1	1050
(12, 8)	74	2	105	-1	35	-2	225	-0	1	2	2	-1	12	-1	3150
(12, 9)	75	11	35	11	35	1	50	1	5	1	1	121	36	11	2100
(12,10)	76	-22	105	-2	35	-2	75	-2	15	2	1	-11	13	-11	1575
(12,11)	77	-2	35	-22	105	-2	75	-2	15	1	2	-11	18	-1	1050
(12,12)	78	4	105	4	105	8	225	-0	1	2	2	1	9	2	1575
(13, 1)	79	-156	35	54	35	-72	25	-0	1	-0	-0	117	2	-78	175
(13, 2)	80	-78	35	13	35	-6	25	-0	1	1	-0	169	12	-13	350

TABLE I DATA INFØRMATIØN FØR QQ(I,J), QM(I,J) and QN(I,J), continued ...

(13, 3)	81	-22	35	27	35	-6	25	-6	5	-0	1	33	4	-33	525
(13, 4)	82	-11	35	13	70	-1	50	-1	10	1	1	143	72	-11	2100
(13, 5)	83	-54	35	-54	35	72	25	-0	1	-0	-0	81	4	-27	175
(13, 6)	84	-27	35	-13	35	6	25	-0	1	1	-0	39	8	-9	700
(13, 7)	85	13	35	27	35	-6	25	-0	1	-0	1	-39	8	13	350
(13, 8)	86	13	70	13	70	-1	50	-0	1	1	1	-169	144	13	4200
(13, 9)	87	54	35	-135	35	-72	25	-0	1	-0	-0	117	2	27	175
(13,10)	88	-27	35	22	35	6	25	6	5	1	-0	-33	4	-9	700
(13,11)	89	-13	35	78	35	6	25	-0	1	-0	1	-169	12	-13	350
(13,12)	90	13	70	-11	35	-1	50	-1	10	1	1	143	72	13	4200
(13,13)	91	156	35	156	35	72	25	-0	1	-0	-0	169	1	78	175
(14, 1)	92	78	35	-13	35	6	25	-0	1	1	-0	-169	12	13	350
(14, 2)	93	26	35	-3	35	-2	25	-0	1	2	-0	-13	4	-13	1050
(14, 3)	94	11	35	-13	70	1	50	1	10	1	1	-143	72	11	2100
(14, 4)	95	11	105	-3	70	-1	150	-1	30	2	1	-11	24	-11	6300
(14, 5)	96	27	35	13	35	-6	25	-0	1	1	-0	-39	8	9	700
(14, 6)	97	9	35	3	35	2	25	-0	1	2	-0	-9	8	-9	2100
(14, 7)	98	-13	70	-13	70	1	50	-0	1	1	1	169	144	-13	4200
(14, 8)	99	-13	210	-3	70	-1	150	-0	1	2	1	13	48	13	12600
(14, 9)	100	-27	35	22	35	6	25	6	5	1	-0	-33	4	-9	700
(14,10)	101	18	35	-4	35	-8	25	-0	1	2	-0	3	2	9	525
(14,11)	102	13	70	-11	35	-1	50	-1	10	1	1	143	72	13	4200
(14,12)	103	-13	105	2	35	2	75	-0	1	2	1	-13	36	-13	3150
(14,13)	104	-78	35	-22	35	-6	25	-6	5	1	-0	-143	6	-13	350
(14,14)	105	52	35	4	35	8	25	-0	1	2	-0	13	3	26	525
(15, 1)	106	-22	35	27	35	-6	25	-6	5	-0	1	33	4	-22	350
(15, 2)	107	-11	35	13	70	-1	50	-1	10	1	1	143	72	-11	2100
(15, 3)	108	-4	35	18	35	-8	25	-0	1	-0	2	3	2	-2	175
(15, 4)	109	-2	35	13	105	-2	75	-0	1	1	2	13	36	-1	1050
(15, 5)	110	-13	35	-27	35	6	25	-0	1	-0	1	39	8	-13	350
(15, 6)	111	-13	70	-13	70	1	50	-0	1	1	1	169	144	-13	4200
(15, 7)	112	3	35	9	35	2	25	-0	1	-0	2	-9	3	3	350
(15, 8)	113	3	70	13	210	1	150	-0	1	1	2	-13	48	1	1400
(15, 9)	114	13	35	-78	35	-6	25	-0	1	-0	1	169	12	13	350
(15,10)	115	-13	70	11	35	1	50	1	10	1	1	-143	72	-13	4200
(15,11)	116	-3	35	26	35	-2	25	-0	1	-0	2	-13	4	-3	350
(15,12)	117	3	70	-11	105	1	150	1	30	1	2	11	24	1	1400
(15,13)	118	22	35	78	35	6	25	6	5	-0	1	143	6	22	350
(15,14)	119	-11	35	-11	35	-1	50	-6	5	1	1	-121	36	-11	2100
(15,15)	120	4	35	52	35	8	25	-0	1	-0	1	13	3	2	175
(16, 1)	121	11	35	-13	70	1	50	1	10	1	1	-143	72	11	2100
(16, 2)	122	11	105	-3	70	-1	150	-1	30	2	1	-11	24	-11	6300
(16, 3)	123	2	35	-13	105	2	75	-0	1	1	2	-13	36	1	1050
(16, 4)	124	2	105	-1	35	-2	225	-0	1	2	2	-1	12	-1	3150
(16, 5)	125	13	70	13	70	-1	50	-0	1	1	1	-169	144	13	4200

TABLE I DATA INFØRMATIØN FØR QQ(I,J), QM(I,J) and QN(I,J), continued ...

(16, 6)	126	13	210	3	70	1	150	-0	1	2	1	-13	48	-13	12600
(16, 7)	127	-3	70	-13	210	-1	150	-0	1	1	2	13	48	-1	1400
(16, 8)	128	-1	70	-1	70	1	450	-0	1	2	2	1	16	1	4200
(16, 9)	129	-13	70	11	35	1	50	1	10	1	1	-143	72	-13	4200
(16,10)	130	13	105	-2	35	-2	75	-0	1	2	1	13	36	13	3150
(16,11)	131	3	70	-11	105	1	150	1	30	1	2	11	24	1	1400
(16,12)	132	-1	35	2	105	-2	225	-0	1	2	2	-1	12	-1	1050
(16,13)	133	-11	35	-11	35	-1	50	-1	5	1	1	-121	36	-11	2100
(16,14)	134	22	105	2	35	2	75	2	15	2	1	11	18	11	1575
(16,15)	135	-2	35	-22	105	-2	75	-2	15	1	2	-11	18	-1	1050
(16,16)	136	4	105	4	105	8	225	-0	1	2	2	1	9	2	1575

BEST AVAILABLE COPY

3. Element Cards with the boundary condition code at each node (2213).

Columns	1-3	The sequence number for the element	
	4-6	The starting matrix row position for the degrees of freedom at nodal point I	(ID(1))
	7-9	The starting matrix row position for the degrees of freedom at nodal point J	(ID(2))
	10-12	The starting matrix row position for the degrees of freedom at nodal point K	(ID(3))
	13-15	The starting matrix row position for the degrees of freedom at nodal point L	(ID(4))
	16-18	Boundary condition code for deflection Z at nodal point I	(w(1))
	19-21	Boundary condition code for $Z_{,x}$ at nodal point I	(w(2))
	22-24	Boundary condition code for $Z_{,y}$ at nodal point I	(w(3))
	25-27	Boundary condition code for $Z_{,xy}$ at nodal point I	(w(4))
	28-30	Boundary condition code for Z at nodal point J	(w(5))
	31-33	Boundary condition code for $Z_{,x}$ at nodal point J	(w(6))
	34-36	Boundary condition code for $Z_{,y}$ at nodal point J	(w(7))
	37-39	Boundary condition code for $Z_{,xy}$ at nodal point J	(w(8))
	40-42	Boundary condition code for Z at nodal point K	(w(9))
	43-45	Boundary condition code for $Z_{,x}$ at nodal point K	(w(10))
	46-48	Boundary condition code for $Z_{,y}$ at nodal point K	(w(11))
	49-51	Boundary condition code for $Z_{,xy}$ at nodal point K	(w(12))

52-54	Boundary condition code for Z at nodal point L	(w(13))
55-57	Boundary condition code for $Z_{,x}$ at nodal point L	(w(14))
58-60	Boundary condition code for $Z_{,y}$ at nodal point L	(w(15))
61-63	Boundary condition code for $Z_{,xy}$ at nodal point L	(w(16))

The 'ID' array at I, J, K and L is assigned for each element for a specific mesh of the elements of the panel. The permutation for I, J, K and L is clockwise and I is corresponding to the origin of each local element as shown in Fig. 2. If ID(I) = 0, all the degrees of freedom at node I are zero. Same situation is applied for other nodes for the element.

The 'w' array defines the boundary condition codes for the degrees of freedom at each node. If w(I) = 0, the associated degree of freedom is zero and if w(I) $\neq$ 0, the associated degree of freedom is taken into account.

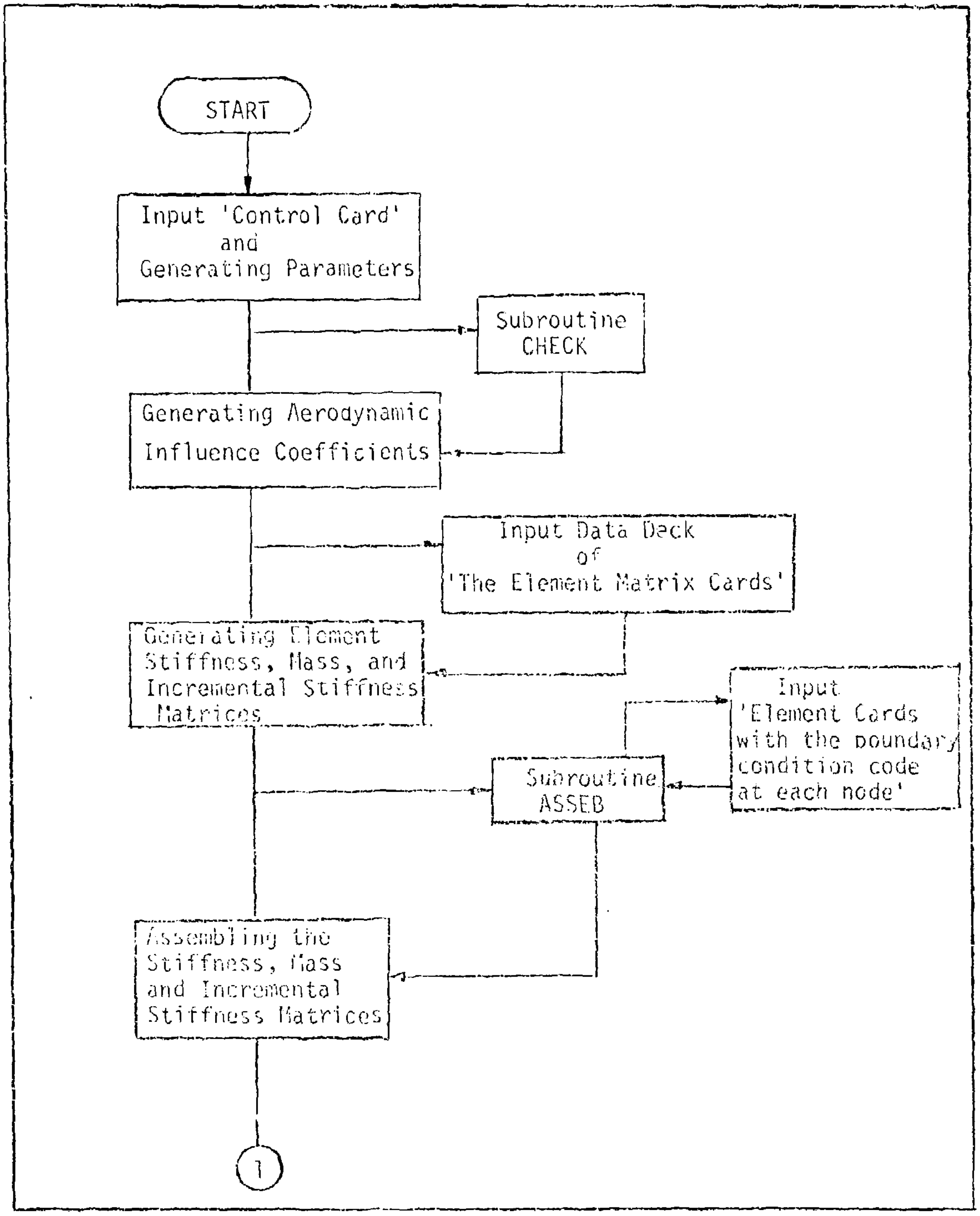

Program Flow Chart

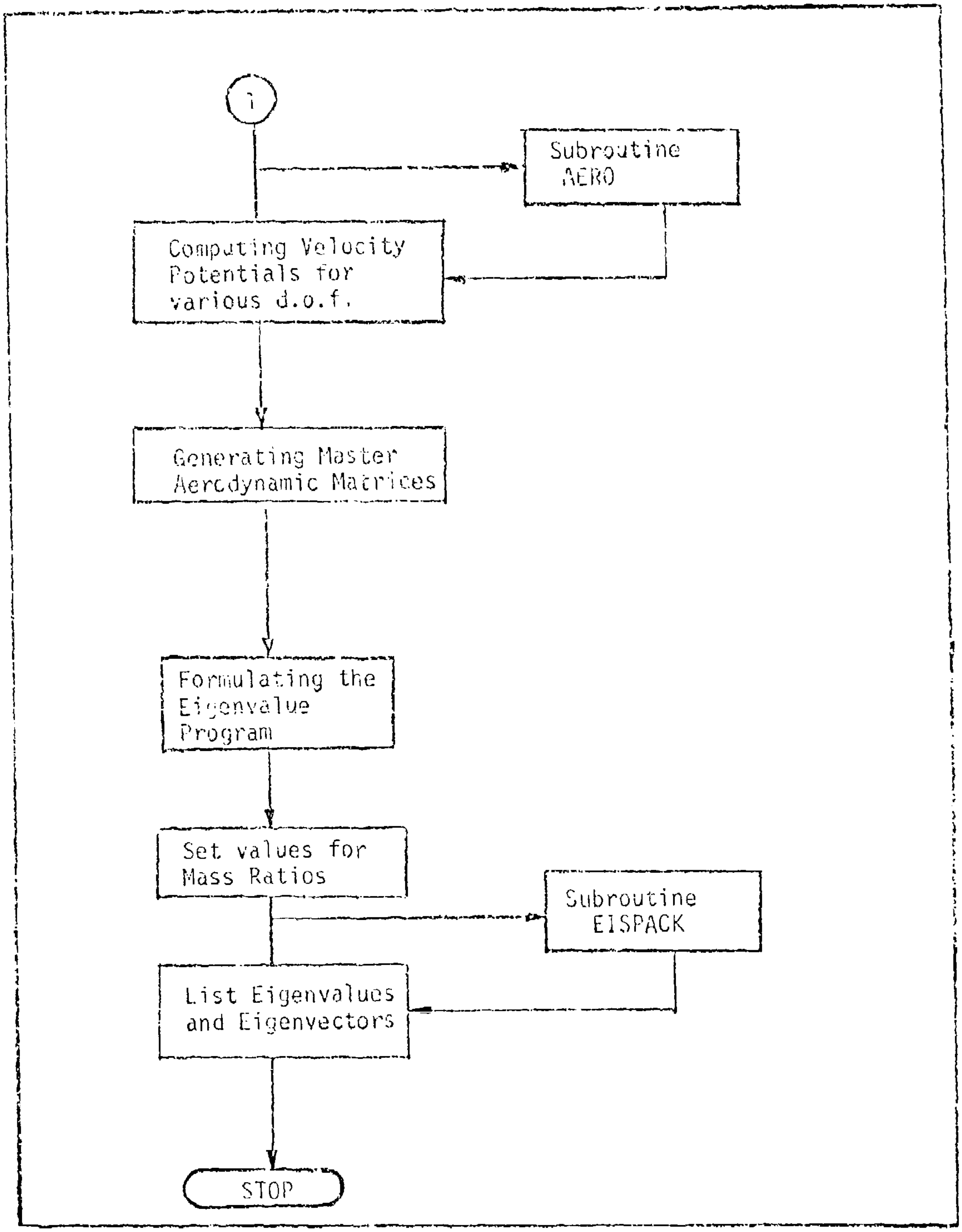

Program Flow Chart continued ....

PROGRAM LISTING AND SAMPLE PROBLEM

```
      PROGRAM FLUTTER (INPUT,OUTPUT,TAPE5=INPUT,TAPE6=OUTPUT)
      COMPLEX CS(18,18),UI(18),RT,CF
      REAL OV(16,16),OM(16,16),GR(2),GRR(16,8),GRI(16,8),IM(18,18),SK(18
     1,18),ON(16,16),SN(18,18),MACH,MU,KL,MU0,V(40,16),VS(40,16),AK(18,1
     28),WI(18,18)
      INTEGER P,S,PMAX,P1,S1,SMAX,JS(8),JM(2),JG(16),JB(2)
      COMMON /BLOCK0/ BM,UB,C,CB
      COMMON /BLOCK1/ IBX,RBX,GRR,GRI,IBY,RBY
      COMMON /BLOCK2/ OO,OM,ON
      COMMON /BLOCK3/ SK,SM,SN
C
C     PANEL FLUTTER FOR CLAMPED PANEL
C
C
C     THE D.O.F.#S FOR EACH NODAL POINT ON THE ELEMENT
C
      IX1(NC)=8*NC
      IX2(NC)=12*NC
      IX3(NC)=NC
      IX4(NC)=4*NC
      PRINT 133
      READ 134, XL,YL,NX,NY,IBX,IBY,NXD,NDX,NDY,SG,MACH,MU0,XINCR
C
C     PANEL PARAMETERS
C
      POISN=0.32
      AO=XL/FLOAT(NX)
      BO=YL/2.0/FLOAT(NY)
      AB=AO/BO
      BA=BO/AO
      XLW=XL/YL
      PRINT 135, XLW,AO,BO
C
C     THE FIRST FREQUENCY PARAMETER FOR CLAMPED PANEL
C
      CK0=4.73
      CK2=0.9825022
      CK3=2.6472354
      CK1=(CK0**4)+((XLW*CK0)**4)+2.*((XLW*CK0*CK2*CK3)**2)
C
C     BOX PARAMETERS
C
      IRT=NX*NY*IBX*IBY
      RBX=1./FLOAT(IBX)
      RBY=1./FLOAT(IBY)
      EPISN=BO/FLOAT(IBY)
      SIGMA=RBX/EPISN
      EL=EPISN/XL
      PRINT 136, EPISN,SIGMA
C
C     REFERENCE REDUCED FREQUENCY PARAMETER
C
      KL=0.50
      PRINT 137, KL
C
C     INITIAL IN-PLANE FORCE PARAMETER
C
```

```
      F=0.1
      PRINT 138, F
C
C     FLOW PARAMETERS
C
      PRINT 139, MACH
      BETA=SQRT(MACH**2-1.)
      OMEGA=((MACH**2)*KL*EL)/(BETA**2)
      BM=BETA*OMEGA/(2.*MACH)
      UD=BM*MACH
      C=1./(2.*3.14159)
      CB=BO
C
C     GENERATING AERODYNAMIC INFLUENCE COEFFICIENTS
C
      RMAX=NX*IBX
      SMAX=2*NY*IBY
      DO 101 I=1,RMAX
      DO 101 J=1,SMAX
         GRR(I,J)=0.
  101 GRI(I,J)=0.
      DO 102 IS=1,RMAX
         R=IS-1
         DS=SIGMA/BETA*(EPISN/2.+EPISN*FLOAT(R))
         JF=IFIX((DS-(EPISN/2.))/EPISN)+2
         IF (JF.GT.SMAX) JF=SMAX
         IF (DS.LT.(EPISN/2.)) JF=1
         JG(IS)=JF
      DO 102 J=1,JF
         S=J-1
         CALL CHECK (R,S,BETA,SIGMA,GR)
         R1=R+1
         S1=S+1
         GRR(R1,S1)=GR(1)
         GRI(R1,S1)=GR(2)
  102 CONTINUE
C
C     GENERATING ELEMENT STIFFNESS MATRIX, ELEMENT INCREMENTAL
C     STIFFNESS MATRIX, AND ELEMENT MASS MATRIX
C
      DO 103 I=1,16
      DO 103 J=1,I
         READ 140, (JS(L),L=1,8),IZ,IY,(JM(L),L=1,2),(JB(L),L=1,2)
         OO(I,J)=(BA**IY)*(FLOAT(JS(1))/FLOAT(JS(2))+(AB**4)*FLOAT(JS(3)
     1   )/FLOAT(JS(4))+(AB**2)*FLOAT(JS(5))/FLOAT(JS(6))+(AB**2)*POISN*
     2   FLOAT(JS(7))/FLOAT(JS(8)))
         OM(I,J)=(BA**IY)*(FLOAT(JM(1))/FLOAT(JM(2)))
         ON(I,J)=(BA**IY)*(FLOAT(JB(1))/FLOAT(JB(2)))*(BA)
  103 CONTINUE
      DO 104 I=1,16
      DO 104 J=I,16
         OO(I,J)=OO(J,I)
         ON(I,J)=ON(J,I)
  104 OM(I,J)=OM(J,I)
C
C     ASSEMBLE ELEMENT STIFFNESS MATRIX, ELEMENT INCREMENTAL STIFFNESS
C     MATRIX, AND ELEMENT MASS MATRIX
C
```

```
      CALL ASSEB (NX,NY,NXD)
C
C     GENERATING VELOCITY POTENTIAL FUNCTIONS
C
      KL=KL/FLOAT(NX)
      CALL AERO (NX,NY,NXD,IBT,KL,V,VS,EPISM,SIGMA,BETA,AD,BA,JG,NDX,NDY
     1)
C
C     GENERATING MASTER AERODYNAMIC MATRIX
C
      DO 123 IIX=1,NDX
         DO 122 IIY=1,NDY
            ND14=4
            IF (IIY.EQ.NDY) ND14=2
            DO 121 ND1=1,ND14
               II=(IIY-1)*4*NDX+(IIX-1)*4+ND1
               IF (IIY.EQ.NDY) II=(IIY-1)*4*NDX+(IIX-1)*2+ND1
               DO 120 JJX=1,NDX
               DO 120 JJY=1,NDY
                  ND24=4
                  IF (JJY.EQ.NDY) ND24=2
               DO 120 ND2=1,ND24
                  JO=(JJY-1)*4*NDX+(JJX-1)*4+ND2
                  IF (JJY.EQ.NDY) JO=(JJY-1)*4*NDX+(JJX-1)*2+ND2
                  Q=0.
                  QS=0.
                  DO 118 NL1=1,NX
                     N1=NL1-IIX
                     IF (N1.LT.0) GO TO 118
                     IF (N1.GT.1) GO TO 119
                     DO 117 NL2=1,NY
                        N2=NL2-IIY
                        IF (N2.LT.0) GO TO 117
                        IF (N2.GT.1) GO TO 119
                        IF (N1.EQ.0) GO TO 105
                        IF (N2.EQ.0) GO TO 106
                        IKL=IX3(ND1)
                        GO TO 108
  105                   IF (N2.EQ.0) GO TO 107
                        IKL=IX2(ND1)
                        GO TO 108
  106                   IKL=IX4(ND1)
                        GO TO 108
  107                   IKL=IX1(ND1)
  108                   DO 116 M=1,IBX
                           DO 115 NS=1,IBY
                              ML=(NL2-1)*IBY+NS
                              MM=(ML-1)*IBX+M
                              XM=FLOAT(M-1)*RBX+RBX/2.
                              YM=FLOAT(NS-1)*RBY+RBY/2.
                              CALL SHAPE (FA,DFA,IKL,XM,YN,BA)
                              IF (JJX-NL1) 109,109,110
  109                         JJ=(JJY-1)*4*(NDX+1)+(JJX-1)*4+ND2+(NX-NL1
     1                        )*4
                              IF (JJY.EQ.NDY) JJ=(JJY-1)*4*(NDX+1)+(JJX-
     1                        1)*2+(NX-NL1)*2+ND2
                              GO TO 111
  110                         VK=0.
```

```
                                  VKS=0.
                                  GO TO 114
  111                             IF (JJY.EQ.NDY) GO TO 113
                                  JJ7=JJ+2*(NDX+1)+((2*NDY-2)-JJY)*4*(NDX+1)
                                  IF (ND2.EQ.3.OR.ND2.EQ.4) GO TO 112
                                  VK=V(JJ,MM)+V(JJ7,MM)
                                  VKS=VS(JJ,MM)+VS(JJ7,MM)
                                  GO TO 114
  112                             VK=V(JJ,MM)-V(JJ7,MM)
                                  VKS=VS(JJ,MM)-VS(JJ7,MM)
                                  GO TO 114
  113                             VK=V(JJ,MM)
                                  VKS=VS(JJ,MM)
  114                             Q=Q+(-FA*VK+DFA/KL*VKS)*(SIGMA*(EPISN**2))
     1                            /(AO*BO)
                                  QS=QS+(-FA*VKS-DFA/KL*VK)*(SIGMA*(EPISN**2
     1                            )) (AO*BO)
  115                           CONTINUE
  116                         CONTINUE
  117                       CONTINUE
  118                     CONTINUE
  119                     AK(II,JQ)=Q
                          AKI(II,JQ)=QS
  120                   CONTINUE
  121                 CONTINUE
  122               CONTINUE
  123 CONTINUE
C
C     FINDING EIGENVALUES AND EIGENVECTORS FOR VARIOUS RATIOS OF AIR
C     MASS TO PANEL MASS
C
      YN=NY*2
      XN=NX
      DO 124 I=1,NXD
      DO 124 J=1,NXD
  124 SK(I,J)=0.01*((XN**5)/CK1*SK(I,J)+F*(XN**2)*(YN)*SN(I,J))
      CALL GINV2 (SK,NXD,NXD,NXD,KZ)
      IF (KZ.EQ.0) GO TO 131
      PRINT 141, SG
      KL=KL*XN
      C10=XN MU0/1225.
      FACTOR=1./MU0
      FACTOR=0.01 FACTOR
      DO 125 I=1,NXD
      DO 125 J=1,NXD
          SM(I,J)=C10*SM(I,J)
  125 CONTINUE
      DO 130 ITER=1,9
          IND=1
          MU=MU0+XINCR
          PRINT 144, MU
          RATIO MU MU0
          FACTOR=FACTOR RATIO
          DO 126 I=1,NXD
          DO 126 J=1,NXD
              SM(I,J)=1./RATIO*SM(I,J)
  126     CONTINUE
          DO 128 I=1,NXD
```

```
      DO 128 J=1,NXD
         AS=0.
         BS=0.
         DO 127 KI=1,NXD
            AS1=SK(I,KI)*(SM(KI,J)-AK(KI,J))
            BS1=SK(I,KI)*(-AKI(KI,J))
            AS=AS+(AS1+(SG*BS1))
            BS=BS+(BS1-(SG*AS1))
127      CONTINUE
         CS(I,J)=CMPLX(AS,BS)
128   CONTINUE
      CALL CGEIG (NXD,NXD,CS,IND,WS)
      DO 129 I=1,5
         CF=CMPLX(FACTOR,0.)
         WS(I)=WS(I)*CF
         AO=REAL(WS(I))
         BO=AIMAG(WS(I))
         G=BO/AO
         RT=CSQRT(WS(I))
         SR=REAL(RT)
         TK=SR*KL
         PRINT 142, WS(I),G,SR,TK
129   PRINT 143, (CS(J,I),J=1,NXD)
      MUO=MU
130 CONTINUE
    GO TO 132
131 PRINT 145
132 STOP
C
133 FORMAT ( 34H1  PANEL FLUTTER FOR CLAMPED PANEL,///)
134 FORMAT (2F5.2,7I3,4F7.4)
135 FORMAT (2X, 20HLENGTH-WIDTH RATIO =,1F6.3/2X, 26HCHORDWISE ELEMENT
   1 LENGTH =,1F6.3,3X, 24HSPANWISE ELEMENT WIDTH =,1F6.3/)
136 FORMAT (2X, 11HBOX WIDTH =,1F6.3,3X, 34HRATIO OF BOX LENGTH TO BOX
   1 WIDTH =,1F6.3/)
137 FORMAT (2X, 19HREDUCED FREQUENCY =,1F6.3/)
138 FORMAT (2X, 33HINITIAL IN-PLANE FORCE PARAMETER=,1F6.3/)
139 FORMAT (2X, 13HMACH NUMBER =,1F5.2/)
140 FORMAT (8I4,2I2,2I4,2I6)
141 FORMAT (2X, 32HSTRUCTURAL DAMPING COEFFICIENT =,1F8.3///)
142 FORMAT ( 15H0  EIGENVALUE= ,1E12.5,1X,1E12.5,3X,  5H G = ,1F8.5,2X
   1, 17HFREQUENCY RATIO =,1F8.5,2X, 22HSTIFFNESS PARAMETER = ,1F8.5)
143 FORMAT ( 14H   EIGENVECTOR,/2X,10E12.5/2X,10E12.5/2X,10E12.5/2X,10
   1E12.5/2X,10E12.5/2X,10E12.5/2X,10E12.5/2X,10E12.5)
144 FORMAT ( 20H0  DENSITY RATIO MU=,1F9.5)
145 FORMAT ( 17H  SINGULAR MATRIX)
C
    END

    SUBROUTINE ASSEB (NX,NY,NXD)
    REAL SK(18,18),SM(18,18),OO(16,16),OM(16,16),ON(16,16),SN(18,18)
    INTEGER W(16),ID(4)
    COMMON /BLOCK2/ OO,OM,ON
    COMMON /BLOCK3/ SK,SM,SN
```

```
      DO 101 I=1,NXD
      DO 101 J=1,NXD
         SK(I,J)=0.
         SM(I,J)=0.
         SN(I,J)=0.
  101 CONTINUE
      NTX=NX*NY
      DO 106 NEM=1,NTX
         READ 107, IN,(ID(I),I=1,4),(W(I),I=1,16)
         DO 105 L=1,4
            IF (ID(L).EQ.0) GO TO 105
            II=ID(L)
            DO 104 M=1,4
               IE=4*(L-1)+M
               IF (W(IE).EQ.0) GO TO 104
               DO 103 LS=1,4
                  IF (ID(LS).EQ.0) GO TO 103
                  JJ=ID(LS)
                  DO 102 MS=1,4
                     IES=4*(LS-1)+MS
                     IF (W(IES).EQ.0) GO TO 102
                     SK(II,JJ)=SK(II,JJ)+QQ(IE,IES)
                     SM(II,JJ)=SM(II,JJ)+QM(IE,IES)
                     SN(II,JJ)=SN(II,JJ)+QN(IE,IES)
                     JJ=JJ+1
  102             CONTINUE
  103          CONTINUE
               II=II+1
  104       CONTINUE
  105    CONTINUE
  106 CONTINUE
      RETURN
C
  107 FORMAT (22I3)
C
      END


      SUBROUTINE AERO (NX,NY,NXD,IBT,KA,V,VS,EPISN,SIGMA,BETA,AO,BA,JG,N
     1DX,NDY)
      REAL V(40,16),VS(40,16),GRR(16,8),GRI(16,8),KA
      INTEGER JG(16)
      COMMON /BLOCK1/ IBX,RBX,GRR,GRI,IBY,RBY
      IX1(NC)=8+NC
      IX2(NC)=12+NC
      IX3(NC)=NC
      IX4(NC)=4+NC
      NY1=NY*2
      NDX1=NDX+1
      NDY1=2*NDY-1
      NE=NX
      DO 116 NES=1,NY
         DO 115 M=1,IBX
         DO 115 N=1,IBY
            NN=(NE-1)*IBX+M
```

```
      NT=(NES-1)*IBY+N
      MT=(NT-1)*IBX+M
      DO 114 JJ=1,NDX1
         DO 113 II=1,NDY1
            N4=4
            IF (II.EQ.NDY) N4=2
            DO 112 ND=1,N4
               JI=(II-1)*4*NDX1+(JJ-1)*4+ND
               IF (II.EQ.NDY) JI=(II-1)*4*NDX1+(JJ-1)*2+ND
               IF (II.GT.NDY) JI=(II-2)*4*NDX1+2*NDX1+(JJ-1)*4+ND
               G=0.
               GS=0.
               DO 110 NK=1,NE
                  N1=NK-JJ
                  IF (N1.GT.1) GO TO 111
                  IF (N1.LT.0) GO TO 110
                  DO 109 NES=1,NY1
                     N2=NES-II
                     IF (N2.GT.1) GO TO 110
                     IF (N2.LT.0) GO TO 109
                     IF (N1.EQ.0) GO TO 101
                     IF (N2.EQ.0) GO TO 102
                     IKL=IX3(ND)
                     GO TO 104
101                  IF (N2.EQ.0) GO TO 103
                     IKL=IX2(ND)
                     GO TO 104
102                  IKL=IX4(ND)
                     GO TO 104
103                  IKL=IX1(ND)
104                  IBF=IBX
                     IF (NK.EQ.NE) IBF=M
                     DO 108 MK=1,IBF
                        MN=(NK-1)*IBX+MK
                        NS=MM-MN+1
                        JX=JG(NS)
                        DO 107 MS=1,IBY
                           MSL=(NES-1)*IBY+MS
                           IF (NT.GT.MSL) GO TO 105
                           ISL=MSL-NT+1
                           IF (ISL.GT.JX) GO TO 108
                           GO TO 106
105                        ISL=NT-MSL+1
                           IF (ISL.GT.JX) GO TO 107
106                        XX=FLOAT(MK-1)*RBX+RBX/2.
                           YY=FLOAT(MS-1)*RBY+RBY/2.
                           CALL SHAPE (FAL,DFAL,IKL,XX,YY,BA)
                           G=G+(FAL*GRR(NS,ISL)+DFAL/KA*GRI(NS,ISL
     1                     ))*(EPISN)/AO
                           GS=GS+(FAL*GRI(NS,ISL)-DFAL/KA*GRR(NS,I
     1                     SL))*(EPISN)/AO
107                     CONTINUE
108                  CONTINUE
109               CONTINUE
110            CONTINUE
111            V(JI,MT)=G
               VS(JI,MT)=GS
112         CONTINUE
```

```
113          CONTINUE
114       CONTINUE
115    CONTINUE
116 CONTINUE
    RETURN
C
C
    END

    SUBROUTINE CHECK (R,S,BETA,SIGMA,GR)
    DIMENSION GR(2), DX(4), DY(4)
    INTEGER R,S
    COMMON /BLOCK0/ BM,UD,C,CD
    A1=2.*FLOAT(S)-1.
    A2=2.*FLOAT(S)+1.
    A3=FLOAT(2*R-1)*SIGMA/BETA
    A4=FLOAT(2*R+1)*SIGMA/BETA
    DO 101 I=1,2
       DX(I)=SIGMA*(FLOAT(R)+0.5)
       I2=I+2
101 DX(I2)=SIGMA*(FLOAT(R)-0.5)
    DO 102 I=1,4,3
102 DY(I)=FLOAT(S)+0.5
    DO 103 I=2,3
103 DY(I)=FLOAT(S)-0.5
    IF (S.EQ.0) GO TO 113
    IF (DY(1).GT.(DX(1)/BETA)) GO TO 105
    IF (DY(4).GT.(DX(4)/BETA)) GO TO 109
    DO 104 JK=1,2
       IK=JK
       CALL GIR (IK,A1,A2,A3,A4,YG3)
       GR(JK)=YG3
104 CONTINUE
    RETURN
105 IF (DY(3).GT.(DX(3)/BETA)) GO TO 107
    DO 106 IK=1,2
       CALL GIRS (IK,A1,A3,A4,YG2)
       GR(IK)=YG2
106 CONTINUE
    RETURN
107 DO 108 IK=1,2
       CALL GIRS (IK,A1,A1,A4,YG2)
       GR(IK)=YG2
108 CONTINUE
    RETURN
109 IF (DY(3).GT.(DX(3)/BETA)) GO TO 111
    DO 110 IK=1,2
       CALL GIR (IK,A1,A2,A2,A4,YG3)
       CALL GIRS (IK,A1,A3,A2,YG2)
       GR(IK)=YG3+YG2
110 CONTINUE
    RETURN
111 DO 112 IK=1,2
       CALL GIR (IK,A1,A2,A2,A4,YG3)
```

```
      CALL GIRS (IK,A1,A1,A2,YG2)
      GR(IK)=YG3+YG2
  112 CONTINUE
      RETURN
  113 IF (R.EQ.0) GO TO 120
      IF (DY(1).GT.(DX(1)/BETA)) GO TO 114
      GO TO 116
  114 DO 115 IK=1,2
      CALL OG3A (IK,A2,A4,YG)
      GR(IK)=YG
  115 CONTINUE
      RETURN
  116 IF (DY(4).GT.(DX(4)/BETA)) GO TO 118
      DO 117 IK=1,2
      CALL GIR (IK,0.,1.,A3,A4,YG3)
      GR(IK)=2.*YG3
  117 CONTINUE
      RETURN
  118 DO 119 IK=1,2
      CALL OG3A (IK,A3,1.,YG)
      CALL GIR (IK,0.,1.,1.,A4,YG3)
      GR(IK)=2.*YG3+YG
  119 CONTINUE
      RETURN
  120 IF (DY(1).LE.(DX(1)/BETA)) GO TO 122
      DO 121 IK=1,2
      CALL OG3A (IK,0.,A4,YG)
      GR(IK)=YG
  121 CONTINUE
      RETURN
  122 DO 123 IK=1,2
      CALL OG3A (IK,0.,1.,YG)
      CALL GIR (IK,0.,1.,1.,A4,YG3)
      GR(IK)=2.*YG3+YG
  123 CONTINUE
      RETURN
C
C
      END

      SUBROUTINE GIRS (IK,YS,XL,XU,YG2)
      COMMON /BLOCK0/ IM,UB,C,CB
      A=0.5*(XU+XL)
      B=XU-XL
      Y1=0.269234655*B
      Y2=0.453089923*B
      DELTA0=A
      DELTA1=A+Y1
      DELTA3=A-Y1
      DELTA2=A+Y2
      DELTA4=A-Y2
      YG2=C*(B/2.)*(0.568888889*FY(IK,DELTA0,YS,DELTA0)+0.47862867*(FY(I
     1K,DELTA1,YS,DELTA1)+FY(IK,DELTA3,YS,DELTA3))+0.236926885*(FY(IK,DE
     2LTA2,YS,DELTA2)+FY(IK,DELTA4,YS,DELTA4)))

      RETURN
C
      END
```

BEST AVAILABLE COPY

```
      FUNCTION FY(IK,DELTA,YL,YU)
      COMMON /BLOCK0/ BM,UB,C,CB
      FK(BM,DELTA,Z)=(COS(BM*SQRT(DELTA**2-Z**2))-1.)/SQRT(DELTA**2-Z**2
     1)
      A=0.5*(YU+YL)
      B=YU-YL
      Y1=0.269234655*B
      Y2=0.453089923*B
      DELTA0=A
      DELTA1=A+Y1
      DELTA3=A-Y1
      DELTA2=A+Y2
      DELTA4=A-Y2
      IF (IK.EQ.1) GO TO 101
      FY=-SIN(UB*DELTA)*(ACOS(YL/DELTA)+(B/2.)*(0.568888889*FK(BM,DELTA,
     1DELTA0)+0.47862867*(FK(BM,DELTA,DELTA1)+FK(BM,DELTA,DELTA3))+0.236
     2926885*(FK(BM,DELTA,DELTA2)+FK(BM,DELTA,DELTA4))))
      RETURN
  101 FY=COS(UB*DELTA)*(ACOS(YL/DELTA)+(B/2.)*(0.568888889*FK(BM,DELTA,D
     1ELTA0)+0.47862867*(FK(BM,DELTA,DELTA1)+FK(BM,DELTA,DELTA3))+0.2369
     2926885*(FK(BM,DELTA,DELTA2)+FK(BM,DELTA,DELTA4))))
      RETURN
C
      END

      SUBROUTINE GIR (IK,YL,YU,XL,XU,YG3)
      COMMON /BLOCK0/ BM,UB,C,CB
      A=0.5*(XU+XL)
      B=XU-XL
      Y1=0.387298334*B
      DELTA0=A
      DELTA1=A+Y1
      DELTA2=A-Y1
      YG3=C*(B/2.)*(0.888888889*FX(IK,DELTA0,YL,YU)+0.555555556*(FX(IK,D
     1ELTA1,YL,YU)+FX(IK,DELTA2,YL,YU)))
      RETURN
C
      END

      FUNCTION FX(IK,DELTA,YL,YU)
      COMMON /BLOCK0/ BM,UB,C,CB
      FS(BM,DELTA,Z)=(COS(BM*SQRT(DELTA**2-Z**2))-1.)/SQRT(DELTA**2-Z**2

     1)
      A=0.5*(YU+YL)
      B=YU-YL
      Y1=0.387298336*B
      IF (IK.EQ.1) GO TO 101
      FX=-SIN(UB*DELTA)*(ACOS(YL/DELTA)-ACOS(YU/DELTA)+(B/2.)*(0.8888888
     189*FS(BM,DELTA,A)+0.555555556*(FS(BM,DELTA,A+Y1)+FS(BM,DELTA,A-Y1)
     2)))
      RETURN
  101 FX=COS(UB*DELTA)*(ACOS(YL/DELTA)-ACOS(YU/DELTA)+(B/2.)*(0.8888888
     189*FS(BM,DELTA,A)+0.555555556*(FS(BM,DELTA,A+Y1)+FS(BM,DELTA,A-Y1))
     2))
      RETURN
C
      END
```

```
      SUBROUTINE OG3A (IK,XL,XU,YG)
      COMMON /BLOCK0/ BM,UB,C,CB
      A=0.5*(XU+XL)
      B=XU-XL
      Y1=0.269234655*B
      Y2=0.453089923*B
      Y=BM*(A+Y1)
      YY=BM*(A-Y1)
      Z=BM*(A+Y2)
      ZZ=BM*(A-Y2)
      X=BM*A
      CALL BESJ (Y,0,BJ1,0.0001,IER)
      CALL BESJ (YY,0,BJ2,0.0001,IER)
      CALL BESJ (Z,0,BJ3,0.0001,IER)
      CALL BESJ (ZZ,0,BJ4,0.0001,IER)
      CALL BESJ (X,0,BJ0,0.0001,IER)
      Y=UB*(A+Y1)
      YY=UB*(A-Y1)
      Z=UB*(A+Y2)
      ZZ=UB*(A-Y2)
      X=UB*A
      IF (IK.EQ.1) GO TO 101
      YG=-0.5*(B/2.)*(0.568888889*SIN(X)*BJ0+0.47862867*(SIN(Y)*BJ1+SIN(
     1YY)*BJ2)+0.236926885*(SIN(Z)*BJ3+SIN(ZZ)*BJ4))
      RETURN
  101 YG=0.5*(B/2.)*(0.568888889*COS(X)*BJ0+0.47862867*(COS(Y)*BJ1+COS(Y
     1Y)*BJ2)+0.236926885*(COS(Z)*BJ3+COS(ZZ)*BJ4))
      RETURN
C
      END
```

```
      SUBROUTINE BESJ (X,N,BJ,D,IER)
      BJ=.0
      IF (N) 101,102,102

  101 IER=1
      RETURN
  102 IF (X) 103,103,104
  103 IER=2
      RETURN
  104 IF (X-15.) 105,105,106
  105 NTEST=20.+10.*X-X**2/3.
      GO TO 107
  106 NTEST=90.+X/2.
  107 IF (N-NTEST) 109,108,108
  108 IER=4
      RETURN
  109 IER=0
      N1=N+1
      BPREV=.0
C
C     COMPUTE STARTING VALUE OF M
C
      IF (X-5.) 110,111,111
  110 MA=X+6.
      GO TO 112
  111 MA=1.4*X+60./X
  112 MB=N+IFIX(X)/4+2
      MZERO=MAX0(MA,MB)
C
C     SET UPPER LIMIT OF M
C
      MMAX=NTEST
      DO 121 M=MZERO,MMAX,3
C
C     SET F(M),F(M-1)
C
         FM1=1.0E-28
         FM=.0
         ALPHA=.0
         IF (M-(M/2)*2) 114,113,114
  113    JT=-1
         GO TO 115
  114    JT=1
  115    M2=M-2
         DO 118 K=1,M2
            MK=M-K
            BMK=2.*FLOAT(MK)*FM1/X-FM
            FM=FM1
            FM1=BMK
            IF (MK-N-1) 117,116,117
  116       BJ=BMK
  117       JT=-JT
            S=1+JT
  118    ALPHA=ALPHA+BMK*S
         BMK=2.*FM1/X-FM
         IF (N) 120,119,120
  119    BJ=BMK
  120    ALPHA=ALPHA+BMK
         BJ=BJ/ALPHA
         IF (ABS(BJ-BPREV)-ABS(D*BJ)) 122,122,121
  121 BPREV=BJ
      IER=3

  122 RETURN
C
      END
```

```
      SUBROUTINE SHAPE (FA,DFA,IK,X,Y,BA)
      F1(Z)=1.+2.*(Z**3)-3.*(Z**2)
      F2(Z)=Z*((Z-1.)**2)
      F4(Z)=(Z**3)-(Z**2)
      DF1(Z)=6.*(Z**2)-6.*Z
      DF2(Z)=3.*(Z**2)-4.*Z+1.
      DF4(Z)=3.*(Z**2)-2.*Z
      IF (IK.EQ.0) GO TO 106
      IF (IK.EQ.1.OR.IK.EQ.3.OR.IK.EQ.5.OR.IK.EQ.7) GO TO 101
      IF (IK.EQ.2.OR.IK.EQ.4.OR.IK.EQ.6.OR.IK.EQ.8) GO TO 102
      IF (IK.EQ.9.OR.IK.EQ.11.OR.IK.EQ.13.OR.IK.EQ.15) GO TO 103
      IF (IK.EQ.10.OR.IK.EQ.12.OR.IK.EQ.14.OR.IK.EQ.16) GO TO 104
  101 AA=F1(X)
      CC=DF1(X)
      GO TO 105
  102 AA=F2(X)
      CC=DF2(X)
      GO TO 105
  103 AA=1.-F1(X)
      CC=-DF1(X)
      GO TO 105
  104 AA=F4(X)
      CC=DF4(X)
  105 IF (IK.EQ.1.OR.IK.EQ.2.OR.IK.EQ.13.OR.IK.EQ.14) BB=F1(Y)
      IF (IK.EQ.3.OR.IK.EQ.4.OR.IK.EQ.15.OR.IK.EQ.16) BB=F2(Y)*BA
      IF (IK.EQ.5.OR.IK.EQ.6.OR.IK.EQ.9.OR.IK.EQ.10) BB=1.-F1(Y)
      IF (IK.EQ.7.OR.IK.EQ.8.OR.IK.EQ.11.OR.IK.EQ.12) BB=F4(Y)*BA
      FA=AA*BB
      DFA=CC*BB
      RETURN
  106 FA=0.
      DFA=0.
      RETURN
C
      END
```

```
PANEL FLUTTER FOR CLAMPED PANEL

LENGTH-WIDTH RATIO = 1.000
CHORDWISE ELEMENT LENGTH = 1.000   SPANWISE ELEMENT WIDTH = 1.000

BOX WIDTH =  .500   RATIO OF BOX LENGTH TO BOX WIDTH =  .500

REDUCED FREQUENCY =  .500

INITIAL IN-PLANE FORCE PARAMETER=  .100

MACH NUMBER = 1.20

STRUCTURAL DAMPING COEFFICIENT =   0.000


DENSITY RATIO MU=   .01500

EIGENVALUE=  5.09752E-01 -1.44227E-02    G =  -.02829  FREQUENCY RATIO =  .71404  STIFFNESS PARAMETER =   .35702
EIGENVECTOR
2.71207E-01 1.73227E-03 3.49503E-01-6.74931E-04 3.81089E-01-1.28203E-03 4.54907E-01-5.78048E-03 5.15697E-01-5.75751E-03
7.94798E-02-1.14777E-02 6.93768E-01-1.03775E-02-2.26185E-02-9.57563E-03 3.60810E-01-1.24987E-02-3.70762E-01 3.94762E-03
4.70692E-01-1.03057E-02-5.14060E-01 1.27013E-02 5.00000E-01 0.          6.26550E-01-4.83439E-03 9.23917E-01-1.21921E-02
1.12643E-01-1.46563E-02 6.32644E-01-1.74853E-02-6.53218E-01 9.42035E-03

EIGENVALUE=  1.31424E-01  5.67010E-04    G =   .00431  FREQUENCY RATIO =  .30252  STIFFNESS PARAMETER =   .18125
EIGENVECTOR
-1.60359E-01-1.27951E-02-1.36713E-01-5.06522E-03-1.94742E-01-1.56964E-02-1.16354E-01-8.20409E-03-9.96963E-03 4.70427E-03
 4.39146E-01 2.77076E-02 7.02060E-02-1.60734E-02 6.51616E-01-2.97707E-03 3.58316E-01 8.31471E-03 6.65135E-03-1.87267E-02
 5.29156E-01-3.09380E-02-1.84926E-01-1.33035E-02-2.63591E-01-2.33017E-02-1.78307E-01-1.45153E-02 6.40818E-02-1.49576E-0[illegible]
 8.15829E-01 1.43044E-02 6.92169E-01-2.27189E-02-5.56703E-02-1.28074E-02

EIGENVALUE=  7.18589E-02 -7.13719E-04    G =  -.00993  FREQUENCY RATIO =  .26807  STIFFNESS PARAMETER =   .13403
EIGENVECTOR
 3.30569E-01-7.85365E-03 4.15737E-01 6.45275E-04-3.41736E-01-7.91461E-03-4.82366E-01-7.69072E-03 5.69927E-01 2.40738E-02
-2.52618E-02 5.61690E-02-6.72746E-01-2.88038E-02-2.65645E-01-1.18713E-02 2.97272E-01 6.31795E-02-4.00658E-01-9.24970E-03
-5.76016E-01 4.70239E-03 4.13108E-01 2.84316E-02-2.93596E-01-1.34572E-02-3.40882E-01-2.06150E-02-5.51195E-01-2.77998E-02
-1.63270E-01 1.93235E-02-5.31106E-01 2.46954E-02 3.20200E-01 4.10527E-02

EIGENVALUE=  5.16318E-02  1.32179E-03    G =   .03722  FREQUENCY RATIO =  .22727  STIFFNESS PARAMETER =   .11363
EIGENVECTOR
-1.17736E-01 5.32891E-02-1.65449E-02 8.54458E-02 3.03037E-02-1.34324E-01 1.72478E-01-5.95052E-02 9.16944E-02 7.10449E-02
 2.07306E-01-1.70097E-01 2.28433E-01 5.52996E-02-1.56286E-01 2.06447E-01-1.70349E-01-2.79402E-01-4.32421E-01-2.13038E-01
-6.76704E-01-2.76921E-02-8.88333E-01-1.71284E-01-5.09649E-02-1.27769E-01 1.55512E-01 3.37926E-03 2.50693E-01 1.03309E-01
-1.05555E-01 1.80141E-01-7.06750E-01-1.45835E-01-9.32594E-01-3.63306E-01
```

```
EIGENVALUE=  4.99984E-02 -2.70008E-03    G =  -.05500  FREQUENCY RATIO =  .22165  STIFFNESS PARAMETER =   .11083
EIGENVECTOR
-1.63754E-01 2.58694E-01-1.30407E-01 1.10518E-01 2.57932E-01-2.16057E-01 1.84875E-01-3.37519E-01-3.55089E-02-3.32093E-02
 4.35613E-01-5.33176E-01-5.87049E-02-2.04364E-01-5.63612E-01 5.35764E-01 4.60902E-01-9.16208E-02 1.67570E-01 4.03024E-01
-1.89898E-01 6.52879E-01 2.36540E-01 6.31718E-01 2.19078E-01-1.39609E-01 7.43524E-02-2.13390E-01-1.06027E-01-2.17721E-01
-4.58719E-01 3.40671E-01-3.08150E-02 6.19561E-01 4.61583E-01 6.10616E-01

DENSITY RATIO MU=   .02500

EIGENVALUE=  5.32925E-01 -2.16467E-02    G =  -.04062  FREQUENCY RATIO =  .73017  STIFFNESS PARAMETER =   .36508

EIGENVECTOR
 2.50000E-01 0.           3.41448E-01-3.51760E-03 3.61083E-01-5.53808E-03 4.56446E-01-1.23192E-02 5.20538E-01-1.24326E-02
 1.25275E-01-1.74406E-02 7.07136E-01-2.16722E-02 2.88874E-02-1.38357E-02 3.96015E-01-2.21435E-02-3.76765E-01 7.79875E-03
 5.10147E-01-2.03298E-02-5.41673E-01 2.31675E-02 4.69379E-01-4.82755E-03 6.22640E-01-1.21634E-02 9.38408E-01-2.59552E-02
 1.84782E-01-2.29647E-02 6.89759E-01-3.27375E-02-6.68778E-01 1.85861E-02

EIGENVALUE=  1.38812E-01  1.04935E-03    G =   .00756  FREQUENCY RATIO =  .37258  STIFFNESS PARAMETER =   .18629
EIGENVECTOR
-1.04603E-01-8.68992E-03-1.16775E-01-2.49426E-03-1.23101E-01-1.31556E-02-8.71043E-02-9.96728E-03-3.76974E-03 8.18527E-03
 3.75465E-01 2.41706E-02 1.10173E-01-2.36345E-02 6.18405E-01-2.38567E-02 4.03026E-01 7.76814E-05 8.77280E-02-3.10660E-02
 6.36505E-01-6.61053E-02-9.69061E-02-2.79283E-02-1.64549E-01-1.93819E-02-1.35186E-01-1.59207E-02 1.06455E-01-2.17587E-02
 7.49558E-01-6.43066E-03 8.15534E-01-5.92423E-02 5.58570E-02-2.93602E-02

EIGENVALUE=  7.65897E-02 -2.53252E-03    G =  -.03307  FREQUENCY RATIO =  .27679  STIFFNESS PARAMETER =   .13839
EIGENVECTOR
 4.12027E-01-1.95277E-01 6.65281E-01-2.99352E-01-4.14071E-01 1.57604E-01-6.30450E-01 2.42194E-01 9.68509E-01-3.81281E-01
 7.40915E-02 1.04675E-01-9.69439E-01 3.72827E-01-7.93337E-01 4.36014E-01 2.24850E-01 1.43230E-01-1.06373E+00 5.65499E-01
-1.59247E+00 9.96205E-01 6.75860E-02 2.77023E-01-3.81301E-01 1.32272E-01-4.26051E-01 1.25330E-01-7.43764E-01 2.73503E-01
-5.60018E-01 4.05967E-01-1.61428E+00 1.07460E+00-2.28128E-01 4.43508E-01

EIGENVALUE=  6.29265E-02  2.92551E-03    G =   .04649  FREQUENCY RATIO =  .25092  STIFFNESS PARAMETER =   .12546
EIGENVECTOR
-1.06237E-02 2.48302E-02-3.42036E-03 2.35291E-02-2.76617E-03-2.01850E-02 1.77626E-02-3.92211E-02 5.77140E-03 3.09169E-03
-1.29227E-03-5.63873E-02 4.29342E-02-4.21253E-02 2.70701E-03 3.83218E-02-1.00462E-01 1.50242E-02-1.14810E-01 6.88837E-02
-1.19270E-01 1.46426E-01-1.87306E-01 2.20100E-01-5.45281E-03-1.51556E-02 1.89380E-02-2.47087E-02 5.00192E-02-3.71381E-02
 1.54123E-03 3.17613E-02-1.59034E-01 1.47531E-01-2.39997E-01 2.00764E-01

EIGENVALUE=  5.60590E-02 -5.09036E-03    G =  -.09080  FREQUENCY RATIO =  .23701  STIFFNESS PARAMETER =   .11851
EIGENVECTOR
-1.55215E-01-8.35883E-02-1.24132E-01-7.18035E-02 1.34613E-01 1.19970E-01 2.43910E-01 1.35685E-01 3.72302E-02 2.84460E-02
 4.04032E-01 3.31513E-01 1.89025E-01-2.16774E-02-3.12504E-01-3.62939E-01 1.07862E-02 4.01859E-01-4.18115E-01 1.12980E-01
-6.03619E-01-2.30812E-01-8.84097E-01 3.72805E-02 9.51827E-02 9.89955E-02 1.36316E-01 6.32020E-02 1.76155E-01-5.39036E-02
-1.97373E-01-2.93916E-01-6.62807E-01-9.57312E-02-8.41283E-01 2.48088E-01
```

```
DENSITY RATIO MU=   .03500

EIGENVALUE=  5.48314E-01 -2.74249E-02    G =  -.05002  FREQUENCY RATIO =  .74071  STIFFNESS PARAMETER =   .37036
EIGENVECTOR
 1.30468E-01 1.85881E-03 1.88863E-01 6.22261E-04 1.94158E-01-1.26495E-03 2.59137E-01-4.89550E-03 2.97823E-01-4.05282E-03
 9.75207E-02-1.08678E-02 4.09453E-01-9.65306E-03 4.76952E-02-9.85934E-03 2.45424E-01-1.25471E-02-2.15796E-01 1.42145E-03
 3.11886E-01-1.11287E-02-3.22890E-01 1.16760E-02 2.50000E-01 0.          3.50007E-01-3.26934E-03 5.41070E-01-1.04582E-02
 1.47464E-01-1.44788E-02 4.27525E-01-1.80856E-02-3.86984E-01 6.75952E-03

EIGENVALUE=  1.46696E-01  9.67724E-04    G =   .00660  FREQUENCY RATIO =  .38301  STIFFNESS PARAMETER =   .19151
EIGENVECTOR
-1.00681E-01-4.54288E-03-1.37432E-01 4.11746E-03-1.04070E-01-1.61930E-02-7.07381E-02-1.98360E-02 1.70118E-02 1.59592E-02
 5.04615E-01 1.65530E-02 2.40488E-01-5.84057E-02 9.08979E-01-9.15125E-02 7.03397E-01-3.74541E-02 2.57288E-01-7.88166E-02
 1.15589E+00 1.95723E-01-5.16120E-03-7.69797E-02-1.39487E-01-2.24390E-02-1.20844E-01-2.58449E-02 2.45044E-01-5.47607E-02
 1.07955E+00-7.06030E-02 1.46338E+00-1.98238E-01 2.66987E-01-8.98861E-02

EIGENVALUE-  8.67425E-02 -5.55596E-03    G =  -.06405  FREQUENCY RATIO =  .29467  STIFFNESS PARAMETER =   .14734
EIGENVECTOR
-2.65344E-02 7.17694E-03-6.20735E-02 7.39889E-03 2.85026E-02 1.56747E-04 4.16231E-02-6.01985E-03-1.01876E-01-7.78799E-04
-2.22429E-02-1.74389E-02 9.45134E-02-1.92665E-02 1.89510E-01-2.90839E-02 1.02498E-01-8.84133E-04 2.81119E-01 1.47933E-02
 4.72562E-01-2.33414E-02 2.81382E-01 6.12224E-03 3.02008E-02 2.13243E-03 2.87092E-02-2.07017E-03 6.98936E-02-2.00229E-02
 1.62050E-01-3.47974E-02 5.19229E-01-2.77407E-02 3.56760E-01 2.27551E-02

EIGENVALUE=  7.20165E-02  3.63030E-03    G =   .05041  FREQUENCY RATIO =  .26844  STIFFNESS PARAMETER =   .13422
EIGENVECTOR
 2.07282E-01 7.79365E-03 2.86757E-01 2.15528E-02-8.09929E-02 2.52052E-02-2.66363E-01-9.98767E-03 2.06329E-01 1.49953E-01

-2.14335E-01 3.67896E-01-5.01226E-01-1.56516E-01-7.64090E-02-3.00804E-01 9.21890E-01 6.08058E-01 1.10741E+00 9.23584E-02
 1.49016E+00-5.37328E-01 2.72452E+00-4.78647E-01-5.44011E-02 2.01386E-02-1.62693E-01-4.64047E-02-4.57607E-01-1.94180E-01
-2.30232E-02-2.30086E-01 1.80859E+00-2.79209E-01 2.97406E+00 4.91414E-04

EIGENVALUE=  6.19934E-02 -6.25723E-03    G =  -.10108  FREQUENCY RATIO =  .24912  STIFFNESS PARAMETER =   .12456
EIGENVECTOR
-2.06958E-01 9.02497E-02-2.19528E-01 1.31835E-01 2.36222E-01-2.01705E-02 4.06739E-01-9.22614E-02 1.19965E-01 1.07294E-01
 9.49457E-01-2.85526E-02 1.81907E-01-2.51758E-01-7.65737E-01-2.18981E-01 7.27124E-01 6.81490E-01-3.02801E-01 7.76834E-01
-1.54335E+00 4.31526E-01-1.69652E+00 1.22374E+00 1.88221E-01-7.25742E-03 2.04225E-01-3.94037E-02 8.80376E-02-2.53765E-01
-6.17539E-01-2.59016E-01-1.25672E+00 6.21582E-01-1.09660E+00 1.52778E+00

DENSITY RATIO MU=   .04500

EIGENVALUE=  5.54946E-01 -3.18754E-02    G =  -.05744  FREQUENCY RATIO =  .74525  STIFFNESS PARAMETER =   .37263
EIGENVECTOR
 1.27393E-01 2.36980E-03 1.95585E-01 1.52735E-03 1.96141E-01-1.54294E-03 2.76377E-01-5.49729E-03 3.20769E-01-3.72462E-03
 1.34285E-01-1.25434E-02 4.47522E-01-1.12455E-02 8.84213E-02-1.24174E-02 2.89749E-01-1.50521E-02-2.31148E-01-8.35919E-05
 3.58810E-01-1.30102E-02-3.61675E-01 1.33098E-02 2.50000E-01 0.          3.69389E-01-3.11467E-03 5.88394E-01-1.15392E-02
 2.07382E-01-1.71204E-02 5.01989E-01-2.21087E-02-4.20157E-01 6.27684E-03
```

```
DENSITY RATIO MU=   .03500

EIGENVALUE=  5.48314E-01 -2.74249E-02    G =  -.05002  FREQUENCY RATIO =  .74071  STIFFNESS PARAMETER =   .37036
EIGENVECTOR
1.30468E-01 1.85881E-03 1.88868E-01 6.22261E-04 1.94158E-01-1.26495E-03 2.59137E-01-4.89550E-03 2.97823E-01-4.05382E-03
9.75207E-02-1.08678E-02 4.09453E-01-9.65306E-03 4.76952E-02-9.85994E-03 2.46424E-01-1.25471E-02-2.15796E-01 1.42145E-03
3.11886E-01-1.11287E-02-3.22890E-01 1.16760E-02 2.50000E-01 0.          3.50007E-01-3.26934E-03 5.41070E-01-1.04682E-02
1.47464E-01-1.44788E-02 4.27525E-01-1.80853E-02-3.86984E-01 6.75952E-03

EIGENVALUE=  1.46690E-01  9.67724E-04    G =   .00660  FREQUENCY RATIO =  .38301  STIFFNESS PARAMETER =   .19151
EIGENVECTOR
-1.00881E-01-4.54288E-03-1.37439E-01 4.11746E-03-1.04070E-01-1.61980E-02-7.07381E-02-1.99360E-02 1.70118E-02 1.59562E-02
 5.04615E-01 1.65530E-02 2.49488E-01-5.84057E-02 9.08978E-01-9.15125E-02 7.03397E-01-3.74541E-02 2.57288E-01-7.86166E-02
 1.15589E+00 1.95723E-01-5.16120E-03-7.69797E-02-1.39487E-01-2.24390E-02-1.20644E-01-2.58449E-02 2.45944E-01-5.47607E-02
 1.07955E+00-7.06030E-02 1.46308E+00-1.98238E-01 2.66987E-01-8.98861E-02

EIGENVALUE=  8.67425E-02 -5.55596E-03    G =  -.06405  FREQUENCY RATIO =  .29467  STIFFNESS PARAMETER =   .14734
EIGENVECTOR
-2.65344E-02 7.17694E-03-6.20715E-02 7.39889E-03 2.85026E-02 1.56747E-04 4.16231E-02-6.01985E-03-1.07876E-01-7.78799E-04
-2.22429E-02-1.74389E-02 9.45134E-02-1.92665E-02 1.89510E-01-2.90898E-02 1.02498E-01-8.84133E-04 2.81115E-01 1.47955E-02
 4.72552E-01-3.35414E-02 2.81382E-01 6.12324E-03 3.02008E-02 2.13243E-03 2.87092E-02-2.07017E-03 6.98916E-02-2.00229E-02
 1.62050E-01-3.47974E-02 5.19329E-01-2.77407E-02 3.56760E-01 2.27551E-02

EIGENVALUE=  7.20165E-02  3.63030E-03    G =   .05041  FREQUENCY RATIO =  .26844  STIFFNESS PARAMETER =   .13422
EIGENVECTOR
2.07282E-01 7.79365E-03 2.86757E-01 2.15528E-02-8.09929E-02 2.52052E-02-2.66363E-01-9.98767E-03 2.06329E-01 1.49953E-01

-2.14335E-01 3.67896E-01-5.01226E-01-1.56516E-01-7.64090E-02-3.00804E-01 9.21890E-01 6.08058E-01 1.10741E+00 9.23564E-02
 1.49016E+00-5.37328E-01 2.72452E+00-4.78647E-01-5.44011E-02 2.01326E-02-1.62693E-01-4.64047E-02-4.57907E-01-1.94180E-01
-2.30232E-02-2.30086E-01 1.80859E+00-2.79209E-01 2.97406E+00 4.91414E-04

EIGENVALUE=  6.19034E-02 -6.25723E-03    G =  -.10108  FREQUENCY RATIO =  .24912  STIFFNESS PARAMETER =   .12456
EIGENVECTOR
-2.06552E-01 9.02497E-02-2.19528E-01 1.31835E-01 2.36222E-01-2.01705E-02 4.06739E-01-9.22614E-02 1.19982E-01 1.07294E-01
 9.49457E-01-2.85626E-02 1.81907E-01-2.51753E-01-7.65737E-01-2.18981E-01 7.27124E-01 6.21490E-01-3.02801E-01 7.76874E-01
-1.54335E+00 4.31526E-01-1.69452E+00 1.22374E+00 1.88221E-01-7.25742E-03 2.04225E-01-3.94037E-02 8.20376E-02-2.53765E-01
-6.17539E-01-2.50016E-01-1.25672E+00 6.21522E-01-1.09660E+00 1.52778E+00

DENSITY RATIO MU=   .04500

EIGENVALUE=  5.54946E-01 -3.18754E-02    G =  -.05744  FREQUENCY RATIO =  .74525  STIFFNESS PARAMETER =   .37263
EIGENVECTOR
1.27393E-01 2.36980E-03 1.95585E-01 1.52735E-03 1.96141E-01-1.54294E-03 2.76377E-01-5.49729E-03 3.20769E-01-3.72462E-03
1.34285E-01-1.25434E-02 4.47522E-01-1.12455E-02 8.84213E-02-1.24174E-02 2.89749E-01-1.50521E-02-2.31148E-01-8.35919E-05
3.58810E-01-1.30102E-02-3.61675E-01 1.33098E-02 2.50000E-01 0.          3.69389E-01-3.11467E-03 5.88394E-01-1.15392E-02
2.07382E-01-1.71204E-02 5.01989E-01-2.21087E-02-4.20157E-01 6.27684E-03
```

```
EIGENVALUE=  8.48193E-02  2.79160E-02    G =   .32912  FREQUENCY RATIO =  .29505  STIFFNESS PARAMETER =   .14753
EIGENVECTOR
 2.73838E-02 3.08450E-02 6.87357E-02 1.86055E-02 5.64523E-02-1.08934E-02 9.36030E-02-7.34521E-03 9.79577E-03 5.52887E-02
-1.06542E-01 1.49245E-01 4.53610E-02-5.25170E-02-4.51729E-02 1.06927E-01 3.61157E-01 1.96636E-01 6.09093E-01-1.26203E-01
 6.08063E-01-1.34523E-01 8.09825E-01-5.47811E-01 6.39462E-02-3.19843E-03 1.22536E-01-5.58964E-02 4.81070E-02-5.04236E-02
-8.19423E-02 1.33127E-01 7.37270E-01-3.91096E-02 1.03565E+00-3.98229E-01

EIGENVALUE=  9.44164E-02 -1.12974E-02    G =  -.11966  FREQUENCY RATIO =  .30782  STIFFNESS PARAMETER =   .15391
EIGENVECTOR
-6.50417E-02 2.67698E-03-1.47682E-01-3.19608E-02 1.28629E-01 1.02468E-01 2.78463E-01 2.37084E-01-2.94163E-01-3.24131E-01
-1.45058E-01-5.69548E-01 5.22790E-01 4.35277E-01 6.32014E-01 5.71665E-01 3.14075E-01 1.76762E-01 9.66599E-01 1.44018E+00
 1.77823E+00 2.38668E+00 1.10025E+00 2.37102E+00 1.46164E-01 1.40600E-01 2.62813E-01 3.03762E-01 4.65054E-01 4.22576E-01
 5.07297E-01 3.96929E-01 1.81207E+00 2.46367E+00 1.22857E+00 2.43933E+00

EIGENVALUE=  7.07209E-02 -2.57349E-02    G =  -.36389  FREQUENCY RATIO =  .27017  STIFFNESS PARAMETER =   .13508
EIGENVECTOR
-2.16520E-02-7.39854E-02 5.42405E-02-1.29479E-01 9.87012E-02-3.02939E-02 2.35089E-01 2.51194E-02-2.24012E-02-1.03209E-01
-2.62906E-01 4.87816E-03 7.57333E-02 8.53733E-02-3.49689E-01-3.16834E-02 2.04445E-01-1.68266E-01 8.66318E-01-3.53159E-01
 9.34454E-01-4.67458E-01 2.05383E+00-4.36256E-01 9.20346E-02-3.59456E-02 2.24342E-01-1.80030E-02 8.40527E-02 6.22851E-02
-3.45990E-01-4.83319E-02 9.99320E-01-6.11273E-01 2.05250E+00-5.98346E-01

DENSITY RATIO MU=   .06500

EIGENVALUE=  5.27670E-01 -3.58407E-02    G =  -.06792  FREQUENCY RATIO =  .72683  STIFFNESS PARAMETER =   .36341
EIGENVECTOR
 1.17861E-01 3.74064E-03 2.09554E-01 4.78854E-03 2.01613E-01-2.15845E-03 3.23816E-01-6.11582E-03 3.87713E-01 1.67754E-04
 2.55066E-01-1.28055E-02 5.57428E-01-1.30575E-02 2.34814E-01-1.71986E-02 4.39353E-01-1.77942E-02-2.64790E-01-7.61677E-03
 5.62942E-01-1.86250E-02-4.75681E-01 1.34288E-02 2.50000E-01 0.          4.20779E-01-1.46708E-03 7.34520E-01-1.05166E-02
 4.12510E-01-1.91731E-02 7.65900E-01-2.81871E-02-5.06411E-01 2.99491E-04

EIGENVALUE=  2.64673E-01 -1.71390E-02    G =  -.06476  FREQUENCY RATIO =  .51473  STIFFNESS PARAMETER =   .25737
EIGENVECTOR
 4.37902E-03-1.74077E-03 5.37378E-02-2.68016E-03 7.65742E-02-1.81183E-02 2.11679E-01-3.34171E-02 2.93609E-01-7.69874E-03
 5.56066E-01-4.77464E-03 6.17164E-01-6.15874E-02 8.24343E-01-4.75925E-02 8.71307E-01-2.55735E-02 4.16254E-02-1.58885E-02
 1.28022E+00-8.57642E-02-3.32455E-01 1.78597E-02 8.07261E-02-1.97224E-02 2.39815E-01-3.43112E-02 7.36350E-01-6.13420E-02
 1.07183E+00-3.93471E-02 1.66740E+00-9.01435E-02-1.18517E-01 9.10428E-03

EIGENVALUE=  9.43066E-02  4.74660E-02    G =   .50332  FREQUENCY RATIO =  .31614  STIFFNESS PARAMETER =   .15807
EIGENVECTOR
 3.75712E-02 3.20938E-02 8.54917E-02-2.39622E-03 7.13685E-02-6.41912E-03 1.11777E-01-8.49976E-02 1.11131E-02 4.19844E-02
-1.15614E-01 1.83143E-01 6.38045E-02-2.17715E-02-3.13250E-02 2.07451E-01 3.60966E-01 1.63741E-01 5.67700E-01-2.30429E-01
 5.86131E-01-8.42902E-02 6.32171E-01-6.69970E-01 8.33220E-02 6.13906E-03 1.53548E-01-7.26543E-02 6.85757E-02-1.92454E-02
-8.03509E-02 2.44447E-01 7.18405E-01 5.82379E-03 8.75560E-01-5.69090E-01

EIGENVALUE=  8.23575E-02 -4.36470E-02    G =  -.52997  FREQUENCY RATIO =  .29628  STIFFNESS PARAMETER =   .14814
EIGENVECTOR
-6.53250E-02-3.29323E-02-3.08282E-02-1.23946E-01 1.23157E-02-1.53127E-01 1.67850E-01-2.62841E-01-9.31677E-02-8.61446E-03
-2.67322E-01 2.10478E-01 8.41301E-02-1.22756E-01-3.57774E-01 1.98189E-01-2.49962E-01-5.54812E-01 4.23183E-01-9.79671E-01
 6.07352E-02-1.12514E+00 1.03143E+00-1.61394E+00 1.84736E-03-1.60736E-01 1.43943E-01-2.90617E-01 6.91950E-02-1.28770E-01
-4.18761E-01 2.20633E-01-1.53191E-02-1.31363E+00 9.67500E-01-1.83985E+00
```

```
EIGENVALUE=  9.39877E-02 -2.03312E-02     G =  -.82270  FREQUENCY RATIO =  .30845  STIFFNESS PARAMETER =   .15422
EIGENVECTOR
1.13344E-01 4.51405E-02 1.73692E-01 1.76758E-01-1.92134E-01-7.48691E-02-3.89459E-01-3.08710E-01 9.36626E-03 5.83171E-01
-5.99415E-01 7.17461E-01-3.51915E-01-3.24207E-01 1.84633E-01-1.05739E+00-8.97665E-01 2.37370E-02-3.65748E-01-1.78309E+00
5.34947E-01-2.16125E+00 1.84537E+00-1.15457E+00-1.77927E-01-1.36909E-01-2.57578E-01-3.96383E-01-2.22149E-01-7.26884E-01

2.12438E-01-5.99033E-01 1.89346E-01-2.09634E+00 4.10725E-01-1.45633E+00

DENSITY RATIO MU=   .07500

EIGENVALUE=  4.28697E-01 -1.50065E-02     G =  -.03570  FREQUENCY RATIO =  .65495  STIFFNESS PARAMETER =   .32743
EIGENVECTOR
9.91578E-02 8.90697E-03 2.19630E-01 1.14132E-02 2.10383E-01-4.01199E-03 4.01410E-01-1.56619E-02 5.08321E-01-1.64673E-03
5.14823E-01-3.91934E-02 8.11365E-01-4.56170E-02 5.88036E-01-7.34697E-02 7.91200E-01-6.88831E-02-2.78021E-01-3.08095E-02
1.04783E+00-9.65312E-02-6.54743E-01 2.42663E-02 2.50000E-01 0.          5.00525E-01-7.07869E-03 1.02428E+00-4.03991E-02
8.81877E-01-7.85979E-02 1.41101E+00-1.23976E-01-6.07372E-01-1.20143E-02

EIGENVALUE=  4.06918E-01 -4.62001E-02     G =  -.11356  FREQUENCY RATIO =  .63885  STIFFNESS PARAMETER =   .31942
EIGENVECTOR
1.56612E-01-3.31363E-01 3.90745E-01-7.49090E-01 3.05106E-01-7.53539E-01 7.05247E-01-1.45245E+00 9.97612E-01-1.78519E+00
1.15010E+00-1.87363E+00 1.56289E+00-2.95974E+00 1.36144E+00-2.28837E+00 1.70938E+00-2.89987E+00-5.05444E-01 9.05852E-01
2.29079E+00-3.90012E+00-1.24198E+00 2.37998E+00 3.99185E-01-8.85854E-01 8.92579E-01-1.78411E+00 1.99059E+00-3.69477E+00
2.00456E+00-3.25579E+00 3.07201E+00-5.22387E+00-1.08923E+00 2.10410E+00

EIGENVALUE=  1.01304E-01  6.52020E-02     G =   .64363  FREQUENCY RATIO =  .33300  STIFFNESS PARAMETER =   .16650
EIGENVECTOR
4.70399E-02 3.68425E-02 1.03030E-01-1.48487E-02 8.30204E-02-2.57378E-03 1.84279E-01-9.69425E-02 1.57537E-02 3.75457E-02
-1.23086E-01 2.07605E-01 6.87556E-02-6.04737E-03-3.40678E-02 2.65492E-01 3.58183E-01 1.45538E-01 5.26127E-01-2.98579E-01
5.60680E-01-5.71072E-02 5.13856E-01-7.43009E-01 9.83163E-02 1.45918E-02 1.77531E-01-8.51432E-02 7.61216E-02-3.19287E-03
-9.02798E-02 3.09101E-01 6.94834E-01 1.96797E-02 7.63207E-01-6.73596E-01

EIGENVALUE=  8.93778E-02 -6.19355E-02     G =  -.69297  FREQUENCY RATIO =  .31474  STIFFNESS PARAMETER =   .15737
EIGENVECTOR
-6.05321E-02-3.77777E-02-1.21006E-02-1.31507E-01-2.20041E-02-1.46934E-01 1.12686E-01-2.66333E-01-5.95163E-02-4.02838E-01
-2.43573E-01 2.31092E-01 1.33265E-02-1.21737E-01-3.81043E-01 2.09726E-01-2.71748E-01-4.48330E-01 3.14103E-01-8.20631E-01
-1.19456E-01-9.07420E-01 8.21760E-01-1.26642E+00-3.84838E-02-1.57821E-01 9.14712E-02-3.03456E-01 3.83135E-03-1.27535E-01
-4.31202E-01 2.61927E-01-2.32374E-01-1.05828E+00 7.46103E-01-1.47328E+00

EIGENVALUE=  1.00212E-01 -2.73917E-02     G =  -.27334  FREQUENCY RATIO =  .31945  STIFFNESS PARAMETER =   .15973
EIGENVECTOR
1.17849E-01 5.19427E-02 1.51406E-01 2.04656E-01-1.89757E-01-3.48161E-02-3.87223E-01-2.38992E-01-1.05652E-01 4.81638E-01
-7.26005E-01 3.59766E-01-1.67419E-01-7.51566E-01 5.97041E-01-9.30731E-01-7.74589E-01-1.85602E-01 9.29666E-02-1.32174E+00
1.02014E+00-9.12196E-01 1.15032E+00 7.55451E-01-1.60316E-01-8.90751E-02-2.17493E-01-3.00128E-01-5.77106E-02-6.04771E-01
4.95292E-01-4.40683E-01 6.59070E-01-8.33513E-01 4.69059E-01 1.65958E-02

DENSITY RATIO MU=   .08500

EIGENVALUE=  4.53302E-01  1.12032E-01     G =   .24715  FREQUENCY RATIO =  .67832  STIFFNESS PARAMETER =   .33916
EIGENVECTOR
-5.14835E-02 2.64032E-02-8.94650E-02 7.87637E-02-7.29096E-02 7.40772E-02-1.07526E-01 1.63074E-01-1.31170E-01 2.14023E-01
-2.85796E-02 2.59027E-01-1.48723E-01 3.50530E-01 3.14726E-02 2.90216E-01-5.40799E-02 3.70376E-01 1.37772E-01-1.15778E-01
-4.15239E-02 4.77348E-01 1.55138E-01-3.07168E-01-9.25319E-02 8.33570E-02-1.49746E-01 1.95971E-01-2.09430E-01 4.37918E-01
-1.60196E-02 4.36990E-01-6.93967E-02 6.49781E-01 2.14071E-01-2.63845E-01
```

```
EIGENVALUE=  4.20653E-01 -1.91773E-01     G =  -.42596  FREQUENCY RATIO =  .60724  STIFFNESS PARAMETER =   .33362
EIGENVECTOR
7.06038E-02-1.22011E-01 2.04812E-01-2.26934E-01 1.85846E-01-2.17265E-01 4.10327E-01-3.82880E-01 5.31832E-01-3.47691E-01
6.19911E-01-1.04004E-01 8.80[illegible]E-01-1.75591E-01 7.43647E-01 6.84563E-03 8.97435E-01-2.16[illegible]E-01-2.87525E-01 3.13235E-01
1.20582E+00-2.21[illegible]E-01-7.43219E-01 4.61913E-01 2.13[illegible]E-01-2.71251E-01 5.0[illegible]E-01-4.25[illegible]E-01 1.09787E+00-5.24705E-01
1.07623E+00-1.07558E-01 1.61482E+00-3.29700E-01-6.55093E-01 5.58429E-01

EIGENVALUE=  1.07486E-01  8.16771E-02     G =   .75939  FREQUENCY RATIO =  .34820  STIFFNESS PARAMETER =   .17410
EIGENVECTOR
-8.32747E-03 3.10637E-02-1.37939E-01 7.31643E-02-1.15187E-01 3.28830E-02-1.27010E-01 1.89958E-01-3.70531E-02-3.65371E-02
7.92718E-02-3.27[illegible]E-01-8.53[illegible]E-02 2.12[illegible]E-02-5.43459E-02-3.91[illegible]E-01-4.20[illegible]E-01-3.52[illegible]E-02-4.[illegible]E-01 6.[illegible]E-01
-6.51139E-01 2.72490E-01-2.43301E-01 1.13551E+00-1.45368E-01 1.30463E-02-2.09733E-01 1.91831E-01-1.02[illegible]E-01 9.11203E-02
-6.40624E-03-4.74705E-01-8.50311E-01 2.17735E-01-5.72095E-01 1.16927E+00

EIGENVALUE=  9.47[illegible]E-02 -7.87858E-02     G =  -.83124  FREQUENCY RATIO =  .23018  STIFFNESS PARAMETER =   .16509
EIGENVECTOR
1.96334E-02 5.03[illegible]E-02-5.44[illegible]E-02 8.60029E-02-3.61831E-02 9.84935E-02-1.61350E-01 1.13900E-01 2.50692E-02 2.13[illegible]E-0[illegible]
2.29797E-01-4.68[illegible]E-02-3.54[illegible]E-02 6.92558E-02 3.20006E-01 2.20031E-02 9.63[illegible]E-0[illegible] 3.25[illegible]E-01-4.55[illegible]E-01 3.09[illegible]E-01
-2.05[illegible]E-01 5.21105E-01-8.7[illegible]E-01 3.50233E-01-2.82737E-02 1.13443E-01-1.61395E-01 1.58401E-01-3.40390E-02 7.62531E-02
3.68[illegible]E-01 6.07535E-03-1.91[illegible]E-01 6.42041E-01-9.03970E-01 4.59441E-01

EIGENVALUE=  1.03068E-01 -3.347[illegible]E-02     G =  -.30571  FREQUENCY RATIO =  .33257  STIFFNESS PARAMETER =   .16623
EIGENVECTOR
-6.46117E-02-4.75364E-02-5.66690E-02-1.46457E-01 1.10070E-01 3.88331E-02 2.04610E-01 1.83853E-01 1.47415E-01-2.33762E-01
4.72[illegible]E-01-1.21[illegible]E-02-5.21[illegible]E-02 4.33[illegible]E-01-5.95553E-01 3.33734E-01 3.40824E-01 2.64649E-01-3.51[illegible]E-01 6.27436E-01
-5.54[illegible]E-01 1.46[illegible]E-02-2.35[illegible]E-01-9.76[illegible]E-01 8.15427E-02 8.48[illegible]E-02 8.44427E-02 1.84914E-01-6.[illegible]E-02 3.20[illegible]E-01
-1.03848E-01 1.27395E-01-4.64045E-01 1.08187E-01-9.04552E-02-2.59[illegible]E-01

DENSITY RATIO MU=   .09500

EIGENVALUE=  4.43391E-01 -2.50358E-01     G =  -.57592  FREQUENCY RATIO =  .69103  STIFFNESS PARAMETER =   .34552
EIGENVECTOR
9.54315E-03 9.70070E-02-3.68713E-02 1.96538E-01-2.62177E-02 1.72520E-01-1.19867E-01 2.55416E-01-1.76700E-01 3.220[illegible]E-01
-3.06091E-01 1.75183E-01-2.34[illegible]E-01 4.5[illegible]E-01-4.01970E-01 1.16775E-01-4.0[illegible]E-01 2.80711E-01 7.11[illegible]E-02-2.6[illegible]E-01
-5.57190E-01 3.39[illegible]E-01 2.79[illegible]E-01-4.35494E-01-2.12576E-02 2.10374E-01-1.34056E-01 3.6830[illegible]E-01-3.95000E-01 5.96985E-01
-5.49154E-01 2.52259E-01-7.39[illegible]E-01 4.77546E-01 2.04350E-01-4.89404E-01

EIGENVALUE=  4.81690E-01  1.77629E-01     G =   .36976  FREQUENCY RATIO =  .7[illegible]537  STIFFNESS PARAMETER =   .35268
EIGENVECTOR
8.66629E-02 1.00748E-02 1.69329E-01-3.14827E-02 1.41098E-01-3.23003E-02 2.35662E-01-1.22312E-01 2.90172E-01-1.74582E-01
1.54195E-01-3.13321E-01 3.75730E-01-3.24466E-01 7.48056E-02-3.92909E-01 2.33506E-01-4.17000E-01-2.64314E-01 6.42402E-02
2.54500E-01-5.40124E-01-3.73779E-01 2.33684E-01 1.74680E-01-2.57566E-02 3.12811E-01-1.30480E-01 5.04856E-01-3.90477E-01
2.06356E-01-5.33125E-01 3.45310E-01-7.35029E-01-4.47745E-01 2.01730E-01
```

```
EIGENVALUE=  1.13320E-01  9.73798E-02    G =   .85933  FREQUENCY RATIO =  .36245  STIFFNESS PARAMETER =   .18122
EIGENVECTOR
8.46356E-02 5.48869E-03 1.08659E-01-1.08206E-01 9.55197E-02-5.69047E-02 6.11954E-02-1.94123E-01 4.20102E-02 1.83424E-02
1.79628E-02 3.01013E-01 7.42469E-02-3.36514E-02 1.63030E-01 3.33672E-01 4.02712E-01-9.70787E-02 2.01375E-01-6.20935E-01
4.56965E-01-3.69276E-01-1.53614E-01-9.77852E-01 1.29403E-01-4.59769E-02 1.34629E-01-3.27412E-01 8.07385E-02-3.78187E-02
1.33396E-01 4.21306E-01 6.33093E-01-3.75567E-01 9.62209E-02-1.10091E+00

EIGENVALUE=  9.96124E-02 -9.47621E-02    G =  -.95131  FREQUENCY RATIO =  .34431  STIFFNESS PARAMETER =   .17215
EIGENVECTOR
7.18246E-03 9.84635E-02-1.44047E-01 1.19257E-01-9.94265E-02 1.51773E-01-3.14180E-01 1.12531E-01 2.20228E-02 4.47269E-02
3.97760E-01 2.37793E-02-7.14356E-02 9.89983E-02 5.31431E-01 1.85096E-01-1.30568E-01 5.03516E-01-9.21254E-01 2.43342E-01
-4.92530E-01 7.10066E-01-1.44432E+00 3.73331E-02-9.11390E-02 1.93772E-01-3.49033E-01 1.72914E-01-7.51235E-02 1.14049E-01
6.19214E-01 1.74487E-01-5.17358E-01 9.06008E-01-1.55765E+00 2.35240E-01

EIGENVALUE=  1.16445E-01 -3.94212E-02    G =  -.33854  FREQUENCY RATIO =  .34596  STIFFNESS PARAMETER =   .17298
EIGENVECTOR
1.07238E-01 4.47033E-02 1.24318E-01 1.29934E-01-1.69449E-01-1.33903E-02-3.51517E-01-1.87345E-01-1.49195E-01 3.43429E-01
-6.50410E-01 8.65978E-02-2.01113E-02-5.96301E-01 7.30495E-01-6.78343E-01-4.72423E-01-3.17315E-01 4.34327E-01-5.79653E-01
8.59934E-01 1.08947E-02 3.22723E-01 1.55176E+00-1.32287E-01-5.66339E-02-1.72236E-01-2.15110E-01 4.53045E-02-4.39453E-01
5.67783E-01-2.55322E-01 5.83367E-01-8.94748E-02 8.05759E-02 5.55670E-01
```